Centro de Investigación Científica y de Educación Superior de Ensenada, Baja California

Doctorado en Ciencias
Ciencias de la Vida
con orientación en Biotecnología Marina

Identification and characterization of potentially harmful dinoflagellates in Todos Santos Bay

Tesis
para cubrir parcialmente los requisitos necesarios para obtener el grado de Doctor en Ciencias

Presenta:

Patricia Esthefanía Paredes Banda

Ensenada, Baja California, México
2020

Tesis defendida por

Patricia Esthefanía Paredes Banda

y aprobada por el siguiente Comité

Dr. Ernesto García Mendoza **Co-director de tesis**	Dra. Elizabeth Ponce Rivas **Co-director de tesis**

Dra. M. del Pilar Sánchez Saavedra

Dr. Allan Douglas Cembella

Dra. María Asunción Lago Lestón

Dra. Patricia Juárez Camacho
Coordinadora del Posgrado en Ciencias de la Vida

Dra. Rufina Hernández Martínez
Directora de Estudios de Posgrado

Resumen de la tesis que presenta **Patricia Esthefanía Paredes Banda** como requisito parcial para la obtención del grado de Doctor en Ciencias en Ciencias de la Vida con orientación en Biotecnología Marina

Identificación y caracterización de dinoflagelados potencialmente tóxicos en la Bahía de Todos Santos

Resumen aprobado por:

_____	_____
Dr. Ernesto García Mendoza	Dra. Elizabeth Ponce Rivas
Co-director de tesis	**Co-director de tesis**

La Bahía de Todos Santos (BTS) se localiza en la costa noroeste de la península de Baja California donde existen fenómenos de surgencia estacional, que producen una alta productividad primaria que sustenta el desarrollo de actividades de maricultura como el cultivo de moluscos bivalvos. El fitoplancton es el alimento principal de los bivalvos. Los dinoflagelados, son un grupo importante del fitoplancton que incluye algunas especies tóxicas que pueden causar florecimientos algales nocivos (FAN). En BTS, los FAN han causado la implementación de vedas sanitarias. Se detectaron espirólidos (SPX) y azaspirácidos (AZA) por LC-MS/MS en bivalvos cultivados en la región, pero las especies productoras de estas toxinas no han sido identificadas. Por lo tanto, el objetivo de este estudio es identificar las especies potencialmente tóxicas en la BTS a través de técnicas moleculares y de microscopía, y relacionar las variables ambientales que favorecen su presencia en la región . Con marcadores moleculares específicos, se identificó por primera vez en el Pacífico noroeste a *Alexandrium ostenfeldii* y *Azadinium spinosum* como las especies productoras principales y probablemente únicas de SPX y AZA, respectivamente. Se detectó un solo análogo de SPX en bajas concentraciones, el 13 desm-SPXC asociado a la presencia de *A. ostenfeldii* que no presentó una estacionalidad clara de aparición. La mayor abundancia celular se registró en octubre del 2013 con 3.62 x 10^3 células L^{-1}. El intervalo de temperatura que favoreció su presencia fue de 17 a 20 °C. En el caso de *Az. spinosum*, se observó una clara estacionalidad de co-ocurrencia de la especie y la toxina, principalmente se presentaron en los meses de invierno. La concentración de AZA-1 (24 µg de Aza kg^{-1}) y abundancia celular de *Azadium* sp. (7.2 x 10^2 células L^{-1}) más altas se registraron en noviembre del 2016. La homogeneidad de la columna de agua y bajas concentraciones de nitrógeno inorgánico (3.60-4 µM) se asociaron con la presencia de esta especie. Además, se aisló y caracterizó una nueva especie de dinoflagelado tecado pequeño, *Heterocapsa calafianiensis*. El análisis filogenético con las secuencias ITS y LSU agrupó a *H. calafianiensis* dentro de un clado separado de las otras especies reportadas para este género. Esta nueva especie presentó un perfil pigmentario Tipo-1 (Chl *c2*, peridinina y dinoxantina) y una tasa de crecimiento alta en condiciones de cultivo (µmax = 0.63 d^{-1}) en comparación con otros dinoflagelados. Esto sugiere un alto potencial para la formación de florecimientos en la región. Se puede concluir que *A. ostenfeldii* tiene una amplia distribución en la BTS, es un componente común del fitoplancton y se presentó en condiciones ambientales distintas a *Az. spinosum*, el cual tiene una distribución oceánica con presencia en la BTS en invierno. Los análogos de SPX asociados con *A. ostenfeldii* en bivalvos no son considerados como un riesgo para la salud. Por otro lado, debido al incremento en las concentraciones de AZA, en BTS es necesario continuar con el monitoreo de *Az. spinosum* y de los azapirácidos, ya que podrían ser un riesgo emergente en la región.

Palabras clave: FANs, toxinas emergentes, variables ambientales, dinoflagelados, marcadores moleculares.

Abstract of the thesis presented **by Patricia Esthefanía Paredes Banda** as a partial requirement to obtain the Doctor of Science degree in Life Sciences with orientation in Marine Biotechnology

Identification and characterization of potentially harmful dinoflagellates in Todos Santos Bay

Abstract approved by:

_____	_____
Dr. Ernesto García Mendoza	Dra. Elizabeth Ponce Rivas
Thesis co-director	**Thesis co-director**

Todos Santos Bay (TSB) on the northwest coast of the Baja California Peninsula is located in a seasonal upwelling region yielding high primary productivity that promotes the development of mariculture activities like bivalve mollusk culture. Phytoplankton is the main food source for the bivalves. Dinoflagellates are an important group of the phytoplankton community and include toxic species, which can cause harmful algal blooms (HABs). In TSB, HABs events have been associated with sanitary closures. Azaspiracids (AZA) and spirolides (SPX) have been detected in cultured bivalves. However, the producer species of these toxins have not been identified. Hence, the present study aimed to identify the potentially toxic species in TSB through molecular and microscopy techniques, and to relate the environmental variables that favored their presence. With specific molecular markers, the dinoflagellates *Alexandrium ostenfeldii* and *Azadinium spinosum* were identified for the first time in the northwest Pacific as the main and perhaps exclusive producer species of SPX and AZA, respectively. *A. ostenfeldii* had no seasonality of appearance, and a single SPX analog, 13 desm-SPXC was detected in low concentrations. The highest cellular abundance was 3.62 x 10^3 cells L^{-1} in October 2013. The temperature range that favored the presence of the species was 17 to 20 °C. In the case of *Az. spinosum*, a clear seasonality of co-occurrence of the species and the toxin was observed during winter months. The highest concentration (24 µg Aza kg^{-1}) of AZA-1 and cellular abundance (7.2 x 10^2 cells L^{-1}) was registered in November 2016. Homogeneity of the water column and low concentrations of inorganic nitrogen (3.60–4 µM) were associated with the presence of the species. Additionally, a new small thecate dinoflagellate species, *Heterocapsa calafianiensis* was isolated and characterized from TSB. Phylogenetic analysis with the ITS and LSU sequences cluster *H. calafianiensis* within a clade separated from the other species reported for this genus. The new dinoflagellate exhibits a classic Type-1 pigment profile (Chl *c2*, peridinin and dinoxanthin) and a high growth rate in culture (μmax= 0.63 d^{-1}) compared with other dinoflagellates. This suggests a high potential for the formation of high biomass blooms in the region. Finally, it may be concluded that *A. ostenfeldii* has a wide distribution in the TSB, is a common component of the phytoplankton, and it was presented in different environmental conditions compared to *Az. spinosum*, which has an oceanic distribution with a presence in TSB during the winter. The presence of SPX analogs associated with *A. ostenfeldii* in bivalve shellfish is not considered to be of human health risk. On the other hand, the monitoring of *Az. spinosum* and azaspiracid are necessary due to the increase of the AZA concentrations, and this could be an emerging toxin risk.

Keywords: HABs, emerging toxins, environmental variables, dinoflagellates, molecular markers

Dedication

Esta tesis se la dedico a Dios porque gracias a ÉL he podido llegar donde estoy, su amor me ha sostenido para permanecer. Toda la Gloria sea a ÉL!!

A mi mamá Ana Banda, tus horas de trabajo, tu amor, tus tiempos de soledad, el haberme puesto alas para volar son el fruto de este gran logro y sueño que nacieron en tu corazón. Gracias por siempre haber creído en mí y por siempre estar conmigo.

A mi papito Agustín que me enseñó, que sin importar el oficio siempre tenía que ser la mejor. Tu sonrisa retumbará hasta mi eternidad!

A mi esposo David J.P. González, eres esa nueva historia en mi vida que me da la fortaleza para ser mejor, gracias mi amor por tu compañía, tu paciencia, tu apoyo y tu amor.

Acknowledgments

Al Centro de Investigación Científica y de Educación Superior de Ensenada, Baja California (CICESE) por permitirme realizar mis estudios de posgrado y por proveer todas las facilidades para llevar a cabo mi tesis de doctorado.

Al Consejo Nacional de Ciencia y Tecnología (CONACYT) por la beca de manutención otorgada para realizar mis estudios de posgrado (No 21892). Así mismo, se agradece el financiamiento de los proyectos FORDECYT 260040-2015, a la red temática RedFAN. Así como al financiamiento dentro del programa de investigación PACES II (Topic II Coast:WP3) del Instituto para la Investigación Polar y Marina Alfred-Wegener (AWI).

A mis directores de tesis el Dr. Ernesto García Mendoza y la Dra. Elizabeth Ponce, gracias por su apoyo académico y financiero a lo largo de estos cuatro años, por hacer que me esfuerce más confiando en que tenía la capacidad para traspasar mis límites. Gracias por ir más allá de lo académico y haberme apoyado y cuidado de manera personal en los momentos difíciles.

A mi comité de tesis la Dra. Pilar Sánchez Saavedra, el Dr. Allan Cembella, la Dra. Asunción Lago Lestón, por compartir sus conocimientos conmigo y haber enriquecido este trabajo realizando sus comentarios oportunos. Allan muchísimas gracias por tus correcciones, por darme la oportunidad de trabajar en tu laboratorio ampliando mis horizontes. Al Dr. Bernd Krock por realizar los análisis de toxinas y a Annegret Müller por toda su ayuda y paciencia durante mi estancia en el AWI. Al Dr. Urban Tillmann por proveer el DNA de *Az. spinosum* y hacer toda la microscopía y descripción morfológica para la identificación de la nueva especie de *Heterocapsa*.

Gracias a mis amigos!! Lau y Faustin desde la maestría me han acompañado, aconsejado y compartido mis alegrías y tristezas, los quiero!. Miriam gracias porque fuiste esa amistad que llegó en el momento que más necesitaba, contigo me río tanto. Gracias al laboratorio FICOTOX, sobre todo a Yaireb por su ayuda con el análisis de toxinas y a Ramón con el análisis de pigmentos.

Mami sin ti yo no habría alcanzado nada de esto, gracias por tu esfuerzo, pero por sobre las cosas gracias por tu gran amor y tu sustento. A mi papito Agustín que está en el cielo, sé que sus bendiciones me han cuidado y está muy orgulloso de mí. A mi abuelita por sus enseñanzas, apoyo y bendiciones.

Gracias esposo mío David J.P González, por enseñarme tanto de la vida, de ti pero sobre todo de mí, has hecho que crezca como persona. Gracias por dar 1 Km extra y ayudarme en el lab. (con mis lágrimas de chinche) aunque no tenías idea, estuviste ahí para mí!!

Gracias a mis tíos Martha, Washington y Héctor por siempre estar allí pendientes de mí y a mi hermana Anita porque compartimos nuestras alegrías y nuestras tristezas.

Table of contents

List of figures

List of tables

Chapter 1. Introduction

In response to favorable environmental conditions, the toxic microalgae can proliferate, aggregate, and accumulated high biomass of cells named (HABs) whose principal characteristic is to have a detrimental effect on plants, animals, and humans (Epstein, 1998). The HABs can alter the food web dynamics with mass mortalities of wild and farmed fish, shellfish and cause human illness and death from toxic seafood or toxin exposure through inhalation or water contact; disease and death of marine mammals, seabirds and the alteration of the marine habitats and trophic structure (Anderson et al., 2002). The human poisoning episodes occur mostly due to the consumption of shellfish, which accumulate the phycotoxins into their tissues, by filtering large volumes of water and they are the vector organisms (Camacho et al., 2007).

Global increases in frequency, magnitude, and geographic extent of HAB events have been recorded over the last two decades (Anderson, 2007; Hallegraeff, 1993; Wells et al., 2020). There were multiple reasons proposed for this expansion, including natural dispersal of species by currents and storms, dispersal through human activities such as ballast water discharge and shellfish translocation, improved detection of HABs and their toxins due to better chemical instrumentation and improved communication among scientists, increased aquaculture operations in coastal waters, and stimulation of HABs as a result of cultural eutrophication or perhaps even climate change. Virtually every coastal region of the world is affected by harmful algal blooms (HABs) commonly called "red tides" (Anderson et al., 2012b).

On a global scale, close to 2000 cases of human poisoning (15% mortality) through fish or shellfish consumption are reported each year and, if not controlled, the economic damage through reduced local consumption and reduced export of seafood products can be considerable (Hallegraeff, 1993).

In Mexico, 61 HABs events caused around 2500 days of sanitary closures between 2003 and 2014 (COFEPRIS, 2018) affecting local economies due to the bans of shellfish harvesting or extracting (Cuellar-Martinez et al., 2018).

Along the Pacific coast of North America, from Alaska to Mexico, harmful algal blooms (HABs) have caused losses of natural resources and coastal economies, and have resulted in human sicknesses and deaths. Two types of HABs pose the most significant threat to coastal ecosystems in this western coast: dinoflagellates of the genera *Alexandrium*, *Gymnodinium*, and *Pyrodinium* that cause paralytic shellfish poisoning (PSP), diatoms of the genus *Pseudo-nitzschia* that cause of amnesic shellfish poisoning (ASP) in humans, and diarrhetic shellfish poisoning from *Dinophysis*; these species extend

throughout the region (Lewitus et al., 2012). While problems from other HABs (e.g., fish kills linked to raphidophytes or *Margalefidinium* (*Cochlodinium*), sea bird deaths caused by surfactant-like proteins produced by *Akashiwo sanguinea*, hepatotoxins from *Microcystis*) are less prevalent but potentially expanding (Lewitus et al., 2012).

In Todos Santos Bay in 2002, a bloom of *Ceratium furca* caused around 15 million-dollar losses in a mass mortality episode on farmed tuna (Orellana-Cepeda et al., 2004). Many events of algal blooms have occurred in the Bay; it is so in 2007 a bloom of *P. australis* caused the death of sea lions and the enclosure of the aquaculture activities and extraction of mollusks (García-Mendoza et al., 2009). In 2010 for the first time, two sanitary bans were implemented associated with positive detection for diarrhetic shellfish toxins (DSTs) using the mouse bioassay (MBA) (Lewitus et al., 2012). Then in 2012, three bans were implemented by the detection of the same toxins (García-Mendoza et al., 2014). During 2016 a mass mortality of tuna was recorded in the Bay with one of the most considerable economic negative impacts estimated of 42 million dollars of losses related to a bloom of *Chatonella* species (García-Mendoza et al., 2018).

1.1 Location and oceangraphic system of Todos Santos Bay

The Baja California state has 1380 km of littoral coast occupying the second place of the states of Mexico. Todos Santos Bay (TSB) is located in the coastal city of Ensenada on the northwestern coast of the Baja California Peninsula between the latitudes 31°42’ to 31°55’ N and longitudes 116°36’ to 116°48’ W. The Baja California Peninsula is located between the Pacific Ocean and the Cortés Sea. TSB has a surface area of approximately 250 km^2 and a mean depth of 50 m. A canyon slightly deeper than 300 m is found in its southwestern part (Torres et al., 2006). TSB has two mouths that connect it with the Pacific Ocean. The northeastern mouth, between Todos Santos Island (TSI) and San Miguel, is approximately 10 km wide, whereas the southwestern mouth measures ~5 km (Argote Espinosa et al., 1991). This region is part of the California Current System (CCS), one of the world’s most productive areas; the general circulation in TSB is primarily due to the CCS, wind stress, and tidal forcing (Farfán Mateos, 2010). Upwelling processes in inshore areas close to the bay introduce cold and nutrient-rich subsurface water, resulting in a lower sea surface temperature in TSB (Torres et al., 2006). Almost all of these coastal water bodies have high primary productivity, and they have an essential influence upon fishery resources as excellent larval recruitment zones, these closely related to coastal upwelling activity (Zaytsev et al., 2003).

Due to these characteristics, in the region, the bivalve mollusk culture has been developed as one of

the most important economic activities. In 1985 the Martesano Company established the first mussels culture using the floating rafts (Cáceres-Martínez, 1997). Currently in the Rincón de Ballenas area, located in the south of the TSB two companies: Acuacultura Oceánica S.P.R. of R.L. and AQUALAP S.A of C.V are operating for the cultivation of *Mytilus galloprovincialis* (Mediterranean mussel) and *Crassostrea gigas* (Japanese oyster) employing the long-line system. In 1993 the Rincón de Ballenas area was approved with sanitary certification No MX0204MC to export the cultivated products (CONAPESCA, 2008). The mariculture activities in the region not only involve the mollusks cultures but also at the North of TSB in the Salsipuedes Bay fattening of T*hunnus thynnus orientalis* (bluefin tuna) is an important aquaculture activity. Baja California produced 2050 tons of oyster, 194 tons of mussels), and a tuna fattening of 4494 tons, which represents MXN 539'935.430 (SEPESCABC, 2018).

The phytoplankton is the foundation of the aquatic food web, meaning that they are the primary producers and the photosynthetic component of plankton (Kyewalyanga, 2016). All bivalves are filter-feeders, mainly feeding on a wide range of phytoplankton species. Mussels process large volumes of water because the amount of organic matter in seawater is low (average 1 mg L^{-1}). Mussels filter, on average, 7.5 L h^{-1} of seawater. As a consequence, they accumulate and concentrate many pollutants and toxins in seawater (Ciminiello and Fattorusso, 2006).

1.2 Dinoflagellates

The main types of phytoplankton are cyanobacteria, diatoms, dinoflagellates, chlorophytes, radophytes, and coccolithophores (Kyewalyanga, 2016).

Dinoflagellates are the second important group of protists in marine and freshwaters. Their adaptation to a wide range of environments is reflected by tremendous morphological and trophic diversity (Taylor, 1987). Dinoflagellate nucleus contains large amounts of DNA and unique cytological features such as permanently condensed chromosomes and a lack of typical eukaryotic histones (Lin, 2011). Dinoflagellates are the second group in importance as primary producers after diatoms, the majority of the species are primary producers (photosynthetic) but also consumers (mixotrophy) in the food web, sometimes at the same time (Burkholder et al., 2008).

Dinoflagellates show a high versatility in the habitat distribution, marine or continental waters, and adaptation to pelagic or benthic environments (Hansen, 2011). Some species are bioluminescent, and another could produce toxins when they are dominant, causing harmful algal blooms (Hackett

et al., 2004). In a checklist of living dinoflagellates, (Gómez, 2012) described 2377 species of these approximately 60 species could synthesize phycotoxins (Méndez, 2008) within these species are *Alexandrium ostenfeldii* and *Azadinium spinosum* which are polyether toxins producers with importance in aquaculture activities due to the economical losses and the hazard in human health.

The variability of the environmental factors reflects the seasonal fluctuation of the dinoflagellates' blooms and its toxicity. The nutrients, temperature, and light affect the metabolism of the organisms (Tosteson et al., 1998). In the laboratory under controlled experimental conditions, it has been confirmed that the temperature and the light have a significative effect in the growth rate and the toxin production on dinoflagellates due their outcome in the biochemical reactions into the cell as in the case of *Azadium spinosum* (Jauffrais et al., 2013). However the specific function of the toxin in the producer organism is not clear but it has been related as a defense mechanism against predation or to reduce the competition with other phytoplanktonic species (Tillmann and Hansen, 2009; Tillmann and John, 2002).

1.2.1 *Alexandrium ostenfeldii*

A. ostenfeldii is a mixotrophic dinoflagellate with a cellular size between 40 – 56 µm length and 40 to 50 µm diameter, it can produce spirolide toxins, some strains also can produce PSP toxins and/or gymnodimines. The cells have a globose appearance; both the epi and hypotheca have margins slightly rounded, the main diagnostics feature is the presence of a ventral pore which is located midway on the right margin of the first apical plate (1') (Fig. 1), and the majority of the cells contain food vacuoles (Almandoz et al., 2014). It was described for the first time by (Paulsen) (Balech and Tangen, 1985) in Iceland. In the beginning, it was thought that the species was exclusive to cold waters and was considered an "Arctic-boreal" species but now is known to be widely distributed in temperate waters (Gribble et al., 2005).

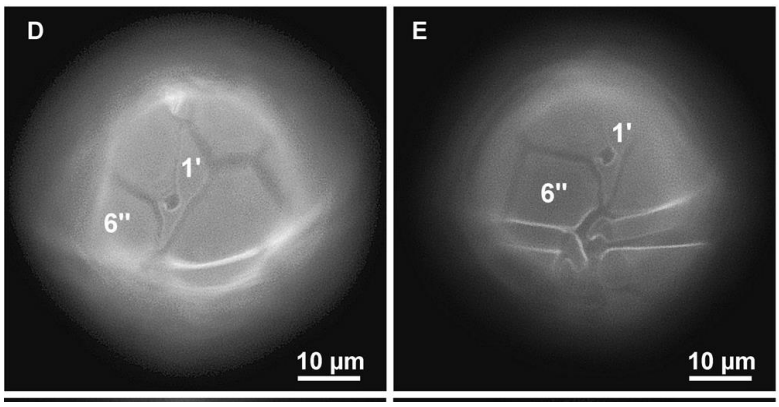

Figure 1. Cells of *A. ostenfeldii* stained with calcofluor and observed by epifluorescence microscope. Morphology of the 1' plate and its ventral pore (**D, E**) (Almandoz *et al*., 2014).

A. ostenfeldii has a wide range of distribution since it has been found in Denmark (Moestrup and Hansen, 1988), Scotland (John et al., 2003), Norway (Balech and Tangen, 1985), Spain (Fraga and Sánchez, 1985), Canada and the Atlantic coast of United States (Cembella et al., 2000b; Gribble et al., 2005), Sweden (Krempt et al., 2009), Argentina (Almandoz et al., 2004) and a report was made for Mexican Pacific coast of Michoacán (Ceballos-Corona, 1998).

Their toxic profiles and toxicity can vary widely depending on the type of strain and its geographic location (Hansen et al., 1992; Mackenzie et al., 1996). For example one strain of *A. ostenfeldii* isolated from Denmark produce saxitoxins and its low power derivatives (Hansen et al., 1992), while New Zealand strains produce high levels of saxitoxins (Mackenzie et al., 1996) and North Atlantic populations like Scotland does not produce PSP toxins but only spirolides (Cembella et al., 2000b).

1.2.2 *Azadinium spinosum*

There is a great interest in the study of this species due to its toxic potential and its relatively small genome around 9 Gbps (Toebe et al., 2013a). *Az. spinsoum* is a small (between 12 to 16 µm length and 7 to 11 µm width) photosynthetic armored dinoflagellate (Fig. 2) belonging to Peridiniphycidae subclass of the Amphidomataceae family (Tillmann et al., 2009a). This species was identified for the first time in 2007 during a research cruise in the North Sea of Scotland (Krock et al., 2009).

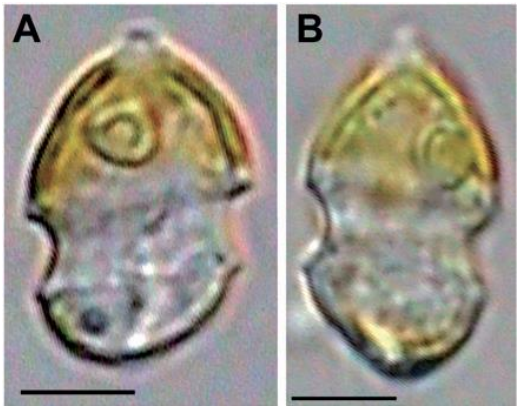

Figure 2. Living cells of *Az. spinosum* observed under optical microscope (Tillmann et al., 2009a).

A*z. spinosum* produces the AZA-1 and AZA-2 analogs (Tillman et al., 2009a) and have a wide geographic distribution. There are records in Denmark (Tillman et al., 2011), Ireland (Salas et al.,

2011), Morocco (Taleb et al., 2006), the Shetland Islands (Tillman et al., 2012b) and in the Mexican tropical Pacific in the Tehuantepec Gulf (Hernández-Becerril et al., 2012). In 1990 it was described as a bloom of *Azadinium.* cf. *spinosum* in Argentina with cell abundance > 9.03 x 10^6 cells L^{-1} (Akselman and Negri, 2012). However, no human intoxication cases were recorded during the Argentina bloom.

1.2.3 *Heterocapsa* genus

Stein initially established the genus *Heterocapsa* in 1880, which is a relatively small armored dinoflagellate in which the identification of their species is difficult because there are few differences in morphological characteristics among their species (Attaran-Fariman and Javid, 2013). One of the main characteristics for the identification of the species is the body-scales structures consisting of a triradiate basal plate and three-dimensional construction that covering the cell surface and allows to reassessed the taxonomy of this genus (Iwataki, 2002; Iwataki et al., 2004). *Heterocapsa* has been known as cosmopolitan phytoplankton, especially in coastal waters like *H. triquetra* and *H. rotundata*. The attention to this genus began when mass mortality in mollusks cultures occurred in Japan, then *H. circularisquama* was described as a toxic species (Horiguchi, 1995; Matsuyama, 1999). After one decade, a new toxigenic species, *H. bohaiensis* was described on the China coast when a bloom caused mortalities in culture prawns (*Penaeus japonicas*) and crab larvae (*Eriocher sinensis*) (Xiao et al., 2018).

1.2.4 Identification of dinoflagellate species

Dinoflagellates species are described based on morphological differences like the shape, wide morphometric data, as well as surface ornamentation (pores, areolae, spines, ridges etc.), the different flagella arrangement and the thecal plates covering the cell (Fensome et al., 1999).

Plate designation systems have been proposed to describe individual thecal plate. In Kofoidian system, the plates immediately above the cingulum are precingulars. Any plates that occur between the apical and precingulars are designated as anterior intercalaries. On the other hand, the plates immediately below the cingulum, except those in the sulcus, are the postcingulars. Any plates in between the antapical pole and postcingular, other than those in sulcus, are termed posterior intercalaries (Taylor, 1987). Besides that, Kofoid's system also used the combination of superscript notation and the number of plates to produce a plate formula: apicals (′), anterior intercalaries (a),

precingulars (′), postcingulars (″), posterior intercalaries (p), and antapicals (‴) (Taylor, 1987) as shown in the figure 3.

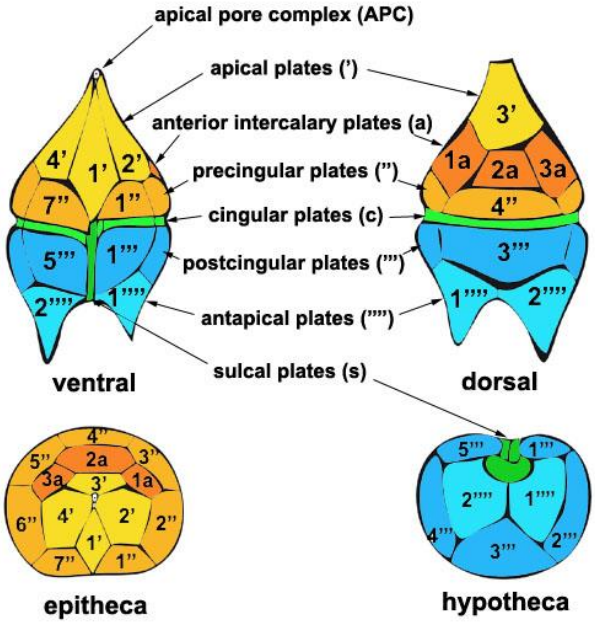

Figure 3. Kofoid system of plate tabulation in dinoflagellates (Hoppenrath and Saldarriaga, 2008).

The accurate identification of species that cause HABs is crucial in the development of strategies for mitigating the adverse impacts of these events. Detection and identification methods are frequently based on traditional microscopy that requires expertise and training. The errors in the identification are often related to the difficult to differentiate the small organisms which require advanced microscopy, the different morphological forms (vegetative cells or cysts) and some closely related species exhibit little or no visible variation making them very difficult to identify (Culverhouse et al., 2003; Godhe, 2001).

The advantage of molecular tools for taxonomic identification such as the Polymerase Chain Reaction (PCR) coupled with gene sequencing and phylogenetic analysis has made possible a faster, efficient and accurate classification of organisms isolated from the field or environmental samples (Ki and Han, 2007; Ki et al., 2004). Genes and spacer of the ribosomal RNA (rRNA) operon are among the most widely used as genetic markers to design specific primers because it occurs as multiple tandem repeats in the nuclear DNA precursor. Each repeat comprises three coding regions, a single rRNA precursor, which is then cleaved to produce mature small subunit, 18S rRNA (SSU), mature 5.8S rRNA, and the mature large subunit, 28S rRNA (LSU) (Casiraghi et al., 2010). The internal transcribed spacer (ITS) regions are between the 5.8S and 18S genes (ITS1) while the ITS2 is between the 5.8S

and 28S genes, they are used efficiently because diverges rapidly during speciation; consequently are used to identify species not only in dinoflagellates (Stern et al., 2010) but also in other groups (Larsson and Jacobsson, 2004; Wastaff, 2004 in Litaker et al., 2007).

The molecular tools are a complement to the traditional morphological identification of the species and not intend to supplant the morphologic characterization.

1.3 Phycotoxins

The term phycotoxin indicates natural metabolites produced by unicellular microalgae (protists) (FAO, 2011). They are a wide array of compounds with diverse chemical characteristics and with biological activity able to produce a harmful reaction or effect in the biological system (Botana, 2014). Dinoflagellates produce most phycotoxins although cyanobacteria have also been reported to produce saxitoxin (STX), and domoic acid (DA) is produced by diatoms (FAO, 2011). Their function is not yet clear; it is thought to have a physiological or defense role. Indeed a certain correlation was observed between the production of diarrheic toxin and photosynthesis activity (Zhou and Fritz, 1994).

The inhibiting activity, called allelopathy has been studied and observed *in vitro* against other microalgae reducing the growth rate or forming cysts (Tillmann and Hansen, 2009) or reducing the grazing of zooplankton and decreasing the hatching rate (Brown et al., 2019; Colin and Dam, 2003). Each compound group typically has several main compounds based on the same or similar structure. However, most groups also have several analogs, which are either produced by the algae or through metabolism in fish or shellfish or other marine organisms (Rossini and Hess, 2010).

One of the most common phycotoxin classifications is based on the toxic effects in humans: paralytic toxins (PSP), diarrheic toxins (DSP), neurotoxins (NSP), amnesic toxins (ASP). Within the lipophilic toxins are the okadaic acid and its derivates, dinophysistoxins, pectenotoxins, yessotoxins, gymnodimines, spirolides, and azaspiracids. These toxins can often be found in combination in shellfish (Trainer et al., 2013). The action mechanism of some phycotoxins is described in Table 1.

Table 1. Classification of toxins according to the symptoms produced in humans (adapted, from Rossini and Hess, 2010 and modified in this study)

Syndrome	Toxins	Major Producer Species	Molecular Target
Paralyzing toxins (PSP)	Saxitoxins	*Alexandrium spp.* *Gymnodinium catenatum* *Pyrodinium bahamense*	Voltage dependent sodium channels (Site 1)
Neurotoxins (NSP)	Brevetoxins	*Karenia brevis*	Voltage dependent Sodium channels (Site 5)
Amnesic toxins (ASP)	Domoic Acid	*Pseudo-nitzschia* spp.	Glutamate receptors
Diarrheic toxins (DSP)	Okadaic acid and Dinophysistoxins	*Dinophysis spp.*	Phosphatase PP1a and PP2a proteins
Lipophilic toxins	Yessotoxins	*Protoceratium reticulatum* *Gonyaulax spinifera* *Lingulodinium polyedrum*	Not well defined
	Spirolides	*Alexandrium ostenfeldii*	Muscarinic and nicotinic receptors
	Gymnodimines	*Karenia selliformis* *Alexandrium ostenfeldii*	Is not clear
	Azaspiracids	*Azadinium spinosum* *Azadinium poporum* *Amphidoma languida*	Gastrointestinal tract

The lipophilic toxins in shellfish can be divided into five groups of toxins with different chemical structures and biological effects: okadaic acid (OA) and its derivatives, dinophysistoxins DTXs; the pectenotoxins (PTXs); yessotoxins (YTXs); the spirolides (SPXs) and the azaspiracids (AZAs). These toxins can often be found in combination in shellfish (Fujiki and Suganuma, 1993).

1.3.1 Azaspiracids

The azaspiracids (AZAs) are polyether compounds with an aza group (cyclic amine), a unique tri-spiro ring assembly, and one carboxylic acid (Satake et al., 1998) (Fig.4). In the last decade, more than 20 analogs were detected (Twiner et al., 2008). In Netherland in 1995 owing to a human intoxication due to the consumption of blue mussels extracted from Ireland AZA-1 was detected for the first time (McMahon and Silke, 1996). Associated with the recognized effect on humans, the regulatory limit for AZA was set at 160 µg Kg^{-1} of AZA-1, AZA-2, and AZA-3; all of these analogs are reported as AZA-1 equivalents (Alexander et al., 2008). The producer species is *Azadinium spinosum* a small photosynthetic dinoflagellate (12- 16 µm) which was isolated in the North Sea and produce the AZA-1 and AZA-2 analogs (Tillmann et al., 2009a).

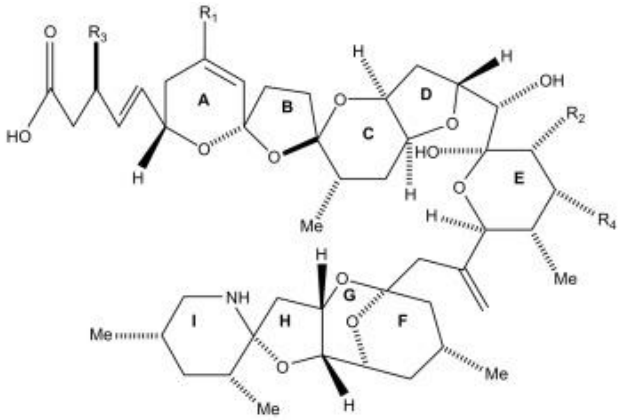

Toxin	Molecular Formula	R1	R2	R3	R4
AZA1	$C_{47}H_{71}NO_{12}$	H	CH_3	H	H
AZA2	$C_{48}H_{73}NO_{12}$	CH_3	CH_3	H	H
AZA3	$C_{46}H_{69}NO_{12}$	H	H	H	H
AZA4	$C_{46}H_{70}NO_{13}$	H	H	OH	H
AZA5	$C_{46}H_{70}NO_{13}$	H	H	H	OH
AZA6	$C_{47}H_{71}NO_{12}$	CH_3	H	H	H
AZA7	$C_{47}H_{71}NO_{13}$	H	CH_3	OH	H
AZA8	$C_{47}H_{71}NO_{13}$	H	CH_3	H	OH
AZA9	$C_{47}H_{71}NO_{13}$	CH_3	OH	H	H
AZA10	$C_{47}H_{71}NO_{13}$	CH_3	H	H	OH
AZA11	$C_{48}H_{73}NO_{13}$	CH_3	CH_3	OH	H

Figure 4. Chemical structure of azaspiracid 1 to azaspiracid 10 (Botana, 2014).

1.3.2 Spirolides

The spirolides (SPX) are polyether compounds, which contain a spiro group linked to tricyclic ethers (Fig. 5). The toxin was detected in 1995 for the first time during biotoxins monitoring cruise into mollusks (*Mytilus edulis* and *Placopecten magellanicus*) collected from Nova Scotia, Canada, the rapid and unusual death in the mouse bioassay when a lipophilic extract was administered by intraperitoneal (i.p.) injection (Hu et al., 1995). It was until the year 2000 that *Alexandrium ostenfeldii* was identified as the producer species of this toxin (Cembella et al., 2000a). 16 SPX analogs have been detected, of which 13 desmethyl spirolide C is the most commonly found in shellfish (Hu et al., 2001). The spirolides are not under sanitary regulation because the effects on humans and the doses necessary to cause harm showed minimal toxicity. In the study conducted by (Munday et al., 2012) using a neuroblastoma cellular model showed that the 13-desme-SPXC had an activity in the muscarinic-acetylcholine receptors. Further, there are no reports of associated poisonings (Otero et al., 2011).

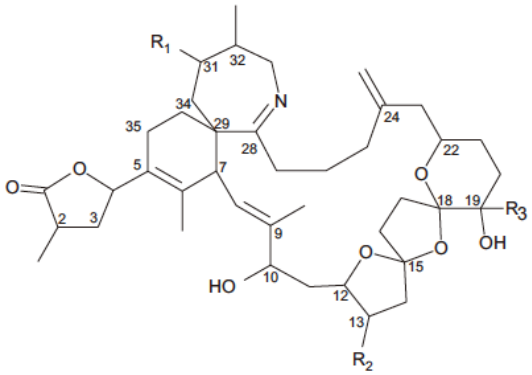

Spirolide	R_1	R_2	R_3	$\Delta^{2,3}$	MW
A	H	CH_3	CH_3	+	691.5
B	H	CH_3	CH_3	-	693.5
C	CH_3	CH_3	CH_3	+	705.5
D	CH_3	CH_3	CH_3	-	707.5
13-desMe-C	CH_3	H	CH_3	+	691.5
13, 19-didesMe-C	CH_3	H	H	+	677.5

Figure 5. Chemical structure of spirolides with its analogs A to C and 13- desMe-C and 13, 19-didesMe-C (Krock et al., 2008)

1.3.3 Phycotoxin detection methods

The routine analysis to detect various types of toxins is the mouse bioassay that allows its characterization, based on careful observation of the animal's symptoms after the toxin extract is injected intraperitoneally (i.p). The quantification of the toxin consists of recording the time of death of the mouse, which is given in mouse units (UR), which is the equivalent of the LD_{50} dose that is needed to kill 20 g mice (Holmes and Lewis, 2002). However, this type of analysis does not allow to differentiate different analogs from toxins, so the use of analytical methods for more accurate detection and quantification has been implemented (Van Dolah et al., 2012).

The liquid chromatography coupled to a mass tandem spectrometer (LC-MS/MS) is an analytic technic that combine the separation of individual toxins compounds through a solid phase with the use of physic parameters (like the hydrophobicity). And shows the relation mass-charge (m/z) of the analytic ions of the toxins in order to identify and quantify the concentrations of the toxin extract. This technique is capable of giving additional confirmatory information through fragmentation patterns of each toxin individually when it is dissociated, and the mass spectrometer detects the fragment ions. The obstacle to the development of this technique is the lack of commercial calibration standards for toxins and the validation of the method (Stobo et al., 2005). Also the high cost of the equipment is one limitation to implement this technique.

1.4 Justification

The harmful algal blooms have increased over the past decades; their frequency and geographic distribution have adverse impacts on public health and the economy in a global form. Sanitary closures have been established in TSB for the detection of diarrheic and amnesic toxins in cultured mollusks. In 2012 three sanitary closures were implemented due to the presence of okadaic acid and dinophysistoxins in shellfish using the mouse bioassay method. Two of these closures were confirmed by the analytical method (LC-MS/MS), but one was a false positive that could be attributed to the presence of spirolides as “fast-acting” toxin causing economic losses (Sánchez-Bravo, 2013). In this study, the azaspiracids and the spirolides were detected for the first time in the cultured mussels of TSB, but the causative species associated with the accumulation of the toxins (*Azadinium spinosum* and *Alexandrium ostenfeldii*, respectively) were not identified. Due to the above, it is proposed to conduct the identification of potentially toxic species in Todos Santos Bay (Ensenada, BC) in field water samples using molecular and microscopy techniques, to confirm if the species that have reported in other regions as producers of azaspiracids and spirolides are the same that produces these toxins here. Besides, the monitoring of the environmental factors allows us to have more information about the distribution and temporality of these species in the TSB. These first records will be the background to put efforts in the future to monitor certain species and toxins of each season, also by the present study can be established whether a toxin and its producing species constitute a hazard in health or environment in the region.

1.5 Hypothesis

Alexandrium ostenfeldii and *Azadinium spinosum* are present in Todos Santos Bay, and these are the species responsible for the accumulation of the toxins in the cultured mussel from the bay.

The azaspiracids and *Az. spinosum* have seasonality in winter months related to low seawater temperature. Spirolides and *A. ostenfeldii* are higher during the summer season.

1.6 Objectives

1.6.1 General objective

- Evaluate the presence of potentially harmful dinoflagellate species in Todos Santos Bay (TSB) and relate them to the accumulated toxins in the mussels cultivated in the bay

1.6.2 Specific objectives

- Identify and characterize the dinoflagellate species of water samples collected in TSB through microscopic and molecular techniques.

- Quantify the toxins accumulated in mussel cultures of *Mytilus galloprovincialis* and relate them to the identified dinoflagellate species.

- Relate the environmental variables with the abundance and spatio-temporal distribution of the species.

- Isolate the potentially harmful dinoflagellate species to describe morphological characteristics and phylogenetic relationships.

Chapter 2. Association of toxigenic dinoflagellates *Alexandrium ostenfeldii* with spirolide accumulation in cultured mussels (*Mytilus galloprovincialis*) from Northwest, Mexico

2.1 Introduction

Spirolides are naturally occurring polyether cyclic imine compounds with a spiro-group attached to the tricyclic ethers. These toxins were first isolated from mussel digestive glands, and toxicity was determined by intraperitoneal mouse bioassay during chemical investigations of polar bioactive molecules from microalgae and shellfish from Nova Scotia (Canada) (Hu et al., 1995). The intact cyclic imine moiety is the pharmacophore that confers biological activity (Hu et al., 1996; 2001). Many spirolides, including those belonging to the A, B, C, D groups and their respective desmethyl derivatives, act as "fast-acting toxins" (FAT) characterized by rapid onset of neurological symptoms followed by death after intraperitoneal injection into mice (Cembella et al., 1999; Richard et al., 2001). Spirolides are not considered in the sanitary legislation for human consumption of shellfish since a toxic effect in humans has not been proven and no poisoning symptoms associated with these toxins have been confirmed (Otero et al., 2011). A few complaints of gastric distress and tachycardia were recorded after the consumption of mussels containing high spirolide concentrations, but these non-specific symptoms could not be definitively ascribed to spirolides (Richard et al., 2001). Cholinergic receptors (muscarinic and nicotinic) are proposed as the main targets for spirolides, and the toxic effects could be related to the activity of the toxin as irreversible antagonists of the muscarinic acetylcholine receptor (Gill et al., 2003) and weak L-type transmembrane calcium channel activators (Sleno et al., 2004).

Spirolides are coextracted in the methanolic extract of the regulated polyether shellfish toxins, such as okadaic acid, dinophysistoxins, azaspiracids, and yessotoxins. The FAT activity of spirolides in methanolic or lipophilic fractions can, therefore, interfere with and cause artifacts in the intraperitoneal mouse bioassay (Trainer et al., 2013). False toxicity positives associated with spirolides can cause unnecessary shellfish sanitary closures that will negatively affect economic activities for coastal aquaculture and harvest of wild shellfish.

The causative species associated with spirolide accumulation in cultured shellfish from Nova Scotia was identified as the mixotrophic dinoflagellate *A. ostenfeldii* (Paulsen) Balech and Tangen (Cembella et al., 2000a). This species is widely distributed in coastal waters around the globe (Cembella, 2018), from the coast of Washington State, USA (Balech, 1995), the northeastern coast of North America (Hargraves and Maranda, 2002), and including north Atlantic and sub-Arctic waters, as well as the

Mediterranean Sea and the brackish Baltic Sea (Suikkanen et al., 2013). Interest in the study of *A. ostenfeldii* and associated toxicity has increased due to the reports of coastal blooms of this species in the Peruvian coast (Sánchez et al., 2004), Narragansett Bay and the New River Estuary along the U.S. east coast (Borkman et al., 2012), and the Baltic Sea coast of Finland (Hakanen et al., 2012). Blooms of this species occurred recently in Oosterschelde, Netherlands, representing a significant concern for public health for poisonings associated with paralytic shellfish toxins, but these blooms were not related to human intoxication by spirolides (Van de Waal et al., 2015). The toxin regulatory situation is complicated by the fact that certain *A. ostenfeldii* populations can also produce other neurotoxins, such as paralytic shellfish toxins (PSTs), and/or the cyclic imines known as gymnodimines. The toxin composition and content of *A. ostenfeldii* depends upon genotypic strain differences and geographic origin (Suikkanen et al., 2013), and is therefore difficult to predict and assess.

The Pacific coast of North America from Alaska to Baja California is relatively underrepresented in studies of the biogeographical distribution of *A. ostenfeldii* and associated spirolides (Cembella, 2018). Todos Santos Bay (TSB), in the northwest of the Baja California peninsula, is the region with the highest production of cultivated mussels in Mexico (Maeda-Martínez, 2008). Sanitary closures have been implemented in the region due to the presence of lipophilic toxins in shellfish harvested from this bay. For the first time in 2012, the 13-desmethyl spirolide C was detected in the cultivated mussels in TSB during almost the whole year with no apparent temporal pattern of appearance (García-Mendoza et al., 2014). Unfortunately, the causative species associated with this spirolide accumulation in shellfish was not identified.

The inability to reliably identify the toxigenic species that produces spirolides is often associated with the complexity in the identification of *Alexandrium* taxa (Touzet et al., 2008), especially by morphological criteria alone. *A. ostenfeldii* has been detected and identified by polymerase chain reaction (PCR) probes involving specific primers to amplify the Internal Transcribed Spacer (ITS) of the rDNA gene (Schwarz, 2011). PCR of ITS regions represents a useful technique to unequivocally evaluate the presence of this species in the phytoplankton community.

The aim of this study was identity *A. ostenfeldii* in-field water samples to evaluate their temporal distribution in TSB as a causative agent for the accumulation of spirolides in cultivated bivalve mollusks from the TSB. The temperature of the water column was measured to relate it to the presence of the species in the Bay. For the identification of *A. ostenfeldii*, two techniques were employed, the PCR with specific primers and the morphological examination of cells by light microscopy. Also, the accumulated spirolides in cultivated mussels (*Mytilus galloprovincialis*) were

analyzed. The combination of these alternative techniques allowed the detection and confirmation of *A. ostenfeldii* in TSB and provided the first report of this species in the northwest Pacific of Mexico.

2.2 Materials and methods

2.2.1 Field samples

Todos Santos Bay (TSB), located on the northwestern coast of the Baja California peninsula, Mexico, is subject to a regular monitoring program for marine biotoxins in shellfish and associated toxigenic plankton by the FICOTOX laboratory of Centro de Investigación Científica y de Educación Superior de Ensenada, Baja California (CICESE). From July 2013 to June 2014 water and mussel samples were collected biweekly from the mussel cultivation area in TSB (St 13; Fig. 6). Water samples for taxonomic analysis and enumeration were collected at the surface and at 10 m depth with a 2 L Niskin bottle. In addition, plankton samples were analyzed from vertical net tows with 20 μm mesh plankton net conducted through the upper 20 m of the water column.

In 2016, the regular monitoring program of FICOTOX was extended to include evaluation of the phytoplankton community where caged tuna aquaculture is located in the region. From August 2016 to August 2017, plankton samples were analyzed from Salsipuedes Bay, where some tuna enclosures are located (St 1, 3, 4 and 6; Fig. 6). Sampling at St 13 continued throughout this period and two more stations (St 11 and 12; Fig. 6) in the southern sector of TSB were also monitored on a monthly. Water samples were collected with a 2 L Niskin bottle at the surface and at the thermocline. The vertical temperature profile of the water column was measured with a conductivity, temperature and pressure profiler (CTD, CastAway, YSI, Ohio, USA). The depth of the thermocline was determined from the temperature profile before the samples were collected.

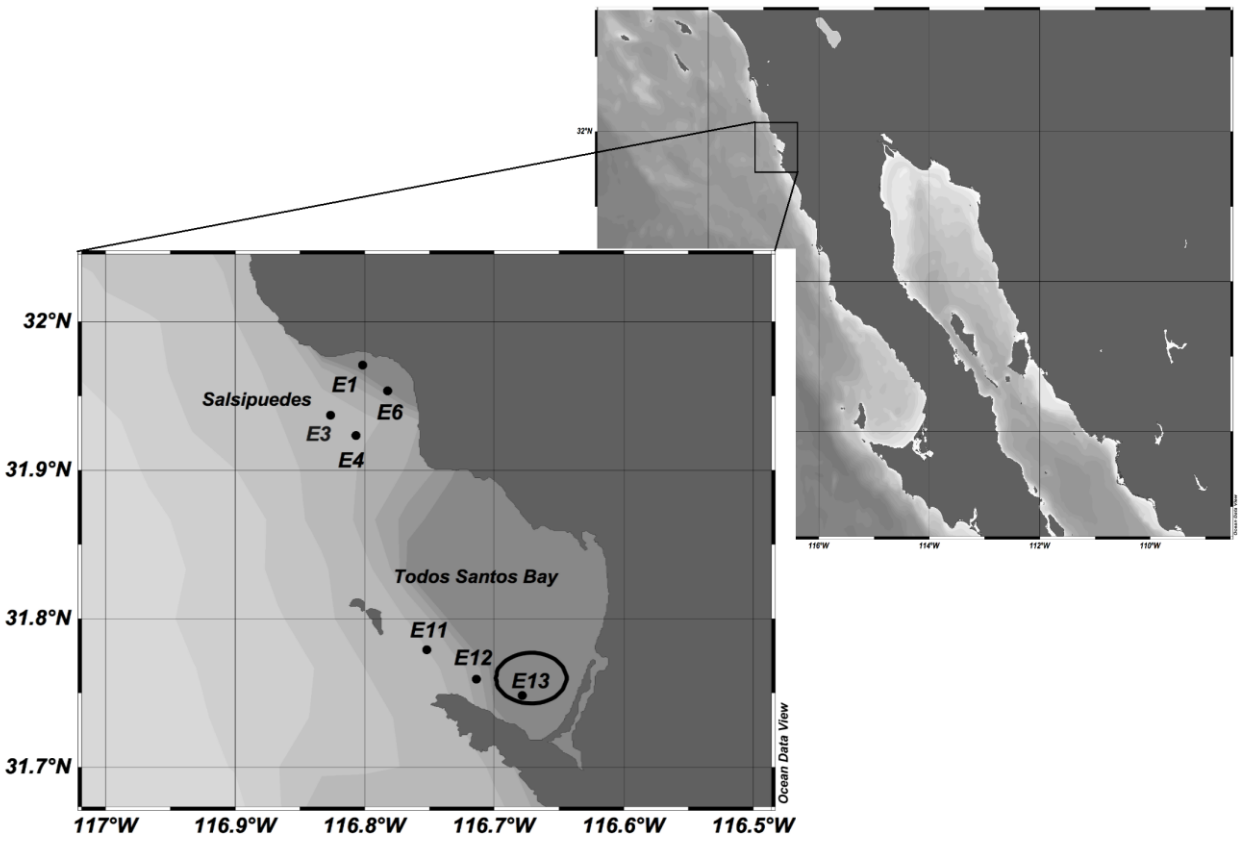

Figure 6. Sampling stations located in Todos Santos Bay (TSB) region. Station 13 enclosed in the circle is inside the mussel cultivation area.

2.2.2 Microscopic evaluation of *A. ostenfeldii* abundance

A 250 mL water subsample from the Niskin bottle was fixed with Lugol's iodine-acetate solution. These samples were analyzed with an inverted microscope (Leica DM13000B, Leica Microsystems, Wetzlar, Germany) according to the Utermöhl method (Lund et al., 1958). A 50 mL sample was sedimented and the complete surface of the sedimentation chamber was analyzed to quantify the cell abundance of *A. ostenfeldii*. For net samples only 10 mL were sedimented and the results were presented as the relative abundance (in %) of *A. ostenfeldii* to total phytoplankton cells collected with the 20 µm plankton net.

The thecal plate arrangement and morphology of cells considered provisionally as *A. ostenfeldii* was evaluated by epifluorescence microscopy. Fixed cells from seawater samples were separated by a capillary, and rinsed twice with deionized water to get rid of salts and residual Lugol's solution. Then, 4 µL of Fluorescent Brightener 28 (Sigma-Aldrich, St. Louis, MO, USA) at a concentration of 1 mg mL^{-1} was added to stain the cellulose thecal plates (Fritz and Triemer, 1985). Plate arrangement was

characterized under an Axio Imager A2 microscope system and digitally photographed with an AxioCam ICc 1 camera and Axiovision software (Carl Zeiss AG, Oberkochen, Germany).

2.2.3 Molecular identification of *A. ostenfeldii*

2.2.3.1 DNA extraction

Seawater (500 mL to 1 L) was filtered through 8 μm pore-size polycarbonate filters (Nucleopore, Whatman, Darmstadt, Germany), under gentle vacuum to avoid cell disruption. Filters were stored in a 50 mL centrifuge tubes at -80 °C until analysis. The DNA was extracted with a DNeasy Plant Mini kit (Qiagen, Hilden, Germany) according to the manufacturer's instructions but with modification of the volume of the lysis buffer to 600 μL. Homogenization of cells was performed with a mini-Bead Beater 24 (BioSpec Products, Bartlesville, United States) at maximum speed (6.5 m/s) for 45 s (Wohlrab et al., 2010), with 170 μm^3 of zirconium beads of 0.1 mm diameter to disrupt the cells. The DNA was resuspended in sterile Milli-Q water. The purity and concentration of DNA was measured by UV-spectroscopy with a NanoDrop 2000 (Thermo Scientific, Wilmington, USA) and the integrity of the DNA was verified on a 1.2% agarose gel via electrophoresis.

2.2.3.2 Polymerase Chain Reaction (PCR) amplification

The primers AOF4 (5'-TGTCAATGCGTGTGCATTCG-3') and AOR3 (5'-CATTGCAACCAATGCACATGA-3') were used for identification of *A. ostenfeldii* during the first monitoring period (2013 to 2014). These primers produce an amplicon of 99 bp of the ITS1, 5.8S and ITS2 region (Schwarz, 2011). The primers were originally designed specifically to differentiate *A. ostenfeldii* from *A. peruvianum* (4 bp), but *A. peruvianum* is now recognized as a heterotypic synonym of the former species (Kremp *et al*., 2014).

For identification of *A. ostenfeldii* in the second sampling period (2016-2017) the primers AOST213F (5'-GGGAAGGGTTGTGGTCATTAGTTA-3') and AOST213R (5'-TTGCCATGTAATTCATTCAGTCATT-3'), which produce an amplicon of 89 bp of the 18S region were used (Elferink et al., 2017).

PCR reactions (30 μL) were performed in a Veriti thermal cycler (Applied Biosystems, USA) using 100 ng of DNA. For ITS amplifications, the master mix was prepared with the following concentrations:

0.4 mM of each dNTP, 0.12 μM of each primer, 4 mM of $MgCl_2$, 1 X GoTaq® Flexi buffer (Promega, Madison, WI, USA), and 1.25 U of GoTaq® DNA polymerase. The PCR was carried out at 94 °C for 4 min, followed by 40 cycles of 94 °C for 30 s, 60 °C for 45 s, 72°C for 1 min, and a final extension step of 72 °C for 7 min.

For the 18S rDNA amplifications the master mix contained the following concentrations: 0.2 mM of each dNTP, 0.30 μM of each primer, 3 mM of $MgCl_2$, 1 X 1 X GoTaq® Flexi buffer (Promega, Madison, WI, USA), and 0.6 U of GoTaq® DNA polymerase. The amplification was carried out under the following conditions: 94 °C for 3 min, followed by 30 cycles of 94 °C for 30 s, 60 °C for 45 s, 72 °C for 1 min and a final extension step of 72 °C for 7 min. The amplicons were analyzed by electrophoresis on 2% agarose gel.

The specificity of the reaction was confirmed with a DNA template from a monoclonal reference culture of *A. ostenfeldii*. Strain CCMP 1773 was acquired from the Provasoli Guillard Center for Marine Microalgae (CCMP, Boothbay Harbor, ME, USA) and cultivated under optimal growth conditions at 15 °C and photon flux density of 100 μmol quanta m^{-2} s^{-1}. The DNA of this strain was used as a positive control. For the negative control the DNA was replaced with ultrapure water in the PCR reaction.

2.2.3.3 Sequences analysis

PCR products of ITS and 18S amplifications were sent for sequence analysis to SeqXcel, San Diego, CA, USA. The analysis of the sequences was carried out using the BLAST tool on the NCBI website and the sequence alignments were performed using the CLUSTAL X software (Thompson et al., 1997) and the BioEdit sequence alignment editor and analysis program (Hall, 1999).

2.2.4 Compositional analysis and quantification of spirolides

Spirolides were determined from particulate plankton by filtration of 300 to 800 mL seawater from the surface and thermocline through Nucleopore polycarbonate filters (3.0 μm pore-size; Whatman, Darmstadt, Germany) under low vacuum. Filters were stored in 50 mL centrifuge tubes at –70 °C until extraction. During extraction, filters were repeatedly rinsed with 1 mL 100% MeOH until complete discoloration of the filters. The methanolic extract was filtered through spin-filters (0.45 μm pore-

size; Millipore Ultrafree, Eschborn, Germany) and centrifuged for 30 s at 800×g. The filtrate was transferred to an autosampler vial and 5 µL were injected into the LC-MS/MS system. The protocol for the detection of spirolides was as described by Krock et al. (2008) for lipophilic toxins. Toxin analyses were performed on a liquid chromatograph (Agilent 1100, Waldbronn, Germany) coupled to triple-quadrupole mass spectrometer (ABI-SCIEX-4000 Q Trap, Applied Biosystems, Darmstadt, Germany) equipped with a Turbo V ion source. Separation of the lipophilic toxins was performed by reverse-phase chromatography on a C8 column (50 mm X 2 mm) packed with 3 µm Hypersil BDS 120 Å (Phenomenex, Aschaffenburg, Germany). The mobile phase comprised two eluents, where eluent A was water and eluent B was acetonitrile-water (95:5 v:v), both containing 2.0 mmol L^{-1} ammonium formate and 50 mmol L^{-1} formic acid. The limit of detection for SPX-1 (13-desmethyl spirolide C) was 0.3 ng mL^{-1}, determined with reference to an external standard solution of 10 ng mL^{-1} SPX-1 obtained from the CRMP, IMB, National Research Council, Halifax, Canada.

Spirolides in mussels from the cultivation area at St 13 were determined from whole mussel samples provided by Acuacultura Oceanica Co., Ensenada, BC, Mexico. Evaluation of lipophilic toxins in mussels was performed according to the standardized procedure of the European Union for the determination of marine lipophilic biotoxins in molluscs (EURLMB, 2011). Complete soft tissues of at least 20 commercial-size mussels were homogenized for the determination of phycotoxins. Toxin extraction was performed with 100% methanol on 2.0 ± 0.01 g of shellfish tissue (EURLMB, 2011). The detection and quantification of lipophilic phycotoxins was performed with the analytical methodology of liquid chromatography coupled to a tandem mass spectrometer (LC-MS/MS). A triple quadrupole Thermo Scientific TSQ Quantum Access Max LC-MS/MS system (San Jose, USA) was used for analysis of mussel samples collected from July 2013 to June 2014, according to the method of Martín-Morales et al. (2013). After extraction, an aliquot of the methanolic extract was filtered through a 0.22-µm-syringe filter and 5 µL were injected into the LC-MS/MS system. The mass spectrometer was operated in positive-ion mode by multiple reaction monitoring (MRM). The Regueiro et al. (2011) method was employed for chromatographic separation with minor modifications for use of a shorter column. Chromatography was performed in reverse-phase mode with a Gemini-NX C18 (Phenomenex,Torrance, USA) (50 x 2 mm; 3 µm) analytical column. The mobile phase was described by Gerssen et al. (2009) to yield alkaline chromatographic conditions; phase A = ammonium hydroxide 6.7 mM, phase B = acetonitrile in ammonium hydroxide 6.7 mM in proportion 9:1 (v:v). A calibration curve of four concentration levels of a certified solution obtained from CIFGA (Lugo, Spain) was used to quantify 13-desmethyl spirolide C. The limit of detection of the method was 0.04 ng mL^{-1}.

For the mussel samples from 2016-2017, toxin analyses were performed by the method of Krock et al. (2008), as described above for analysis of spirolides in plankton samples. An aliquot of methanolic extract of mussel tissue was transferred to a spin-filter (pore-size 0.45 µm; Millipore Ultrafree, Eschborn, Germany) and centrifuged for 30 s at 800×g. The filtered sample was transferred to an autosampler vial and 5 µL were injected into the LC-MS/MS system.

2.3 Results

2.3.1 Occurrence of *A. ostenfeldii* in Todos Santos Bay

Light microscopic analysis of the phytoplankton community in 134 water samples collected from August 2016 to August 2017 revealed that *A. ostenfeldii* occurred in 20.9% of the samples. The species was detected in the same number of samples from the surface and the thermocline, indicating that *A. ostenfeldii* was present throughout the mixed layer. Nevertheless, the cell abundance was higher at the surface than at the thermocline. There was no apparent seasonality for the species presence and the low cell abundances did not allow the definition of a clear pattern. The only discernible trend was the low cell abundance during the winter (November – February) when cell densities were consistently low or below the detection limit (Fig. 7A and B).

At the surface, *A. ostenfeldii* was detected at all stations except St 4, but at low abundance during the sampling period (Fig. 7A). The maximum abundance of 480 cells L^{-1} was registered at St 6 (Salsipuedes) at the end of September 2017 (Fig. 7A). A relatively high abundance of 400 cells L^{-1} in June 2017 and 240 cells L^{-1} at the beginning of March 2017 were also recorded from St 11 (Rincón de Ballenas). The species was not observed at the thermocline from St 6 and at the other stations the abundance was low (20 to 80 cells L^{-1}) or absent (Fig. 7). The highest abundance of *A. ostenfeldii* in the thermocline was 353 cells L^{-1} detected at St 11 in June (Fig. 7B). An abundance of 160 cells L^{-1} was found at the end of September from the same station.

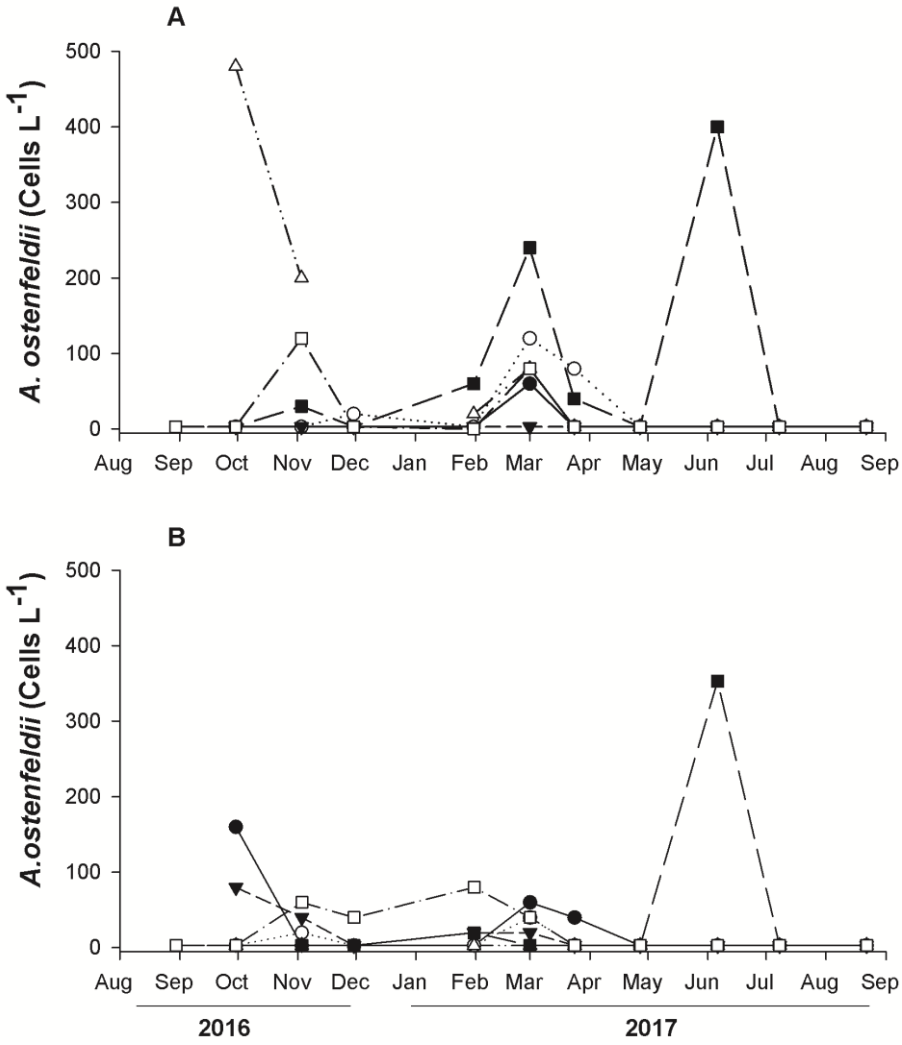

Figure 7. Temporal variation of cell abundance of *A. ostenfeldii* at seven sampling stations located in Todos Santos Bay region: Station 1 (closed circles), Station 3 (open circles), Station 4 (closed triangles), Station 6 (open triangles), Station 11 (closed square) and Station 12 (open square). Samples were collected at surface (**A**) and at the thermocline (**B**) from August 2016 to August 2017.

2.3.2 Morphological characterization of *A. ostenfeldii*

The cells of *A. ostenfeldii* presented a globose appearance with slightly rounded margins (Fig. 8A and G). The theca is very thin and not easily detected with light microscopy (Fig. 8H). The specimens from TSB were typically observed as solitary cells varying in size from 25 to 35 µm in diameter. In some water samples, both vegetative cells and cysts were found (Fig. 8I). The cingulum is equatorial and slightly excavated with no presence of cingular lists (Fig. 8B and C). The hypotheca and epitheca have the same height. The tabulation of the cells is typical of *A. ostenfeldii* showing an insert-type tabulation characterized by the contact of the plate 1' with 1'', 6''', 2', 4' and the apical pore complex APC (Fig. 8B and C). This complex is completely occupied by a big comma-shaped pore (Fig. 8B). The sixth precingular plate (6'') is wider than tall. The 1' plate is elongated and asymmetric, with a

prominent ventral pore in the inflection. The sulcal plate series is clearly distinguished. The key plate for describing the sulcus is S.p. This plate contacts with s.d.p, s.sp, 5’’’, 4’’’, 2’’’’ and 1´´´´´ (Fig. 8D and E).

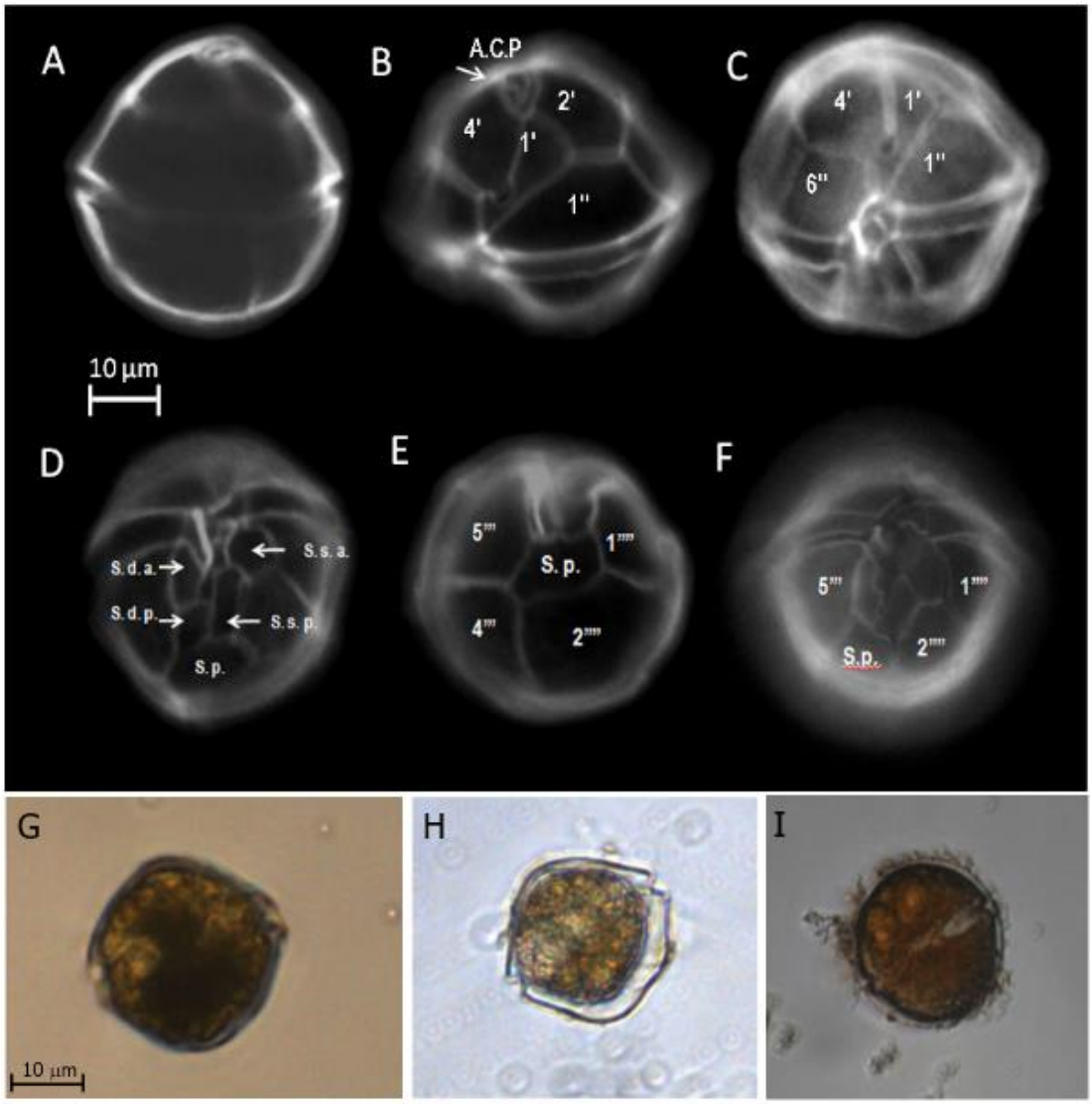

Figure 8. Morphological characteristics of *Alexandrium ostenfeldii* collected in water samples from Todos Santos Bay region. The cells were stained with calcofluor to evaluate the thecal plate arrangement with epifluorescence microscopy. (**A**) shape of the cells; (**B**) apical pore complex (APC) complex occupied by a prominent comma-shaped pore; (**C**) first precingular (1’) plate with a ventral pore; (**D**) ventral view showing the sulcal plates; (**E**) antapical view showing the sulcal posterior plate; (**F**) ventral view; (**G** and **H**) vegetative cells observed by inverted optical microscopy; (**I**) presence of cysts in the water samples.

2.3.3 Molecular identification of *A. ostenfeldii*

Molecular identification of *A. ostenfeldii* was conducted on 57 samples analyzed by PCR from the south of TSB (Rincón de Ballenas, St 13), where mussel farms are located. With the AOF4 and AOR3

primers, the 99 bp ITS fragment was detected in 52.6% of the samples collected from July 2013 to June 2014, confirming the presence of *A. ostenfeldii* in the study area. As expected, given the higher plankton biomass collected among the three alternative samples (at surface, from 10 m depth and vertical net haul) the highest number of positive results (68.4%) were obtained from net haul samples, figure 4 shows an example of the PCR results. The expected size amplicon was detected in all three fractions of samples from April 8, 2014, collected at the surface, from 10 m and by net haul (Fig. 9), suggesting that this species was present throughout the mixed layer of the water column. In contrast, the absence of an amplicon in the samples from April 22, 2014, indicates that *A. ostenfeldii* was not present on this date (Fig. 9).

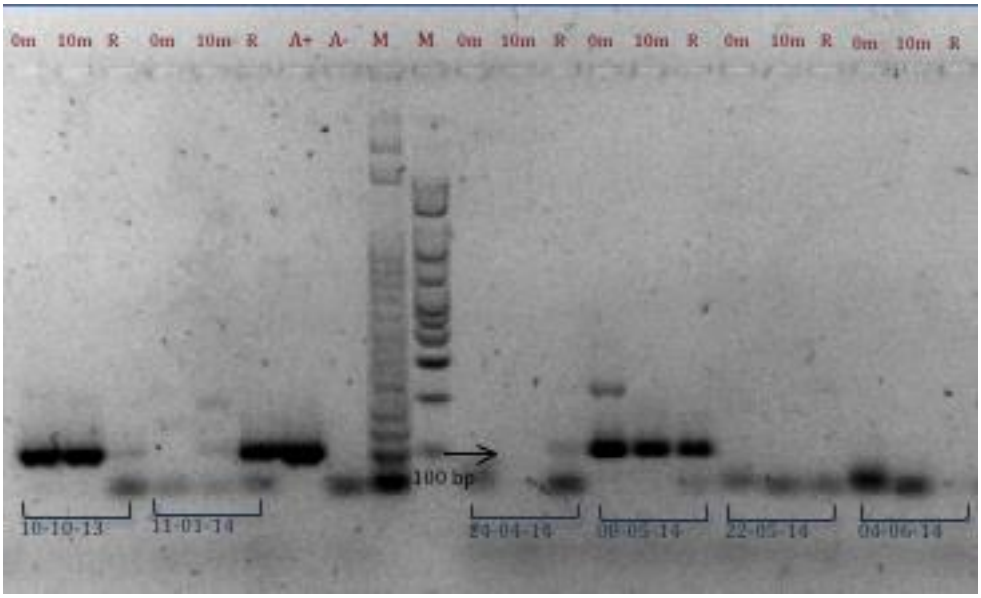

Figure 9. PCR amplification of samples from Station 13 using AOF4 and AOR3 primers. The 99 bp ITS fragment indicates the presences of *A. ostenfeldii*. Results of samples collected at different dates are presented (October 10, 2013; November 1, 2014; April 24, 2014; May 8 and 22, 2014 and June 4, 2014). Samples were collected at 0 and 10 m discrete depth in the water column and by vertical phytoplankton net tows (R). A+: positive PCR control and A-: negative PCR control. M: molecular marker of 50 and 100 bp bioline.

The samples collected from August 2016 to August 2017 at seven stations and analyzed by PCR with the alternative primers AOST213F and AOST213F also confirmed the presence of *A. ostenfeldii* within the TSB region. The 18S amplification fragment of 89 bp was detected in 23.7% of 156 samples processed. For example, in samples of March 1, 2017, the expected amplification fragment was observed in samples from all stations, except in the surface sample from St 4, St 6 at the thermocline, and from St 13 at both surface and thermocline (Fig. 10).

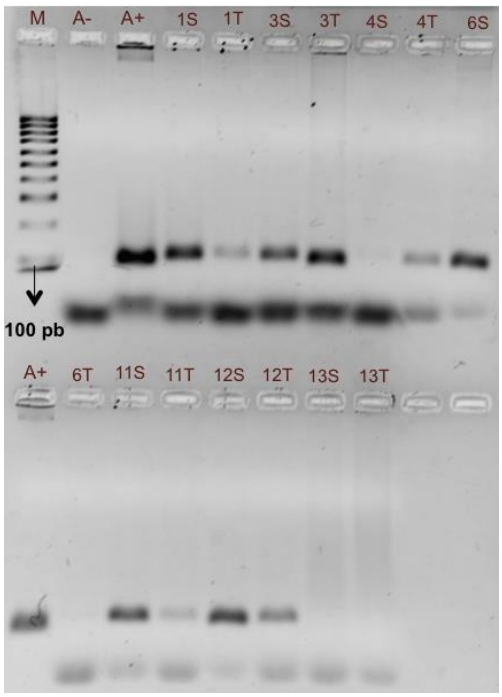

Figure 10. PCR amplification of samples from seven different stations in Todos Santos Bay region using AOST123F and AOST123R primers. The 89 bp fragment indicates the presence of *A. ostenfeldii*. Results of samples collected on March 1, 2017 are presented. The samples were collected at surface (S) and thermocline (T) in the water column. A+: positive PCR control and A-: negative PCR control. M: molecular marker of 100 bp bioline.

A. ostenfeldii was detected in 70.5% of the 213 samples from the two sampling periods analyzed by PCR and light microscopy. The PCR method yielded a higher positive detection (by 26.7%) compared to light microscopy. In contrast, PCR results were negative for only 1.88% of the samples in which *A. ostenfeldii* was registered by light microscopy.

PCR products were sequenced, the alignments and blast analysis conducted with the 99 bp ITS fragment sequence from the sample of August 8, 2013 (St 13) showed 98% identity with *A. ostenfeldii* sequences found in the NCBI GenBank (JX841278.1).

The phylogeny of *A. ostenfeldii* based on the ITS molecular marker was built with 30 nucleotide sequences of 99 bp long. The phylogenetic tree was inferred using the Maximum Likelihood method based on the Hasegawa- Kishino-Yano model. The initial tree for the heuristic search was obtained by Neighbor-Join. Nodal support was estimated by bootstrap analyses with 1000 replicates (Epstein, 1985). The sequences of *A. ostenfeldii* used to build the tree, were obtained from the water samples, the strain of TSB formed a cluster with the Northeast Pacific strain from Canada, and was closely related with the *A. peruvianum/ostenfeldii* strain from the Southeast Pacific (Peru) (Fig. 11). In the

neighbor branch are the strains isolated from Denmark. The outgroup species were *A. tanatum*, *A. lusitanicum* and *A. minutum*.

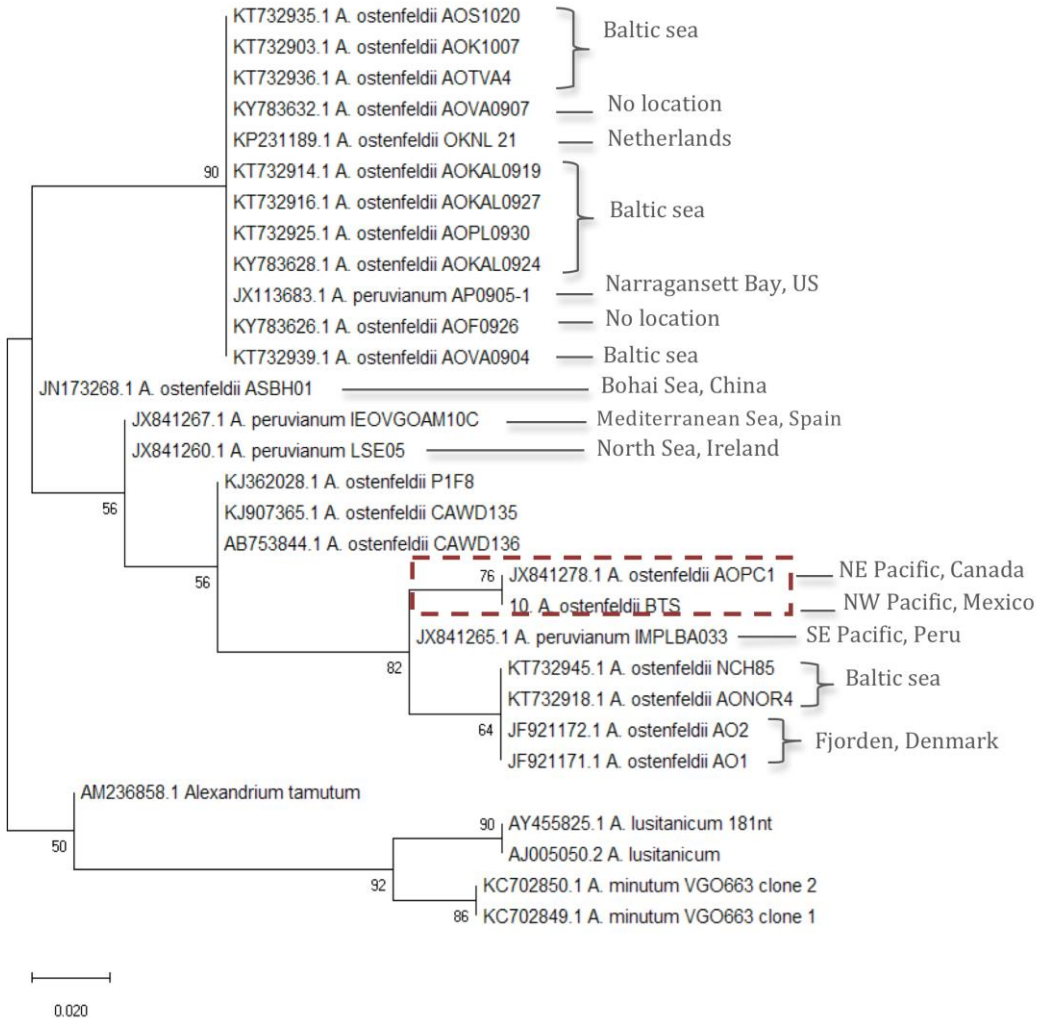

Figure 11. Phylogenetic tree of *A. ostenfeldii* based on the maximum likelihood internal transcribed spacer (ITS) rDNA sequences. The numbers in the left of the branches are statistical support values (values < 50 are not shown).

2.3.4. Spirolide detection in plankton and mussels

The presence of spirolide was confirmed in mussel samples collected at Rincón de Ballenas (St 13), but the analog 13-desmethyl spirolide C was the only analog detected by LC-MS/MS in mussels. The chromatogram presented in Fig. 12 shows the quantitative detection of 13-desmethyl spirolide C in a mussel sample of September 2014. The retention time (RT) (4.25 min) of the 164 *m/z* ion that coincided with the RT of the 695.501 to 444.30 *m/z* transition used as the confirmatory ion for 13-desmethyl spirolide C. The chromatogram of analogs 13-19 didesmethyl spirolide C and the spirolide

B are also presented in Fig. 12, but these analogs were not detected in mussels; the corresponding signals for these analogs were absent or below the detection limit and/or the retention times did not align with those of the expected transitions.

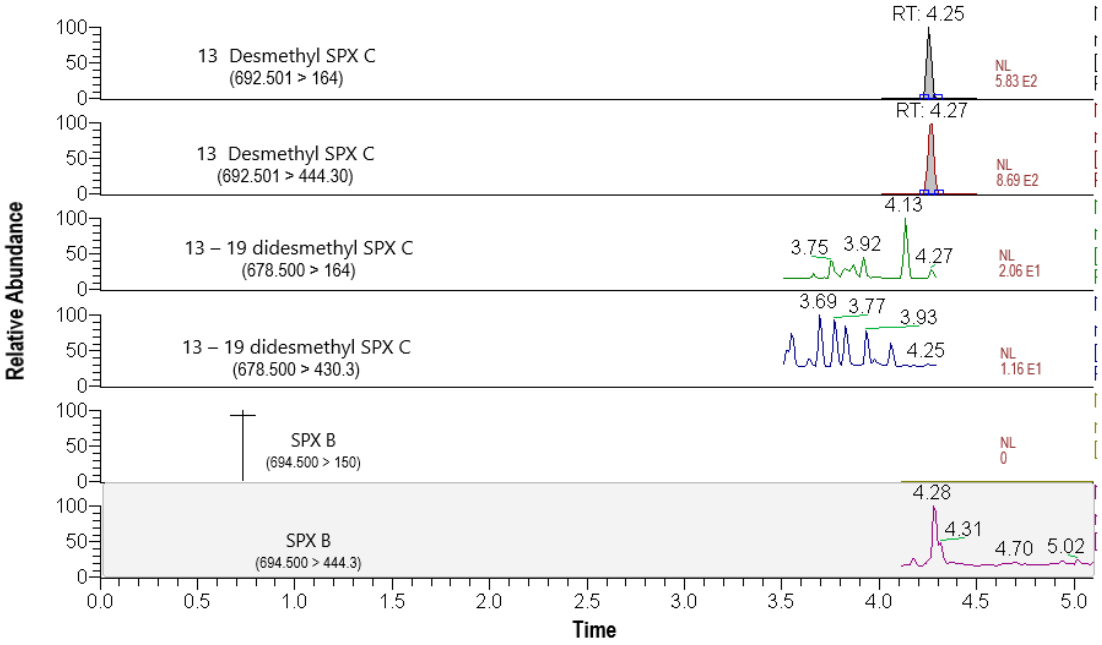

Figure 12. LC-MS/MS chromatograms (in MRM mode) of 13-desmethyl spirolide (SPX) C transitions (692.501 > 164 *m/z* and 692.501 > 444.30 *m/z*). Mass transitions of 13-19-didesmethyl spirolide (SPX) C and spirolide (SPX) B are also shown but were not detected in this sample of Mediterranean mussels (*M. galloprovincialis*) from Todos Santos Bay collected on September 12, 2014.

The cell abundances of *A. ostenfeldii* detected in Rincón de Ballenas area (St 13) at the surface and 10 m or the thermocline depth were compared with the spirolide accumulation in cultivated mussels (Fig. 13). *A. ostenfeldii* was detected in 50% of the samples during the first sampling period from July 2013 to June 2014. The species was heterogeneously distributed from surface to 10 m depth since the detection and abundances coincided in samples from both depths. There was no clear seasonality pattern of occurrence for *A. ostenfeldii* or for the spirolides in mussels. The cell abundance of *A. ostenfeldii* varied throughout the sampling period of 2013–2014 (from 0 to 3.6 x 10^3 cells L^{-1}). Nevertheless, these variations are not reflected in the concentration of 13-desmethyl spirolide C in mussels, which varied from below the detection limit (0.04 µg kg^{-1}) and remained <1.05 µg kg^{-1} throughout the sampling period (2013-2014) (Fig. 13). The maximum *A. ostenfeldii* cell abundance was found in October 2013 (3.62 x 10^3 and 3.59 x 10^3 cells L^{-1} in surface waters and at 10 m depth, respectively); the concentration of 13-desmethyl spirolide C was 0.54 µg kg^{-1}. In the second sampling period from August 2016 to August 2017, *A. ostenfeldii* was absent from all samples, except

for a sample obtained at the end of August 2016 (280 cells L^{-1}) at the thermocline. According to the LC-MS/MS results, the concentration of 13-desmethyl spirolide C remained below the detection limit in most of the samples, therefore, no spirolides were detected in the 154 samples of plankton particulate matter.

Certain populations of *A. ostenfeldii* are capable of producing PSP toxins (saxitoxin and derivatives) in addition to or instead of spirolides (Cembella, 2018). As a confirmation, for three samples (from July 8, 2013; August 22, 2013; October 10, 2013) where the cell abundance of *A. ostenfeldii* was high, but the concentration of spirolides in mussels was low, analysis of PSP toxins was carried out on mussels samples. No PSP toxins were detected in these samples.

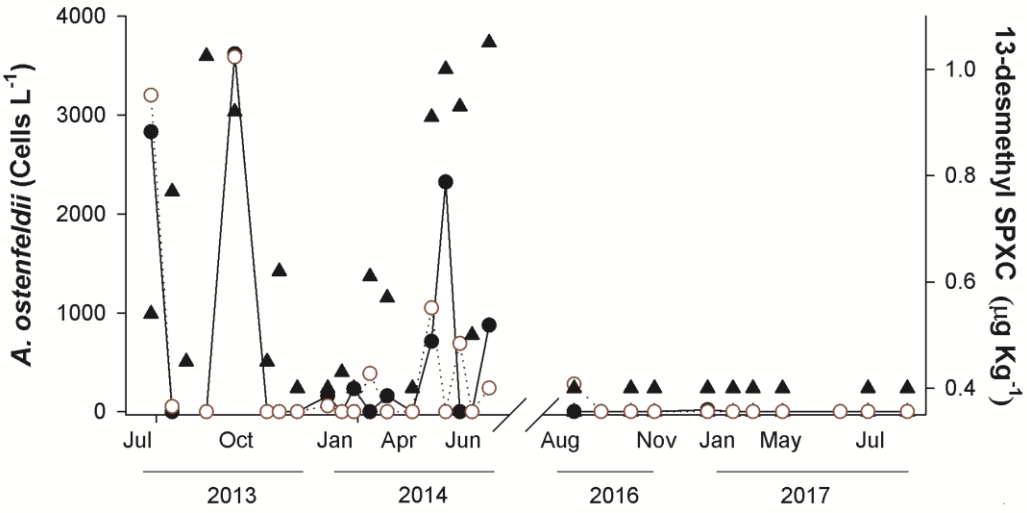

Figure 13. Concentration of 13-desmethyl spirolide (SPX) C (closed triangles) in the Mediterranean mussel *Mytilus galloprovincialis* collected from July 2013 to June 2014 and from August 2016 to August 2017 in Rincón de Ballenas (Todos Santos Bay). The abundance of *A. ostenfeldii* cells at surface (closed circles) and 10 m or thermocline depth (open circles) is also shown.

2.3.5 Water temperature associated with the presence of *A. ostenfeldii*

In an attempt to establish trends of *A. ostenfeldii* cell abundance in relation to water temperature, water temperatures at surface, 5 m and 10 m depth at St. 13 are presented together with *A. ostenfeldii* cell abundance during July 2013 to June 2014 and from August 2016 to August 2017 (Rincón de Ballenas) (Fig. 14). The highest cell abundance of *A. ostenfeldii* was associated with temperatures between 17 to 20 °C (Fig. 14). From 2013 to 2014, the maximum surface temperature of 22.1 °C was registered in September 2013. The water column was stratified as evidenced by a decrease of 5 °C from surface waters at 5 m (17 °C) and 8 °C at 10 m depth (14 °C). Under these

conditions, *A. ostenfeldii* was not detected. Abundance of *A. ostenfeldii* was <500 cells L^{-1} during the winter period with lower water temperature (November to April 2013-2014). Strong water stratification was present during the period 2016 – 2017, with a decrease of 8.5 °C from the surface to 10 m depth. During this period, a higher maximum surface temperature of 22.9 °C was detected in August 2016 and August 2017. The species was not detected during this period (Fig. 14). When the water column was homogeneous for temperature and during periods of lower water temperature between November 2013 and April 2014 cell abundance was reduced or remained below detection.

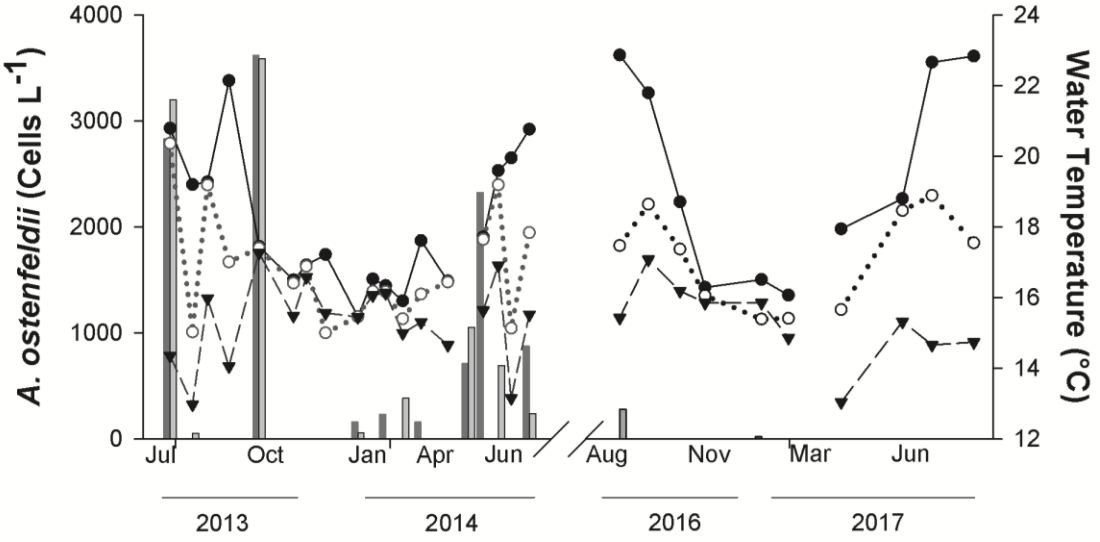

Figure 14. Temperature at surface (closed circles), 5 m (open circles) and 10 m depth (closed triangles) at Station 13 (Rincón de Ballenas) in Todos Santos Bay. The cell abundance of *A. ostenfeldii* in samples at surface (dark grey bar) and 10 m or thermocline (light grey bar) is also presented.

Bioassays were performed to analyze the effect that environmental factors like the temperature and irradiance have on the toxin production, then we worked with a strain isolated in Netherland (AON-13), the only strain so far that can produce spirolides, gymnodimines and PSP toxins. The results of these experiments are shown in the supplementary material.

2.4 Discussion

2.4.1 Dynamics of *A. ostenfeldii* in Todos Santos Bay

The dinoflagellate *A. ostenfeldii* was found in TSB with variable abundances and as a common

component of the phytoplankton community, but this species did not exhibit a clear seasonal occurrence pattern during the sampling period. The maximum cell density (3 x 10^3 cells L^{-1}) registered at St 13 during late summer to fall 2013 was typical for this species from coastal North Atlantic waters and Scandinavian fjords. In such low water temperature and moderate salinity environments the species tends not to form high biomass blooms, but rather is commonly found as a non-dominant component of the phytoplankton community at low maximal cell abundances ranging typically from 10^2 to 10^3 cells L^{-1} (Balech and Tangen, 1985; Moestrup and Hansen, 1988; Gribble et al., 2005). For example, *A. ostenfeldii* in coastal waters of Nova Scotia tends to form sub-surface aggregations at relatively low cell abundances of less than 4 x 10^3 cells L^{-1} (Cembella et al., 2001). In Casco Bay, along the Gulf of Maine, USA, a maximum abundance of 244 cells L^{-1} was registered during June 2001 (Gribble et al., 2005). These low abundances contrast with the high bloom concentrations reported from certain locations in northern Europe, typically characterized by a low salinity regime. Maximum cell abundances as high as 2.1 x 10^5 cells L^{-1} have been recorded from the coast of Finland in the northern Baltic Sea (Hakanen et al., 2012) and in the virtually freshwater Ouwerkerkse Creek, Netherlands, an extreme bloom of *A. ostenfeldii* yielded maximal cell densities of 4.5 x 10^6 cells L^{-1} (Van de Waal et al., 2015). In any case, the association of extreme blooms of *A. ostenfeldii* with low salinity environments is clearly not applicable to seasonal dynamics of this species in TSB. In comparison with habitats of *A. ostenfeldii* in the North Atlantic, TSB represents an environment characterized by higher seasonal surface water temperatures but only slightly higher salinity, which does not vary dramatically on an annual basis.

Temperature is one of the most important environmental variables that determine the biogeography of phytoplankton species (Butterwick et al., 2005), and which has a direct physiological influence and consequences on metabolic rates and hence growth rate (Anderson, 1998). Suggesting a possible regulatory role of temperature in determining the temporal distribution of *A. ostenfeldii* in TSB. In spite of the lack of a definitive seasonal cell abundance pattern, and absence of a clear relationship between the presence of *A. ostenfeldii* and the ambient temperature, the species was not present in the water column during the winter. The cell abundance of *A. ostenfeldii* in TSB decreased from August 2016 to August 2017 to the comparable period in 2013 to 2014, which indicates that the temporal cell distribution and abundance may be related to prior temperature anomalies. Under this scenario, a low cell abundance of *A. ostenfeldii* could be related to shifts in the phytoplankton community associated with the abnormally warm water conditions in the region, which initiated three years before 2016, associated with El Niño events, with temperature anomalies above 3 ^{o}C (Garcia-Mendoza et al., 2018). These anomalies were accompanied by low phytoplankton biomass. In the California Current System status report, these changes are also described for the phytoplankton community, for which the productivity and cell concentrations of diatoms were below average for

the southern California coast during 2016 (McClatchie et al., 2016). Jacox et al. (2017) reported that the water temperature anomalies caused changes in the structure and composition of the phytoplankton community, perhaps disadvantageous to *A. ostenfeldii*, while favoring an increase in cell abundances of species better adapted to these conditions. These warm water conditions recorded in TSB in the last few years have caused blooms of other genera such as *Cochlodinium* and *Chattonella* that had been previously registered only in low densities in the bay.

A. ostenfeldii is often considered a "cold-water" species, but "blooms" (or at least maximal cell abundance) consistently occur during the warm period of the annual cycle in the respective environments. In TSB, two peaks of high cell abundance were detected in October, 2013 and May, 2014, when the surface water temperature was 17 °C, but also when surface water was around 20 °C. These results suggest an optimal temperature range of 17 – 20 °C for *A. ostenfeldii* in TSB. By comparison, massive blooms of *A. ostenfeldii* in the northern Baltic Sea occurred at water temperatures close to 20 °C (Hakanen et al., 2012). In Narragansett Bay, Gulf of Maine, USA, maximum cell abundances were found within a temperature range from 14.0 to 17.0 °C and the species (cited as synonym *A. peruvianum*) was not detected from the water column during autumn when the temperatures were between 13 to 17 °C (Borkman et al., 2012). In contrast, in the Beagle Channel, Argentina the species was recorded at lower temperatures (7.5 – 10 °C) during austral spring (Almandoz et al., 2014). The fact that *A. ostenfeldii* is globally distributed (Cembella, 2018) indicates that temperature-adapted variants are common and that comparisons of temperature tolerance ranges among geographically separate populations are not strictly valid.

Due to the increasing global temperature, the surface ocean is anticipated to become more stratified (Stocker et al., 2013). Garneau et al. (2011) recorded the maximum cell abundance for *A. catenella* in summer-autumn along the coast of Oregon and northern California, during the dry season (reduced freshwater runoff) with weak upwelling and low nutrients in surface waters. Stratification of the water column forming a superficial stable layer may favor the growth of *Alexandrium* over other phytoplankton species during low nutrient conditions in this stratified layer (Horner et al., 1997). Under such circumstances, the influence of the ambient water temperature on the temporal and spatial distribution of *A. ostenfeldii* may also be indirect, via contribution to stratification of the water column. More stratification of the water column should favor the growth and persistence of species such as *A. ostenfeldii*, a facultatively mixotrophic dinoflagellate with vertical migration capabilities. This interpretation is consistent with the evidence that cells were absent from the water column at TSB during winter (the 2013 – 2014 monitoring period) and remained <500 cells L^{-1} during 2016 – 2017 when the water column was well mixed and homogeneous. Yet a simple association of *A. ostenfeldii* with high stratification is not supported by the data on the apparent lack of cells in the

upper water column during August 2016, during a period of high surface water temperature (22.9 °C) and strong stratification.

Nutrients are known to influence the dynamics of phytoplankton communities in rivers, estuaries, and coastal zones (Anderson et al., 2002). In the same way, inorganic macronutrients could directly influence the growth of *A. ostenfeldii* but there were no massive blooms recorded during the sampling periods in TBS. Furthermore, the high mixotrophic potential of this species renders it unlikely that inorganic macronutrient concentrations were directly correlated with or driving cell growth or biomass yield in TSB. This suggestion agrees with both Collos et al. (2007) and Brandenburg et al. (2017) who reported that the proliferation of cells of *Alexandrium* species was independent of the inorganic nutrient concentrations because of mixotrophic feeding of the species. During a bloom in the Baltic Sea, the abundance of *A. ostenfeldii* cells was related with warm water, but was not significantly correlated with dissolved inorganic nutrient concentrations, however, nutrient concentration was related to the high concentration of resting cysts in the sediment (Hakanen et al., 2012).

2.4.2 Species detection and identification

The presence of *A. ostenfeldii* in TSB was independently confirmed by both light microscopy and positive PCR assays applied to 213 field samples during the two multi-annual periods. There were significant discrepancies between the results of the alternative methods, e.g., the molecular approach yielded 27.6% higher positive detection of the species than microscopy. By comparison, positive registration of toxic dinoflagellate species in the Mediterranean Sea by microscopy did not coincide with the detection of the species by PCR. These differences were especially evident with members of the genus *Alexandrium*, and varied among species; the PCR method gave 38% higher detection for *A. catenella*, 36% for *A. minutum* and 20% for undefined *Alexandrium* species (Penna et al., 2007).

These discrepancies are related to differences in cell detection limits for the respective methods. The nominal detection limit of the Utermöhl method is 20 cells L^{-1} in a sedimentation volume of 50 mL when the whole chamber is counted (Edler and Elbrächter, 2010). In comparison, with a reported PCR amplification with 1 pg of genomic DNA for *Alexandrium* (Penna et al., 2007) and an estimated 115 pg per cell nuclear DNA content for *A. ostenfeldii* (Kremp et al., 2009), it is then theoretically possible to detect a single cell of this species in a field sample by PCR technique. Therefore, the

possibility of detecting species that are poorly represented in the phytoplankton community, like *A. ostenfeldii,* increased significantly due to the use of the PCR technique.

In a few cases (1.88%), *A. ostenfeldii* cells were identified from TSB samples by microscopy but were not detected by PCR. This may be attributable to the misidentification of *Alexandrium* taxa due to the difficulty of morphological discrimination among closely related species within this genus (Touzet et al., 2009; Cembella, 2018). In TSB, *A. ostenfeldii* may be present in different life history (vegetative cells, gametes, zygotes) and growth stages of variable morphology. Furthermore, other species of *Alexandrium* genus, such as *A. catenella* (Peña-Manjarrez, 2005), may be present in TSB, and could be misidentified as *A. ostenfeldii* in the absence of critical taxonomic analysis.

2.4.3 Accumulation of spirolides in mussels

The dinoflagellate *A. ostenfeldii* was likely responsible for the accumulation of spirolides in mussels collected in the TSB region during 2012 (García-Mendoza et al., 2014). Among the diverse structural sub-types and known analogs of spirolides, only 13-desmethyl spirolide C was detected in cultivated mussels from TSB. This result indicates that *A. ostenfeldii* populations in the region produce primarily or exclusively this spirolide analog and not other toxins such as paralytic shellfish toxins (PSTs) associated with certain *A ostenfeldii* strains from global locations. In a phylogenetic study comparing multiple *A. ostenfeldii* strains from widely biogeographically distributed populations, six groups were defined that cluster genetically and according to toxin profile (Kremp et al., 2014). Group 1 strains produce both 13-desmethyl spirolide C and PSTs (Van Wagoner et al., 2011). In contrast, Group 2 members produce mostly or exclusively 13-desmethyl spirolide C (Franco et al., 2006; Touzet et al., 2008). The strain present in TSB, therefore, seems to belong to this latter group, the toxin profile and the phylogenetic analysis with Maximum Likelihood tree cluster with Group 2. Populations of *A. ostenfeldii* Group 2 have been registered mainly from eastern Canada, northeast USA, Spain and Irish coasts (Cembella et al., 2000b; Mackinnon et al., 2004; Percy et al., 2004). However, it is necessary to isolate local strains to characterize their toxin profile and to confirm their phylogenetic relationships with other populations of *A. ostenfeldii*. Besides, it is essential to evaluate the toxin content of vegetative cells and cysts since this might influence the concentrations of spirolides in mussels.

From 2013 to 2014 13-desmethyl spirolide C was detected in 78.9% of the samples analyzed. There was no apparent seasonality in the presence of this toxin, as typified by the time-series data from 2012 when 13-desmethyl spirolide C was detected in most (80%) of the mussel samples analyzed and

was present all year long without a clear pattern of appearance (García-Mendoza et al., 2014). In contrast, during the period from 2016 to 2017, 13-desmethyl spirolide C was below the detection limit, and this was related to the absence of the causative species.

Concentrations of 13-desmethyl spirolide C in this study were lower than the concentrations recorded in shellfish from other regions. In Catalonia, NW Mediterranean Sea, 2 to 16 µg kg^{-1} of 13-desmethyl spirolide C was detected in mussels and oysters (García-Altares et al., 2014). In shellfish samples from the Chinese coast, the highest concentration of 13-desmethyl spirolide C was 8.96 µg kg^{-1} (Wu et al., 2015) and in Norwegian blue mussels, the concentration of this toxin reached 226 µg kg^{-1} (Rundberget et al., 2011). The concentration of this spirolide previously reported in mussels from TSB was higher during the year 2012 (3 µg kg^{-1}) (García-Mendoza et al., 2014) than recorded in this present study (1.05 µg kg^{-1}).

In July, 2013 among the highest abundance for the species was recorded (2.8 and 3.2 x 10^3 cells L^{-1}), but the concentration of the 13-desmethyl spirolide C was low (0.54 µg kg^{-1}). The toxin cell quota is variable and dependent upon environmental conditions; the physiological state of the cell and the growth phase influence the cellular concentration of the toxin (Boczar et al., 1998; Anderson et al., 2012a). This variability could explain the fact that even though one of the highest abundance of *A. ostenfeldii* was recorded and the presence of the species was confirmed by PCR, the concentration of 13-desmethyl spirolide C was near the detection limit. Environmental conditions during this sampling period could influence the spirolide production in *A. ostenfeldii* present in the bay, and this could explain why there was not a clear correlation between the abundance of the species and the accumulation of spirolide in mussels.

At the end of August, 2013 and the middle of September 2013 *A. ostenfeldii* was not detected in the water samples, but one of the highest concentrations of 13-desmethyl spirolide C in this study (1.02 µg kg^{-1}) was recorded from mussels. Jensen and Moestrup (1997) have proposed that the wide variation in cell concentrations of this species can also be due to rapid shifts between pelagic and benthic stages in shallow waters. Furthermore, *A. ostenfeldii* has been found to actively produce temporary cysts in cultures (Hakanen and Kremp, unpubl. data) and live field samples, although the trigger mechanisms are not always understood. It has been reported that when there is only low abundance of *A. ostenfeldii* vegetative cells in the water column, the population may have already undergone a life history transition by forming resting cysts deposited to benthic sediments as "seedbeds" for subsequent blooms (MacKenzie et al., 1996). These resting cysts remain toxic and can be ingested by shellfish directly from the sediments or via resuspension events driven by wind and other hydrodynamic mechanisms disrupting the sediments. In such cases, the relatively high

concentration of 13-desmethyl spirolide C in the absence of vegetative cells in the water column could be associated with a rapid proliferation of cysts and remobilization from the sediments. A routine operation conducted at shellfish aquaculture farms is the lifting and physical displacement of lines that sink by the weight of the product (oyster modules, mussel socks, etc.), and which thereby causes sediment disruption and resuspension. We cannot, therefore, discard the possibility that *A. ostenfeldii* cysts were available for the mussels during previous days before sampling the water column and that the mussels accumulated the toxin from such cysts, even when vegetative cells could not be detected.

2.5 Conclusions

Integration of analytical techniques, ie. optical microscopy, specific primers for species identification by PCR and LC-MS/MS for toxin determination in plankton and shellfish tissue matrices, allowed the confirmation of *A. ostenfeldii* as the primary and perhaps exclusive source of spirolide in Todos Santos Bay, and is the first record of the species in the northwest Pacific coast of Mexico. The species is a common component of the phytoplankton community but typically occurs in low cell abundances. The analog 13-desmethyl spirolide C was the only spirolide detected in mussels from TSB, which suggests a very restricted toxin profile is produced by the dinoflagellate. The species was not consistently detected when strong stratification and higher temperatures were recorded in the water column, indicating that these environmental conditions are not favorable for the accumulation of *A. ostenfeldii* in the region.

Chapter 3. Accumulation of azaspiracids in cultivated mussels (*Mytillus galloprovincialis)* and molecular identification of *Azadinium spinosum* in Northwest Baja California, Mexico

3.1 Introduction

Azaspiracids (AZAs) are polyether compounds with a unique tri-spiro ring assembly, a cyclic amine (aza group), and a carboxylic acid (Satake et al., 1998). AZAs were detected for the first time when a human intoxication occurred in the Netherlands in 1995 related to the consumption of blue mussels (*Mytilus edulis*) cultivated in Killary Harbor, Ireland (McMahon and Silke, 1996). The intoxication symptoms were very similar to the diarrheic shellfish poisoning (DSP); however, the shellfish contained negligible amounts of DSP toxins. Then a new group of biotoxins was discovered; the azaspiracids, with AZA-1 being the first analog detected (Satake et al., 1998). The identification of AZA-2 (8-methyl azaspiracid) and AZA-3 (22-desmethyl azaspiracid) was associated with a second intoxication outbreak that occurred in County Donegal, Ireland (Ofuji et al., 1999). In the last decade, more than 30 analogs of azaspiracids have been identified (Twiner et al., 2008).

Since the first outbreak, several intoxications associated with AZA have been documented. Between 1997 to 2007, around 24 cases of poisoning were registered in Ireland, 30 cases in France, and 16 in the United Kingdom (Twiner et al., 2008). The highest number of cases occurred in Belgium where 400 persons got intoxicated by the consumption of mussels cultivated in Denmark (Furey et al., 2010). In the USA, 2 cases linked to the consumption of imported mussels from Ireland were confirmed by the FDA (Klontz et al., 2009). AZA intoxication outbreaks have not yet been registered in Latin America, which could be explained by the fact that the intoxication symptomatology is similar to bacterial infection.

The primary toxicological target of AZA is the gastrointestinal tract. These toxins cause fluid accumulation in the small intestine and vacuolar degeneration of epithelial cells, which is characterized by necrotic atrophy of lamina proper of the villi (Ito et al., 2000). AZA can induce cytotoxicity and affect several cellular processes as the increase of cytosolic calcium or can alter the F-actin cytoskeleton (Román et al., 2002). Also, neurotoxic effects have been reported (Furey et al., 2010). Associated with the recognized impact on humans, the regulatory action limit for AZA was set at 160 µg Kg^{-1} of AZA-1; when other analogs are detected in shellfish as AZA-2, and AZA-3, following the toxic equivalence factor (TEF), these analogs are reported as AZA-1 equivalents (Alexander et al., 2008). These toxins are considered in the sanitary legislation of Mexico, but they are not monitored by the regulatory agency.

Thirteen years after AZA-1 was detected, *Azadinium spinosum* was recognized as the microalga that produces this toxin (Krock et al., 2009; Tillmann et al., 2009a). This small photosynthetic dinoflagellate (12 to16 µm in length) was isolated from the Scottish East Coast (Tillmann et al., 2009a). *Az. spinosum* has been registered in Ireland (Salas et al., 2011), Denmark (Tillmann et al., 2011) Argentina (Akselman and Negri, 2012), Mexico (Hernández-Becerril et al., 2012), and Korea (Potvin et al., 2012). Not only *Az. spinosum* produces AZA, but other species like *Az. poporum* and *Az. dexteroporum* produce different analogs of AZAs (Krock et al., 2012; Percopo et al., 2013; Tillmann, et al., 2017a). Production of these toxins is not restricted to *Azadinium* genus also *Amphidoma languida* that belongs to the Amphidomataceae family produces AZA-3, AZA-38, AZA-39, AZA-2, and AZA-43 (Krock et al., 2012; Tillmann et al., 2017b) As in other toxic dinoflagellates, the production of AZA is different in strains isolated from distinct geographical locations. For example, *Az. dexteroporum* isolated from the subarctic does not produce azaspiracids (Tillmann et al., 2015), while Mediterranean strains biosynthesize different analogs of azaspiracids (Rossi et al., 2017).

Todos Santos Bay (TSB) is located in the Northwest of the Baja California Peninsula. This region has high primary productivity associated with upwelling events that occurred mainly during spring and-summer (De la Cruz-Orozco et al., 2017). As a consequence, TSB has a high potential for the cultivation of mollusks (Maeda-Martínez, 2008). Baja California produced approximately 2000 tons of oyster (*Crassostrea gigas*), and 200 tons of mussels (*Mytilus galloprovincialis*) (SEPESCABC, 2018). The AZAs can affect the development of shellfish cultivation since they were detected in mussels cultivated in TSB (García-Mendoza et al., 2014). However, the species that produced the AZAs in the region have not been identified. The identification of *Azadinium* and *Amphidoma* species by light microscopy is difficult due to their small size (between 12 to 16 µm) (Tillmann et al., 2009a, 2012a). Therefore, molecular tools are used to assess the presence of these species in natural samples (Wietkamp et al., 2019). This work proposes to conduct the identification of *Az. spinosum* in TSB, as well as trying to relate the environmental conditions involved in the presence of the species. For this the polymerase chain reaction (PCR) method with specific primers (Toebe et al., 2013a) was employed to detect the presence of *Az. spinosum* in field samples from the Bay. And the azaspiracids were measure in the cultivated mussels to associate the accumulation of the toxin and the abundance of *Az. spinosum*, then its period of appearance could be established. This information will contribute to evaluate the risks of AZA intoxication due to the consumption of mussels cultivated in this region and know the temporal and spatial distribution of *Az. spinosum* in TSB.

3.2 Material and methods

3.2.1 Study area and sample collection

This work is part of the regular monitoring program of marine biotoxins in shellfish cultivated in TSB and associated toxigenic plankton perfomed by FICOTOX laboratory of the Centro de Investigación Científica y de Educación Superior de Ensenada, Baja California (CICESE). The study area was in TSB and Salsipuedes Bay, they are located on the Northwestern coast of the Baja California peninsula in Mexico.

In this study, the results of the two-sampling periods are presented. The first was from June 2013 to June 2014, here the only sampling station was in TSB into the mussels cultivation area (St. 13; Fig. 15). During this period the detection of the species in water samples with PCR was done, and the AZAs into the cultured mussels were detected.

The second sampling period was from August 2016 to August 2017, here the sampling area was extended, and two more stations were placed in TSB (St 11 and 12; Fig. 15) and continued monitoring the St 13 (Fig. 15). Four more sampling stations in Salsipuedes Bay (St. 1, 3, 4, and 6; Fig. 15). From this period, water samples were analyzed to detect the presence of *Az. spinosum* by light microscopy. Water samples were collected once a month at the surface and the thermocline with a 2 L Niskin bottle. The detection of the species with molecular markers and the quantification of the AZAs continued.

The vertical temperature profile of the water column was measured with a conductivity, temperature, and pressure profiler (CTD, CastAway, YSI, Ohio, USA). The depth of the thermocline was determined from the temperature profile before the samples were collected.

Inorganic nutrients (nitrate + nitrite, ammonium, phosphates, and silicates) were also analyzed. An aliquot of 15 mL of water samples was taken and stored at -20 °C. The samples were analyzed in the Colima University with the segmented continuous-flow autoanalyzer Skalar Scan ++ (Skalar Analytical B.V, Netherlands) with a precision of 0.01 µM as described in Solórzano (1969); Strickland and Parsons (1972), and (Grassoff et al., 1983).

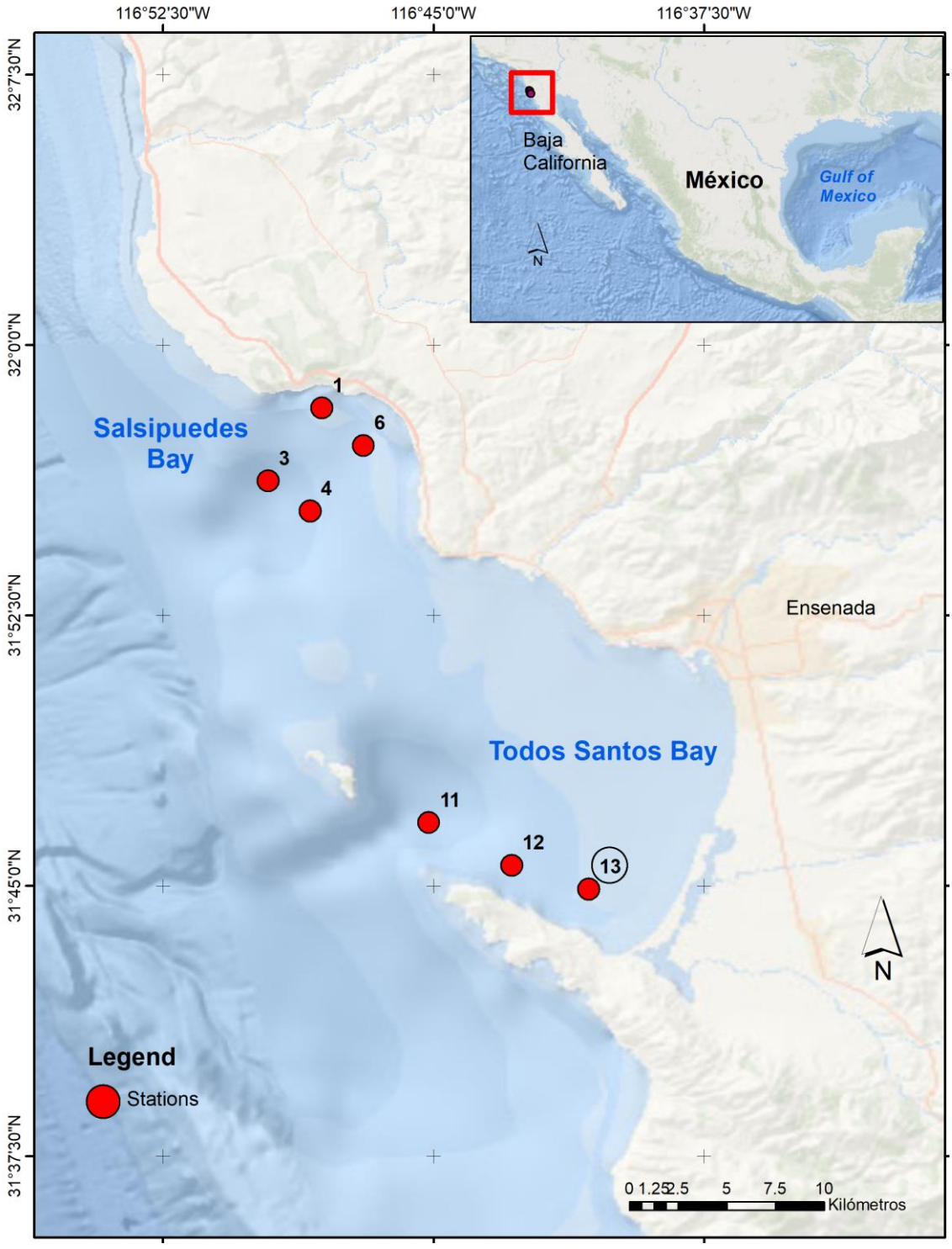

Figure 15. Study area was located in Todos Santos Bay with three sampling stations (St 11, 12 and 13). Station 13 enclosed in the circle is located inside the mussel cultivation area. And in Salsipuedes Bay with four sampling stations (St 1, 3, 4 and 6).

3.2.2 *Az. spinosum* morphological identification and abundance

An aliquot of 250 mL from surface and thermocline water samples were fixed with Lugol's iodine-acetate solution. These samples were analyzed with an inverted microscope (Leica DM13000B, Leica Microsystems, Wetzlar, Germany) according to the Utermöhl method (Lund et al., 1958). A 50 mL sample was sedimented, and the entire surface of the sedimentation chamber was analyzed to quantify cells that morphologically resembled *Azadinium* species. These are reported as *Azadinium* sp.

3.2.3 Molecular analysis

3.2.3.1 DNA extraction

The genomic DNA was extracted from seawater field samples from both Bays through filtration (500 mL to 1 L) using 8 μm pore-size polycarbonate filters (Nucleopore Whatman, Darmstadt, Germany), under gentle vacuum to avoid cell disruption. Filters were stored in 50 mL sterile centrifuge tubes at -80 °C until analysis. The DNeasy Plant Mini kit (Qiagen, Hilden, Germany) was used for DNA extraction, following manufacturer**'**s instructions with a slight modification in the volume of the lysis buffer to 600 μL. The mechanic disruption of the cells was carried out using the mini-Bead Beater 24 (BioSpec Products, Bartlesville, United States) with two rounds of shaking for 40 s at a speed of 6.0 m/s using 170 μm^3 of zirconium beads of 0.1 mm diameter (Wohlrab et al., 2010). Concentration and purity of DNA were determined using the NanoDrop 2000c spectrophotometer (Thermo Scientific, Wilmington, USA), and integrity was assessed by agarose gel electrophoresis. The samples were stored at -20 °C until testing by PCR.

3.2.3.2 Polymerase Chain Reaction (PCR) amplification

The identification of *Az. spinosum* from the field genomic DNA was done by the amplification of a 72 bp fragment of the 28S ribosomal DNA (rDNA) using specific primers designed by Toebe et al. (2013a).

Amplifications were performed in a Veriti thermal cycler (Applied Biosystems, USA). The PCR reaction (30 μL) consisted of 0.2 mM of each dNTP, 0.30 μM of each primer, 3 mM of $MgCl_2$, 1 X GoTaq® Flexi

buffer (Promega, Madison, WI, USA), 0.6 U of GoTaq® DNA polymerase, and 100 ng of genomic DNA. The amplification was carried out under the following conditions: 94 °C for 3 min, followed by 30 cycles of 94 °C for 30 s, 58 °C for 45 s, 72 °C for 1 min, and a final extension step of 72 °C for 7 min. Genomic DNA from the monoclonal strain 3D9 of *Az. spinosum* donated from Alfred Wegener Institute (AWI) was used as a positive control. For the negative control the DNA was replaced with ultrapure water in the PCR reaction.

3.2.3.3 Sequencing and phylogenetic analysis

The 72 bp fragments obtained from the 28S rDNA PCR amplifications were sequenced at SeqXcel, San Diego, CA, USA. The analysis of the sequences was carried out using the Basic Local Alignment Search Tool *(BLAST)* of the *NCBI* website to find the closely related sequences. Multiple sequence alignments were performed using the CLUSTAL X software (Thompson et al., 1997)

A phylogenetic analysis was performed with positive detections for *Az. spinosum* in water samples from 2013 – 2014 and 2016 – 2017 monitoring. The tree was built by the Maximum likelihood (ML) method based on the Kimura 2-parameter model. Nodal support was estimated by bootstrap analyses with 1000 replicates (Felsenstein, 1985) and the evolutionary analyses were performed in MEGA 7 software (Kumar et al., 2016). Sequences from *Amphidoma languida* were used as an outgroup.

3.2.4 Analysis and quantification of azaspiracids in mussels

The accumulation of the azaspiracids was evaluated from July 2013 to June 2014, and from August 2016 to August 2017. The mussels were donated by Acuacultura Oceanica Company, Ensenada, B. C., Mexico, and they were collected in the station 13 into the farming area of TSB. The analysis was performed following the standardized operating procedure of the European Union for the determination of marine lipophilic biotoxins in mollusks (EURLMB, 2015). The complete soft tissue of at least 20 commercial-size mussels was homogenized, the toxin was extracted with 100% methanol on 2.0 ± 0.01 g of shellfish tissue. The detection and quantification of the azaspiracids were performed with the analytical methodology of liquid chromatography coupled to a tandem mass spectrometer (LC-MS/MS). A triple quadrupole Thermo Scientific TSQ Quantum Access Max LC-MS/MS system (San Jose, USA) was used for the analysis of mussel samples collected from July 2013

to June 2014. For the chromatographic separation, the method of Regueiro et al. (2011) was employed with minor modifications for the use of a shorter column. Chromatography was performed in reverse-phase mode with a Gemini-NX C18 (Phenomenex, Torrance, USA) (50 x 2 mm; 3 µm) analytical column. The mobile phase was described by Gerssen et al. (2009) to yield alkaline chromatographic conditions; phase A = ammonium hydroxide 6.7 mM, Phase B = acetonitrile in ammonium hydroxide 6.7 mM in proportion 9:1 (v:v). A calibration curve of four concentration levels of certified standards obtained from CIFGA (Lugo, Spain) was used to quantify AZA-1. The limit of detection of the LC-MS/MS analysis was 0.04 ng mL^{-1}.

The mass spectrometer analysis was according to the method of Martín-Morales et al. (2013). After extraction, an aliquot of the methanolic extract was filtered through a 0.22-µm-syringe filter, and 5 µL were injected into the LC-MS/MS system. The mass spectrometer was operated in positive-ion mode by multiple reaction monitoring (MRM).

For the mussel samples from 2016-2017, toxin analyses were performed with the method of (Krock et al., 2008), for lipophilic toxins. An aliquot of methanolic extract of mussel tissue was transferred to a spin-filter (polypropylene membrane of 0.45 µm pore-size; Millipore Ultrafree, Eschborn, Germany) and centrifuged for 30 s at 800×g. The filtered sample was transferred to an autosampler vial, and 5 µL were injected into the LC-MS/MS system. Toxin analyses were performed on a liquid chromatograph (Agilent 1100, Waldbronn, Germany) coupled to an ABI-SCIEX-4000 Q Trap triple-quadrupole mass spectrometer (Applied Biosystems, Darmstadt, Germany) equipped with a Turbo V ion source. Separation of the lipophilic toxins was performed by reverse-phase chromatography on a C8 column (50 mm X 2 mm) packed with 3 µm Hypersil BDS 120 Å (Phenomenex, Aschaffenburg, Germany). The mobile phase had two eluents, where eluent A was water, and eluent B was acetonitrile-water (95:5 v:v), both containing 2.0 mmol L^{-1} of ammonium formate and 50 mmol L^{-1} of formic acid. The limit of detection for AZA-1 was 0.3 ng mL^{-1}, determined with reference to an external standard solution of 10 ng mL^{-1} AZA-1 obtained from the CRMP, IMB, National Research Council, Halifax, Canada.

3.2.5 Statistical analysis

To establish the relationship between the abundance of *Az. spinosum* in the water samples from TSB and the accumulation of the azaspiracids in the cultivated mussels, Pearson's correlation was used. Statistical analyses were carried out using STATISTICA 7 ® (StatSoft)

After proving the homoscedasticity of the data, a principal component analysis using R software was performed between the set of environmental variables (temperature and inorganic nutrients) and the abundance of *Az spinosum* to determine which variable had more effect on the presence of the species in TSB.

3.3 Results and discussion

3.3.1 Temporal variation of *Az. spinosum* in TSB and Salsipuedes

One hundred forty-seven samples were analyzed by light microscopy to evaluate the abundance of *Azadinium* sp. in the seven stations. *Azadinium* type species were observed in 20% of the samples. Cell abundance was higher at the surface than at the thermocline. *Azadinium* has a clear seasonality of appearance in the Bay since it was observed mainly during the winter of 2016 and also at the beginning of the spring of 2017 and was absent in the summer months of 2017 (Fig. 16A and B).

Azadinium sp. showed the maximum abundances in the surface at the beginning of November, 2016 in all stations of the Salsipuedes area (Fig. 16A). The maximum abundance was 720 cells L^{-1} registered in station 4 and decreased at the end of November 2016. *Azadinium* was not detected in any station at the end of January 2017 but was recorded again at the beginning of March 2017 reaching a maximum abundance of 440 cells L^{-1} in station 4.

The abundances of *Azadinium* sp. at the thermocline were noticeably lower in comparison with abundances at the surface. The maximum abundance recorded was 360 cells L^{-1} at the end of November 2016 at station 4 (Fig. 16B). *Azadinium* sp was not detected in any station after this date during the sampling period.

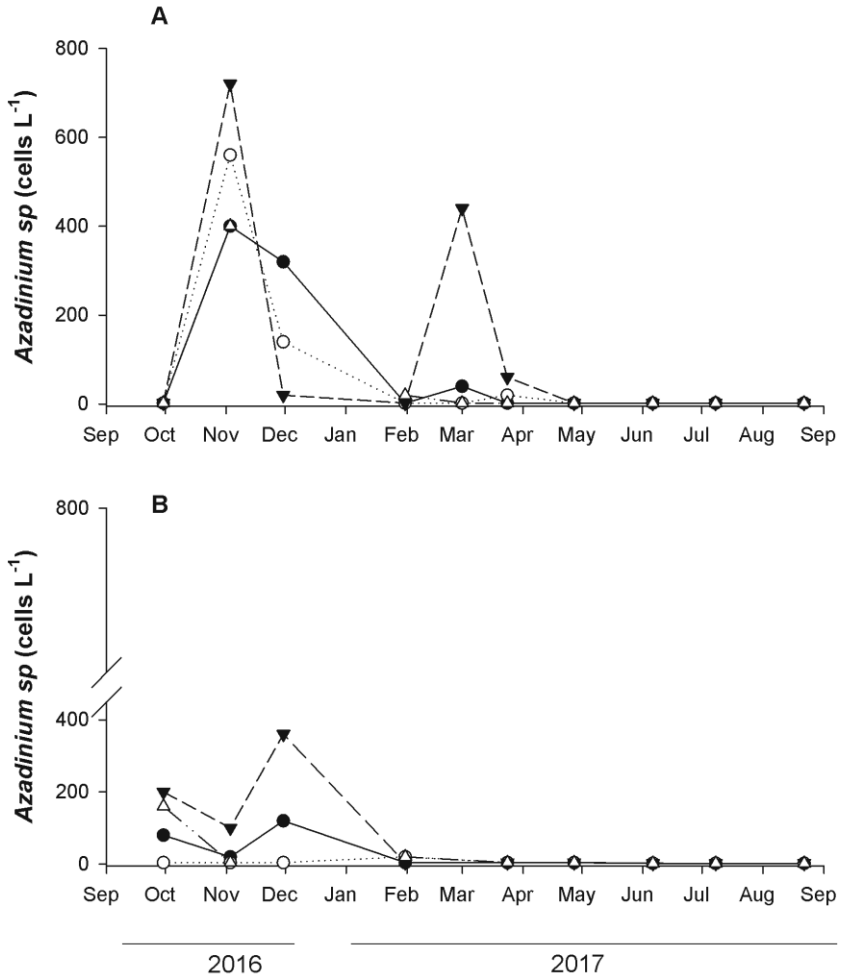

Figure 16. Temporal variation *of Azadinium* sp. abundance in four sampling stations located in Salsipuedes area: station 1 (closed circles), station 3 (open circles), station 4 (closed triangles), station 6 (open triangles). Samples were collected at surface (**A**) and in the thermocline (**B**) from August 2016 to August 2017.

The morphological identification of the *Azadinium* species is difficult due to their small size (between 12 to 16 µm) and requires high magnification microscopy to see their distinctive characteristics (Tillmann et al., 2009a). The first and unique record of *Az. spinosum* in Mexico waters was in Tehuantepec Gulf, and the abundance was less than 300 cells L^{-1} (Hernández-Becerril et al., 2012). In this study, *Az. spinosum* was identified only by its morphological characteristics, and azaspiracids in the samples were not measured. The abundance reported by Hernández-Becerril et al. (2012) is similar to the abundance of *Azadinium* sp. found in Todos Santos and Salsipuedes bays, this suggest the population of *Azadium* cf *spinosum* in the Mexican Pacific is a minor component in the phytoplankton community with low densities. However, these are low compared with abundances reported in other regions. For example, in Ireland, Tillmann et al. (2014a) reported cells as "*Azadinium* like" with maximum abundance around 24000 cells L^{-1}. In the Southeast of the Chilean coast, *Az. poporum* was identified and cells as "*Azadinium* like" was reported with a maximum

concentration of 6800 cells L^{-1} (Tillmann et al., 2017a). *Az. poporum* was monitored for three years by the qPCR technique in South Korea, and a maximum abundance of about 5000 cells L^{-1} was registered (Potvin et al., 2012). The highest abundance (9 x 10^6 cells L^{-1}) of *Azadinium* cf. *spinosum* was recorded during a bloom detected on the northern coast of Argentina (Akselman and Negri, 2012). Non-intoxication cases were registered, and the azaspiracids were not analyzed during this event in Argentina (Akselman and Negri, 2012) Another bloom of *Azadinium* occurred in the Peruvian coast with water discoloration and cell densities of up to 1 x 10^6 cells L^{-1} of *Az. prolongum* (Tillmann et al., 2017b). In Ireland continuous monitoring of *Azadinium* and AZAs has been established due to the poisoning cases, but no bloom of the species has been recorded (Tillmann et al., 2014a). Knowledge on the occurrence and distribution of the species is a quite inconstant and incomplete, and quantitative abundance data of Amphidomataceae are hardly available and patchy, this makes difficult to compare the cell abundance of different regions because most studies focus on characterizing a specific strain morphological, genetic and toxicological, but environmental variables were not measured.

3.3.2 Species detection and identification

3.3.2.1 Morphological description

Cells of *A.* cf *spinosum* are elongated and dorsoventrally compressed, the cingulum is wide, and deep, the episome is larger than the hiposome (Fig. 17A). The specimens from Todos Santos Bay had a length of 11 to 13 µm (Fig. 17B). Analysis of the species with scanning electron microscopy (SEM) did not allow the detection of the thecal arrangement because the thecas were transparent, and the cells collapsed during the sample preparation. However, it was possible to observe the two main morphological characteristic of *Az. spinosum*: a prominent apical pore complex (APC) in the episome, and the single small antapical spine (Fig. 17C).

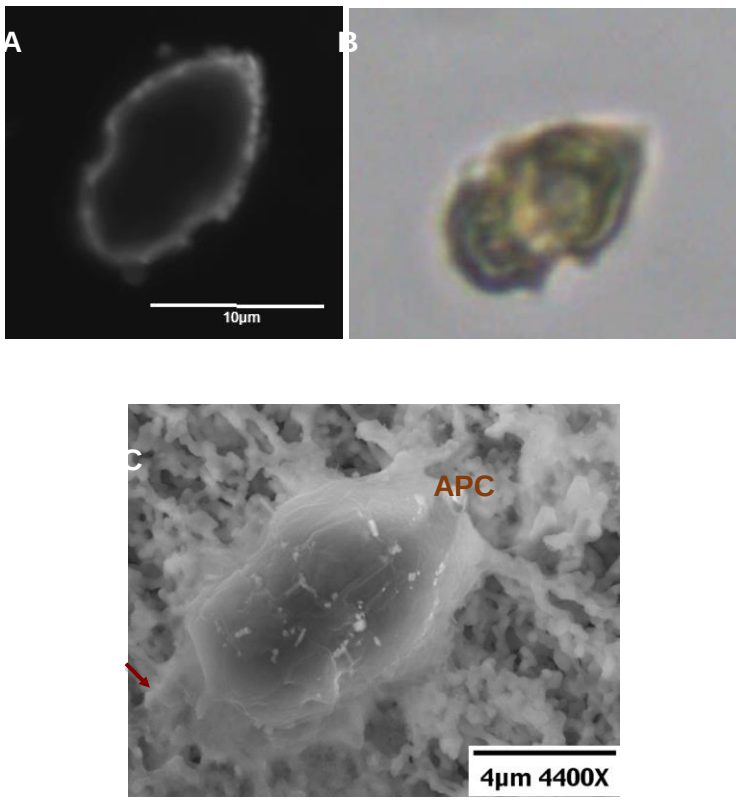

Figure 17. *Azadinium* cf *spinosum* cells. **(A)** epifluorescence image of cells shape **(B)** Light microscopy of cells fixed with Lugol´s solution and **(C)** Scanning electron micrographs showing the prominent apical pore complex (APC) and the little antapical spine (arrowed).

3.3.2.2 Molecular identification of *Az. spinosum*

The molecular identification of *Az. spinosum* was conducted by PCR in the 145 water samples from Salsipuedes and Todos Santos Bays (seven stations) obtained from August 2016 to August 2017. The PCR is a useful tool for the identification of *Azadinium* species since they have a very similar morphology to the genus *Heterocapsa* (Wietkamp et al., 2019). The amplification of the 28S rDNA fragment (72 bp) confirmed the presence of the species in the region (Fig. 18A), and *Az. spinosum* was detected in 21.37 % of the analyzed samples.

Figure 18A shows the results of the PCR amplification of samples collected in November 2016. Positive results (presence of 72 bp fragment) were detected in most of these samples. In contrast, figure 16B shows that the species was not present on the samples of May 2017, supporting the light microscopy results.

In the 2013 to– 2014 period, 38 water samples were analyzed from station 13, and the species was detected in 31% of these samples. Positives samples were observed from the middle of autumn (October 10, 2013) to the end of April 2014.

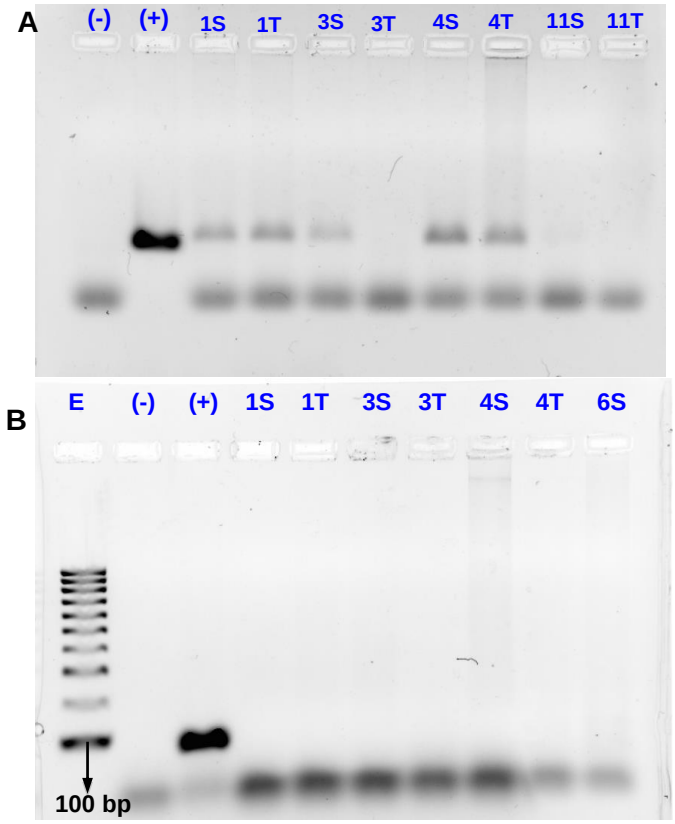

Figure 18. PCR amplification of samples using Asp 48F and Asp 120R primers. The 72 bp 28S rDNA fragment indicates the presence of *Az. spinosum*. Results of samples collected on different dates are presented: **(A)** samples of November 20, 2016 collected from surface (S) and thermocline (T). **(B)** samples of May 27, 2017. (+): positive (DNA of *Az. spinosum*) and (-): negative (ultrapure water) PCR controls. E: molecular marker of 100 bp Bioline.

In this study the molecular technique with the use of specific primers was essential for the detection of the species since its identification by microscopy was complex and despite the time spent preparing samples, it was not successful. The only record of *Az. spinosum* for the Northwest Pacific is in Puget Sound, Washington State, USA and was achieved using qPCR with the same primers used in this study. Kim et al. (2017) reported the positive signal for the species in water samples, but as in the case here, identification of the species by microscopy was not possible.

The alignment done showed that the amplified sequences obtained from field samples of one fragment of 28S gene had 98% identities with *Az. spinosum* (accession number: LS974160, JX559885, JN65101) with 100% of the coverage of the sequence (74 bp).

In the phylogenetic tree, the best scoring of the Maximum likelihood (ML) for the large ribosomal subunit (LSU gene) (-ln = 228.10) is shown in Fig. 19. The (ML) inference analysis indicates that TSB strain cluster together with Scotland, Ireland, and Norway strains in a well-supported clade of 88% with a 1000 bootstrap replicate. *Az. spinosum* isolated from Norway and the North Sea form a separate clade, which shows that they are different populations. Due to the lack of a strain isolated from the TSB, there was not possible to sequencing the entire LSU gen or ITS regions to establish the differences between Pacific strains and European strains (Salas et al., 2011; Tillmann et al., 2009a; 2012b). So far, a strain of the Pacific has not been isolated. Then with this short sequence (28S), which is useful to identify the species apparently, the strain of the bay is the same as the Scotland and Ireland strains. The ballast water is one of the main conveyance of non-endemic phytoplanktonic species introduction (Burkholder et al., 2007). Around 50 million cubic meters of ballast water is discharged into the waters of the Mexican coast (Mendoza et al., 2014). Ensenada is an important port; then, the European strain may have been transported through ballast water. But it is necessary to isolate the strain of the bay to confirm this and to establish if there are one or more genotypes.

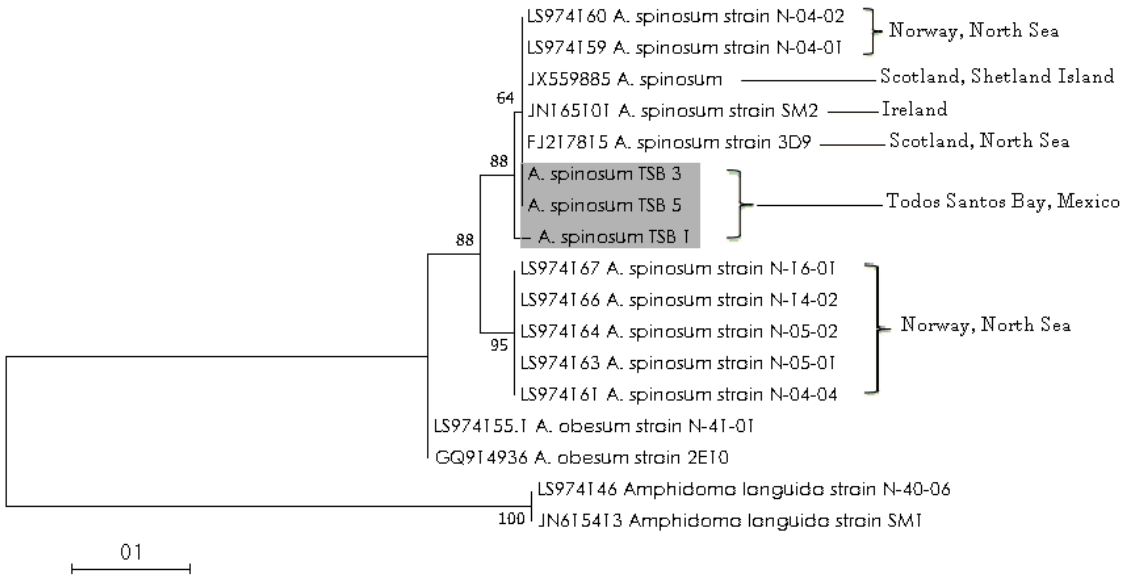

Figure 19. Phylogenetic tree of *Az. spinosum* based on the maximum likelihood of large ribosomal subunit (LSU 28S) rDNA sequences obtained from the water samples of Todos Santos Bay. The numbers in the left of the branches are statistical support values (values < 50 are not shown). Sequences from *Amphidoma languida* were used as outgroup. Bootstrap values (1000 replicates).

3.3.3 Azaspiracids accumulated in cultivated mussels

The accumulation of azaspiracids in mussels from TSB was confirmed. Of the 32 analogs searched, only AZA-1 was detected in this study by LCMS/MS. It is known that *Az. spinosum* is the only species

that produces this analog but also produces AZA-2; then, typically AZA-1 is the dominating analog in shellfish, and AZA-2 is accumulated in less proportion due it is the same toxic profile of the producer species (*Az. spinosum*) as strain 3D9 produced AZA-1 (74.6%) and AZA-2 (25.4%) (Salas et al., 2011; Tillmann et al., 2012b; Jauffrais et al., 2012) The toxin profile found in mussels from Spain was AZA-1 (54%), AZA-2 (29%), and AZA-3 (17%) (Braña Magdalena et al., 2003). A similar toxin profile was found in mussels from Ireland and Norway (James et al., 2002). Here, the analog AZA-2 was not detected, probably related to the low concentrations of toxins found in the mussels.

The chromatogram presented in Figure 20 shows the presence of AZA-1 in the mussel sample of November 2016 collected from station 4 in Salsipuedes Bay. AZA-1 presented a retention of 11.80 min, and the transition monitored was 842 m/z → 824 (Fig. 20B), the confirmatory transition was 842 m/z → 672. This retention time coincided with the standard solution of AZA-1 (10 pg μL^{-1}) (Fig. 20A).

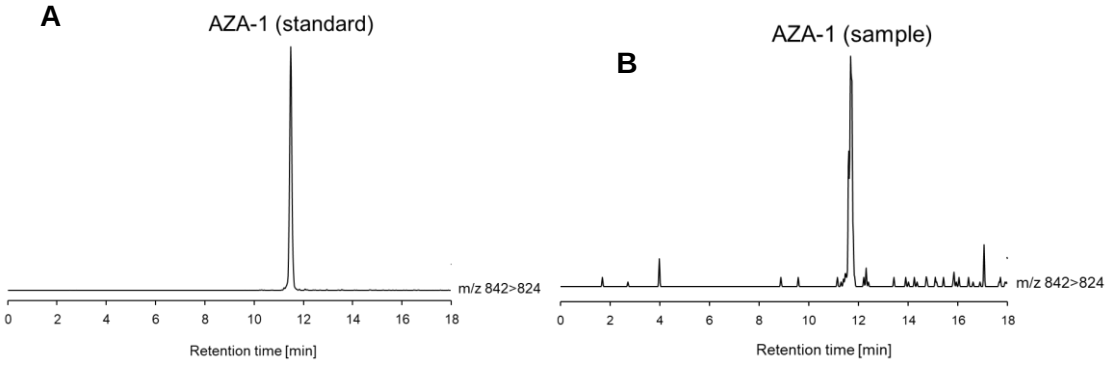

Figure 20. LC-MS/MS chromatogram (in SRM mode) of azaspiracid 1 (AZA-1) transition 842 > 824 *m/z*. (**A**) Standard solution of AZA-1 (10 pg μL^{-1}) (**B**) detection of AZA-1 in Mediterranean mussel collected in November 2016 in St 4 (Salsipuedes Bay).

Azaspiracids were monitored only during the first sampling period (2013-2014). A total of 19 samples were analyzed, and AZA-1 was detected in 36% of the samples (Fig. 21). The presence of the toxin had a clear seasonality of occurrence in TSB since it was detectable mainly during the winter. The maximum concentration of AZA-1 (15.29 µg kg^{-1}) occurred at the beginning of February 2014. Also on November 2013 a high concentration 12.25 µg kg^{-1} was recorded.

From the 12 mussel samples collected from August 2016 to August 2017, AZA-1 was present in 50% of the samples. During this period also the toxin was present mainly during winter and continued

until the beginning of spring. The seasonality of appearance of azaspiracids was also registered in the Southwest and Northwest coast of Ireland. These toxins were present from June through to November, reaching a peak during September and October in 2013 (Tillmann et al., 2014a). This same pattern of toxin appearance has been detected in Northern and Western European waters. High concentrations of AZAs were detected from mid-summer to mid-winter (Furey et al., 2003; James et al., 2002).

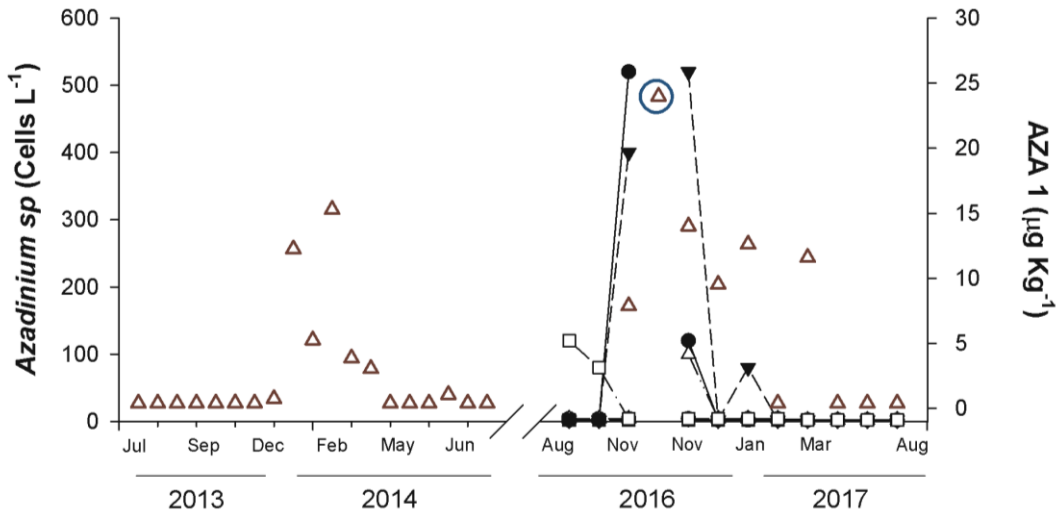

Figure 21. AZA-1 concentration (red open triangles) in *M. galloproviancialis* collected from July 2013 to June 2014 and from August 2016 to August 2017 in St 13, Rincón de Ballenas (TSB). The abundance of *Azadinium* sp. in St 11 at the surface (closed circles) at thermocline depth (open circles), St 12 at the surface (closed triangles) at the thermocline (open triangles) and St 13 at the surface (closed square) at the thermocline (open square). The AZA-1 concentration enclosed in a blue circle corresponds to St. 4.

During 2016- 2017, (Fig. 21), the presence of *Azadinium* sp. was observed in stations 11, 12 (Punta Banda), and 13 (Rincón de Ballenas) located in the south of the TSB close to the mussels cultivation area. The presence of the genus in the water samples had the same seasonality as the toxins accumulated in the mussels. The maximum concentration of AZA-1 (23.99 µg kg^{-1}) was registered at station 11 at the beginning of November (Fig. 21). This was the only mussels sample (not cultivated) collected from this station. This concentration of AZA-1 is related to the highest abundance registered in the same station with 520 cells L^{-1}. On the same date, the accumulation of AZA-1 in mussels from the cultivation area (St 13) was approximately 7.88 µg Kg^{-1}, and the *Azadinium* sp. was not detected in this zone. The maximum concentration of AZA-1 for cultured mussels in the Rincón de Ballenas area was at the end of November 2016 with 14.0 µg kg^{-1}. As happened at the beginning of November the species was not detected in the mussels cultivation area (St 13), but in station 12, an abundance of 520 cells L^{-1} was registered. These results showed that apparently, *Azadinium* sp. in

TSB is an oceanic species that seems to enter into the bay by oceanographic processes as the flow of an intense current (15 cm/s) from the North entrance (Salsipuedes Bay) with Southeast direction towards the TSB and currents of less intensity (5 cm/s) within the bay near to the coast (Larrañaga, 2013), then *Azadinium* sp. cells from Salsipuedes Bay could be transported into the TSB and the superficial current in front of Punta Banda (St 11) is another entrance of water during the winter where the winds have a southeast direction (Argote Espinosa et al., 1991), explaining the higher concentration of cells and azaspiracids in St 11 compared to St 13. The transportation of dinoflagellates cells into the bay has already been described; Ruiz de la Torre (2013) using drifter buoys, could observed that the combination of the daytime breeze and the direction and speed of the wind, forms a superficial current (between 1 to 3 m) that displaced this surface layer into the bay with the transportation of *Lingulodinium polyedrum* cells, which caused the coastal bloom. This distribution of *Az. spinosum* from deeper offshore locations towards the coast has also been described before by Tillmann et al. (2014a) in the Northwest and Southwest of Ireland. Further, Raine et al. (2010) in the Southwest of Ireland demonstrated that the wind causes an intrusion of offshore waters, which contain a high amount of cells of HABs species into the bay, causing the coastal blooms. Although the geography of Ireland bay is different to TSB, the oceanographic processes in both cases cause the oceanic *Az. spinosum* enters the Bay, and this also explains the temporality of appearance of *Az. spinosum* and it is not present as common species in the phytoplankton community.

In this study, we found a relation in the azaspiracids accumulation and the presence of *Azadium* sp.. These results agreed with Tillmann et al. (2014a), who after 11 years of monitoring azaspiracids on Irish shellfish, concluded that the detection of the azaspiracids is a useful indicator to characterize the temporal distribution of *Az. spinosum*; this is in agreement with the relationship found for TSB.

The Pearson correlation was used to quantify the relationship between the abundance of the genus in the three stations close to the mussel cultures (St 11, St 12, and St 13) and the azaspiracids accumulated in the mussels. The highest correlation with r^2= 0.5317 (p < 95) was in station 12; nevertheless, the correlation was not significant. In station 13, which corresponds to the mussels extraction area, no relation was found between the toxin accumulated and the abundance of the genus. One possible reason could be the small number of the samples analyzed in this study, which influenced the correlation analysis. However, as mentioned before, it seems that the population of *Azadinium* sp. comes from outside the TSB and moves into, then the abundances are lower. Another point that should be considered is the possible underestimation in cell counts related to the cell size of the species that makes very difficult to accurately identify by optical microscopy.

Azaspiracids accumulation in the mussels was relatively low, no more than 20% of the regulatory level of 160 µg Kg^{-1}. In the Portuguese coast, azaspiracids were also accumulated in low concentrations (2.4 – 8.9 µg Kg^{-1} of AZA-1 -eq.Kg^{-1}) in several shellfish species (Vale et al., 2008). Similarly, in the Galician, Cantabrian, and Basque coasts, the maximum concentration detected in *M. galloprovincialis* was around 5.4 of AZA-1 -eq.Kg^{-1}, in this study the producer species could not be identified and the AZAs in bivalves was linked to upwelling relaxation in the Galicias Rías (Blanco et al., 2017). As in other regions where the AZAs are accumulated in low concentrations, the abundance of the producer species also is low abundances as was the case of this study or even could not be detected as occurred in the Portuguese and Galician coast. On the other hand, azaspiracids are a recurrent problem for human health in Ireland because mussels frequently reach concentrations above the regulatory limit. The highest level reported in *Mytilus edulis* from Ireland was 8970 µg Kg^{-1} (Salas et al., 2011).

3.3.4 Environmental variables

3.3.4.1 Vertical distribution of temperature water in the bay

A temperature profile was performed in the water column from 2016 to 2017 to correlate the presence of *Azadium* sp. with the environmental factors. In summer (August-2016), warm water was recorded with an average surface temperature in the Salsipuedes area of 18.19 °C with stratification at 10 m depth. In the south of the Bay (Rincón de Ballenas) the water was warmer with an average of 22.14 °C, 4 degrees higher than in Salsipuedes area and the stratification was found at 5 m depth with a significant decrease in the temperature of about 5 degrees in this water layer (Fig. 22). The temperature differences have already been observed by Calva-Chávez (2014) with an overage of 3 or 4 degrees hotter inside the Bay than outside, which suggests that the water is trapped and heated by solar radiation; this is known as an upwelling trap.

At the beginning of autumn, the surface water had more homogeneity since an average of 19.81 °C was registered in Salsipuedes, and 20.31 °C in Rincon de Ballenas (Fig. 22). However, during September 2016 the stratification decreased. At the beginning of October, the stratification was broken. The water column was homogeneous, characteristic of the start of the winter season (Durazo, 2015). During winter (November to February) (Fig. 22) the water column was homogeneous in the entire Bay, until the beginning of the spring (March 2017) (Fig. 22), and the thermocline was deeper in the Punta Banda stations. This was found around 15 m depth, while at Salsipuedes stations, the homogeneity of the column water continued.

Salsipuedes and Todos Santos Bays are part of the California Current System (CCS). (Pérez-Brunius et al. (2006) described that these regions have an evident seasonal variability; in spring, subarctic water is more present in the California Current (CC). The water body is characterized by a relatively high concentration of nutrients, and in the winter, the upper ocean becomes more homogeneous, this favored the presence of *Azadinium* sp. During the 2016-2017 monitoring, the water temperature seasonality was confirmed, both on the surface and in the water column.

According to these results, the presence of *Azadinium* sp. and its toxins seems to be favored when the water column is homogeneous or with moderate stratification (end of October until the end of March). In the Celtic Sea, Tillmann et al. (2014a) suggested that *Az. spinosum* population was present when the water is moderately stratified, which is consistent with our results. In the bloom of *A.* cf. *spinosum* in Argentina, Akselman and Negri (2012), described that the bloom occurred when the water column showed a weak stratification. *Az. prolongum* on the Peruvian coast was also recorded when the water column showed a moderate stratification (Tillmann et al., 2017d). The stratification has an impact on the nutrient exchange, therefore in the winter, the wind mixes the column water, and the nutrients are distributed and available in the surface water to be assimilated by *Azadinium* sp.

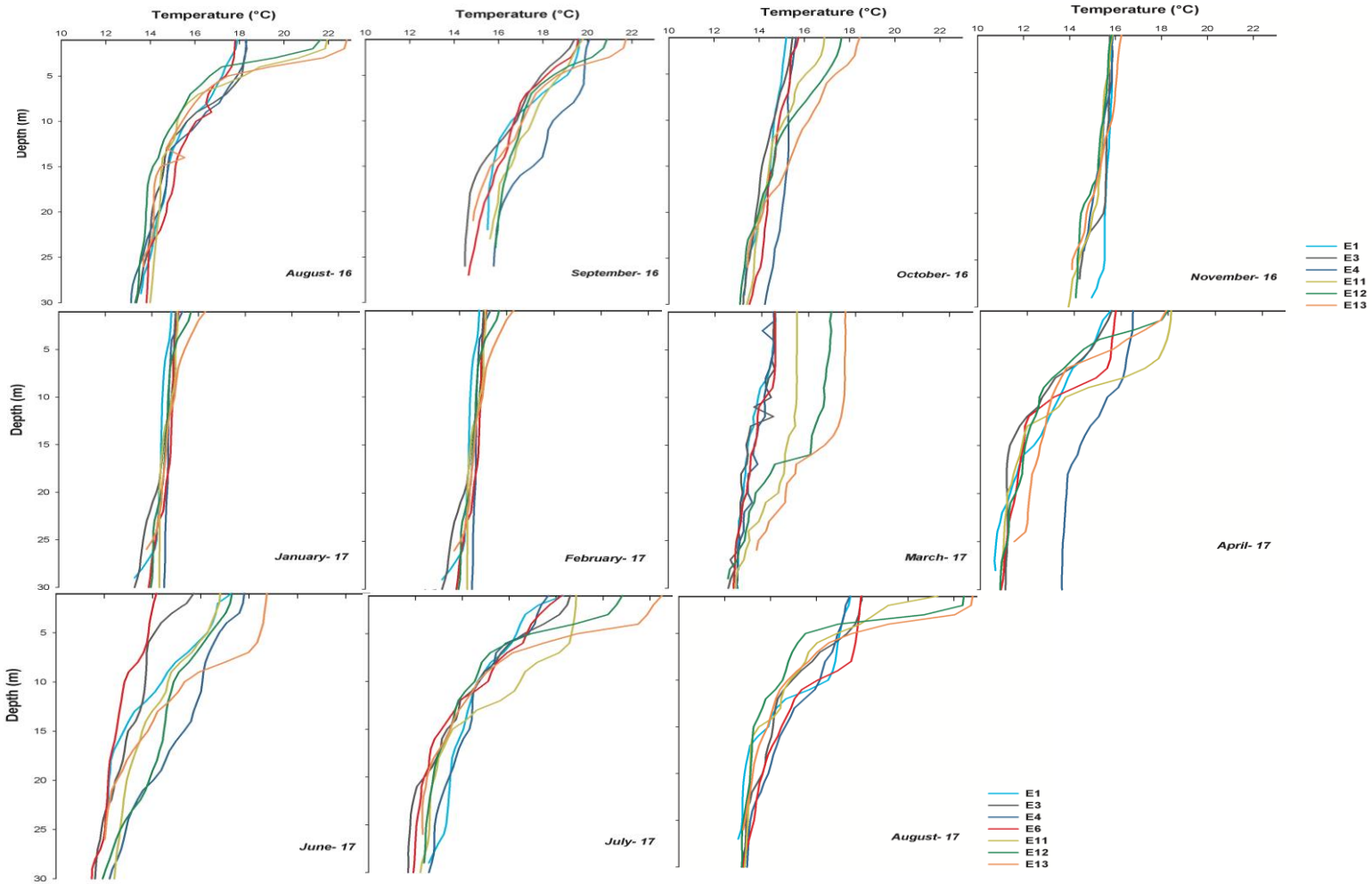

Figure. 22 Vertical distribution of temperature in the seven sampling stations from Salsipuedes to Todos Santos Bay. Station 1 (E1) light blue, Station 3 (E3) brown, Station 4 (E4) blue, Station 11 (E11) yellow, Station 12 (E12) green and station 13 (E13) orange.

3.3.4.2 Relationship between *Azadinium* sp. cell abundance and environmental variables

A principal component analysis (PCA) was done to characterize the relations between the environmental and biological parameters. The PCA generated five eigenvalues with a Kaiser, Meyer, Olkin (KMO) index of 0.75. The first two components explained 90% of the total variance of the data. The component 1 (PC1) represented 70% of the variance and corresponded to the concentration of the inorganic nutrients: nitrate and nitrite (NO_3 + NO_2), ammonium (NH_4), phosphate ($P0_4$) and silicate (SiO_2) in the surface. The abundance of *Azadinium* sp. had a negative correlation with nitrate and nitrite. When the concentration of these nutrients was low (about 3.60 to 4 µM), the cell abundance was higher (Fig. 23).

The second component (PC2) represented 20% of the variance and corresponded to the temperature. The correlation between abundance and low temperatures (around 14 and 16 °C) was in the critical point (r^2 0.23 and p=0.054), but it was not significant (Fig. 23).

Nitrogen is required for the synthesis of amino acids, nucleic acids, chlorophylls, and toxins. The change of its concentration and composition influence the primary and secondary metabolism of the dinoflagellates (Dagenais-Bellefeuille and Morse, 2013). The dinoflagellates tend to thrive under more nutrient-poor environments (Wyatt, 2014), and typically, a significant concentration of NO_3 leads to a rapidly growing of diatoms (Lomas and Glibert, 1999).

In the ocean, nitrogen is mostly in the form of nitrate (88%), while oxidized nitrogen and ammonium are less than 0.3% (Gruber, 2008). Nevertheless, the dinoflagellates prefer the NH_4 source because its assimilation does not involve a redox reaction and therefore requires a little energy, by contrast to the uptake of NH_3 (Zehr and Ward, 2002). Another advantage of dinoflagellates is their molecular transporters, which allows them to incorporate different forms of nitrogen from the environment like urea (urease), amino acids (aminotransferase), showing its high physiological plasticity (Dagenais-Bellefeuille and Morse, 2013)

There are not many studies about the environmental conditions which favored the presence of *Azadinium* sp. During the Argentina bloom of *Az*. cf *spinosum* the nitrate values were between 6 to 12µM (Akselman and Negri, 2012). On the other hand, in the monitoring during a bloom of *Az. prolongum* in the Peruvian coast the nitrate concentrations were low between 3.8 and 4.5 µM (Chacay station) (Tillmann et al., 2017d). The concentration of NO_3 + NO_2 when *Az. poporum* was isolated in the Chilean Coast was 11.41 µM (Tillmann et al., 2017a). *Az. spinosum* cultivated in the laboratory with different

sources of nitrogen did not show an effect on the toxin cell quota or in growth. Not even the different media used strongly affected growth and toxin cell quota and did not indicate any unusual nutrient requirement (Jauffrais et al., 2013).

The temperature range associated with the presence of *Azadinium* sp. and AZAs (between 14 and 16 °C) is similar to other regions. For example, on the Irish coast *Az. spinosum* was present at the end of summer months, reaching an abundance peak in October and September (Tillmann et al., 2014a) when the seawater temperature was between 14 to 15.5 °C, which represents that the temperature range between the Scottish strains is similar to the strain we have in the TSB.

In Argentina, water temperature during the bloom was between 7.7 to 9.0 °C (Akselman and Negri, 2012). In the laboratory, a wide range of growth temperatures was recorded for the cultivation of *Az. spinosum* (10 – 26 °C). In that study, the authors found that the temperature does determine the growth and the AZA cell quota. The best temperature for *Az. spinosum* growth (0.46 d^{-1}) was at 22 °C, but the AZA cell quota was lower (8 fg $cell^{-1}$), while at the lowest temperature (10 °C) the higher AZA cell quota (220 fg $cell^{-1}$) and the lowest growth (0.12 d^{-1}) were obtained (Jauffrais et al., 2013). The non-high toxicity of *Azadinium* sp. strain in TSB could be related to the seawater temperature in the winter season (between 14 to 15 °C).

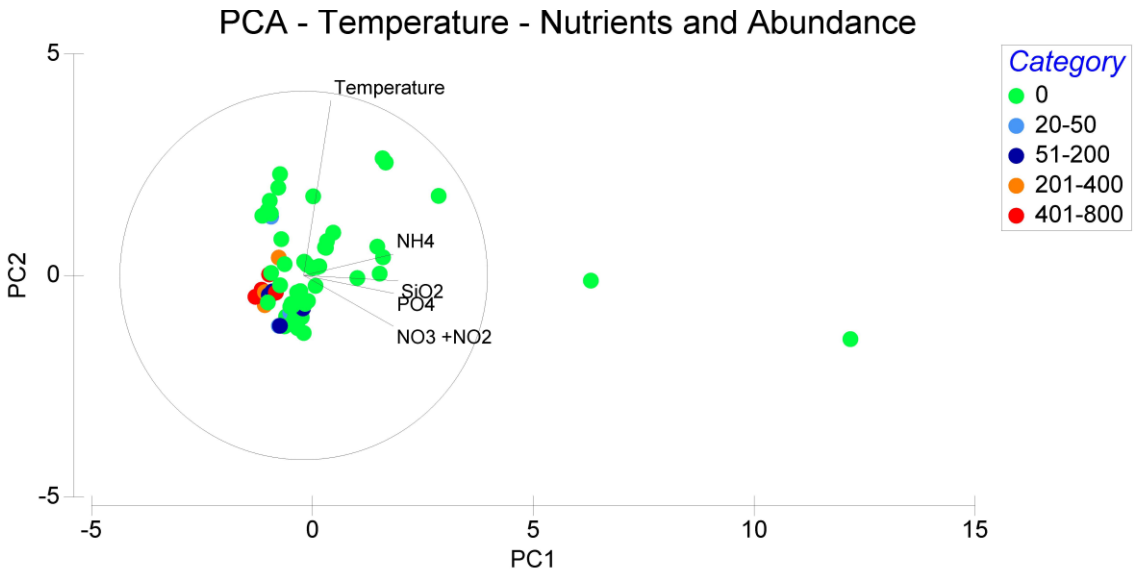

Figure. 23 Results of principal component analysis (PCA) that shows the relationship between the abundance of *Azadinium* sp. (category) and the environmental variables (temperature and nutrients) of Salsipuedes and Todos Santos Bay. These results correspond to the data from the surface water of the seven sample stations in the 2016-2017 monitoring.

Predict the conditions for the presence of the one species is complicated; multiple factors interact in the environment. In this study, the analysis of some physical and chemical variables was done. However, it is necessary to consider also the ecology of the species and biological interactions. It is little known about the ecology of *Az. spinosum* due to their difficulty to be identified and quantified (Tillmann et al., 2014), but the seasonality observed in the TSB could be correlated to the low competition with other phytoplankton species in the winter, making them more successful. During the 2016 – 2017 period, the conditions in the Bay were still anomalous due to the warm anomaly "Blob" from 2013 to 2014 and the "El Niño Godzilla" event in 2015-2016. Then abundance of diatoms and dinoflagellates decreased significantly (Fimbres, 2019). Then it was not possible to see the biological interactions. Furthermore, it is necessary to mention that nitrate limitation is not the only or main factor for the presence of the species in the TSB.

3.4 Conclusions

The first record of *Azadinium spinosum* in the Northwestern of Mexican Pacific was obtained in this study by the use of species-specific primers. The evidence of its presence was the detection of AZA-1 accumulated in the cultivated mussels. Both toxin and the species presented a clear temporality of appearance during the winter. Cold months seem to provide the conditions for the accumulation of this species in the region associated with a homogeneous column with distributed nutrients. The nutrients do not be a limitation for the species. Contrary to be expected, the low water temperatures were not correlated with the abundance of *Azadinium* sp. The distribution of the species in the TSB was oceanic, the seasonal surface currents transport the cells into the coast. The temperature range for the higher abundance in Salsipuedes and Todos Santos Bays was between 14 to 16 °C, and this temperature could be related to the non-high toxicity of *Az. spinosum*. Although the concentrations of azaspiracids are below the maximum permissible limit; there has been an annual increase. Therefore it is necessary to continue monitoring both the species and the toxin, which could be an emerging risk in the region.

Chapter 4. Morphological and molecular characterization of the marine dinoflagellate *Heterocapsa calafianiensis* sp. nov. (Dinophyceae) from Todos Santos Bay, México

4.1 Introduction

The *Heterocapsa* genus has had a confusing story in its classification. Stein (1883) established the genus *Heterocapsa*. However, the formal type of the name was based on the identification of the species *H. triquetra* (=*Glenodinium triquetrum,* Ehrenberg) by Loeblich and Loebich (1966). Unfortunately, *G. triquetrum* applies to a species belongs to *Kryptoperidinium* (Gottschling et al., 2018; Tillmann et al., 2017c). After extensive review, and due that not validly published species name has existed for *H. triquetra*, Tillmann et al. (2017c) describe a new species named *H. steinii*, and Gottschling et al. (2018) proposed to conserve the genus *Heterocapsa* with *H. steinni* as a conserved type.

Heterocapsa is a genus of relatively small dinoflagellate species. The smallest recognized species of the genus is *H. minima* (7.5 µm lenght), and *H. pacifica* is the largest species (30 µm lenght). The genus incudes twenty species (Iwataki, 2008), and *H. bohaniensis* is the species more recently added to the group (Xiao et al., 2018)

The most important characteristic to identify *Heterocapsa* species is the presence of organic three-dimensional body scales on the surface of the plasma membrane, which are unique to the genus (Iwataki et al., 2004), but not all of the species have these structures (Horiguchi, 1995; Iwataki et al., 2002). Also, the position of the pyrenoids and nucleus, and the pattern of the thecal plates are important morphological traits (Iwataki et al., 2004). General plate pattern of the genus according Kofoidean notation is: Po, X, 5', 3a, 7'', 6C, 5S, 5''', 0-1p, 2'''' (Salas et al., 2014).

Heterocapsa is ecologically important since this group since it is a conspicuous component of the phytoplankton community of coastal environments. Some species like *H. triquetra* and *H. rotundata* are cosmopolitan and contribute to carbon and nutrient cycling in coastal environments as they can form dense coastal blooms (Lindholm and Nummelin, 1999; Throndsen et al., 2007). Some species can have a deleterious effect on the environment and affect other organisms. *H. bohaiensis* and *H. circularisquama* produce toxins that affect the marine fauna. A mass mortality of cultivated bivalves and gastropods occurred in Japan during a *H. circularisquama* bloom that caused economic losses of around 93 million US dollars (Matsuyama et al., 1997, 2001). Moreover, blooms of *H. bohaiensis* caused high mortalities of

prawns (*Penaeus japonicus*) and larvae of crabs (*Erincheir spensis*) in aquaculture ponds located in Liaodong coast, China (Yang et al., 2015). The toxic effect of *H. circularisquama* is related to a potent light-dependent hemolytic toxin named H2-a, which is a porphyrin derivate (Miyazaki et al., 2005). This toxin tends to accumulate in the plasma membrane, and it is suggested that it has a necrotic mechanism (Kim et al., 2008). The compound that causes the toxicity in *H. bohaiensis* is a hemolytic toxin, but its action mechanism is still unclear (Zhang et al., 2019). The lethal effect of this toxin in rotifers was not affected by light conditions, as compared to *H. circularisquama* H*2-a* toxin.

In Mexico, there are some reports about the genus, a bloom of *H. rotundata* with cell concentration of 110.74 x 10^3 cells L^{-1} was recorded in the Jamapa estuary, Veracruz (Aké-Castillo et al., 2016). In Bahía de la Paz, two blooms of *H. triquetra* and *H. niei* were recorded within culture ponds (Gárrate-Lizárraga et al., 2006). The toxigenic *H. circularisquama* is considered a potentially toxic species in the Yucatán Peninsula (Herrera Silveira et al., 2010).

As in other coastal environments, in Todos Santos Bay (TSB), the *Heterocapsa* species are registered as a common component of the phytoplankton community (Fimbres Martínez, 2019). However, since the records are at the genus level, the species that are in the Bay and their toxic potential are unknown. TSB is located in the northwest of the Baja California Peninsula, Mexico, and in the region, the mariculture activities like the mollusks bivalves cultures, and tuna fattening have economic importance. Due to the *Heterocapsa* ability to form blooms and their toxic potential, it is necessary to characterize the species that are in the TSB. The aim of the present study was to isolate *Heterocapsa* species from TSB to characterize their phylogenetic relationships with strains from other regions and identify the isolated species by light microscopy and scanning electron microscopy to the morphological description and employing molecular test with specific primers to amplify the LSU (large ribosomal subunit) and ITS (internal transcribed spacer) rDNA. Additionally, the pigment profile was analyzed and the evaluation of the population growth in control conditions was performed, to know their potential to form blooms in the region.

4.2 Material and methods

4.2.1 Isolation and culture of *Heterocapsa calafianiensis* sp.nov

In November 2016 during winter season, two strains (named G3 and G8) of *H. calafianiensis* were isolated from Salsipuedes (Latitude: 31° 92'33'' N Longitude: 116°80'70'' W) and one strain (A1-B5) from the Punta Banda area (Latitude: 31°74'83'' N, Longitude: -116°67'83'' W), located in Todos Santos Bay region (Northwest Baja California Peninsula, Mexico). The California Current System influences this region (Pérez-Brunius et al., 2006)

Cultures were established from cells isolated from surface water samples collected with a 2 L Niskin bottle. At the laboratory, the sample was concentrated with a 10 µm mesh. *Heterocapsa* cells were picked up with a capillary micropipette under an inverted light microscope (Leica DM13000B, Leica Microsystems, Wetzlar, Germany) and placed in 96 cell-tissue culture plates with medium diluted with seawater (50:50). The strains were maintained in GSe medium 70% (70 medium: 30 seawater) (Blackburn et al., 2001). The temperature and salinity (16 °C; approx. 33 PSU) used for the maintenance of the strains are the same when the cells were collected from the field. Following bibliographic references a medium irradiance of 100 µmol quanta m^{-2} s^{-1} were choose in the culture.

4.2.2 Microscopy

Living or fixed cells (formaldehyde: 1% final concentration, or neutralized Lugol solution: 1% final concentration) were observed with an inverted microscope (Axiovert 200M; Zeiss; Munich, Germany) and a compound microscope (Axiovert 2; Zeiss), both equipped with epifluorescence and differential interference contrast optics. Photographs were taken with an Axiocam MRc5 digital camera (Zeiss, Germany). Videos of living cells were recorded using a digital camera (Gryphax, Jenoptik, Germany) at full-HD resolution. Single frame micrographs were extracted using Corel Video Studio software (Version X8). Cell length and width were measured at 1000 x microscopic magnification using freshly fixed cells (formaldehyde, 1% final concentration) from dense but healthy and growing strains (based on stereomicroscopic inspection of the living material) at late exponential phase and the Axiovision software (Zeiss). The shape and location of the nucleus was determined after staining of formalin-fixed

cells with 4'-6-diamidino-2-phenylindole (DAPI, 0.1 μg ml^{-1} final concentration) for 10 min (Tillmann et al., 2009a).

For scanning electron microscope (SEM), cells were collected by centrifugation (Eppendorf 5810R; 3220 *x* g for 10 min) from 2–15 mL of the culture, depending on cell density. The supernatant was removed and the cell pellet re-suspended in 60% ethanol prepared in seawater (final salinity ca. 13) in a 2 mL microtube at 4 °C for 1 h in order to strip off the outer cell membrane. Subsequently, cells were pelleted by centrifugation (Eppendorf 5415R; 16,000 *x* g for 5 min) and re-suspended in a 60:40 mixture of deionised water and seawater (final salinity approx. 13 PSU) at 4 °C for 30 min. After centrifugation and removal of the diluted seawater supernatant, cells were fixed with formaldehyde (2% final concentration in a 60:40 mixture of deionised water and seawater) and stored at 4 °C for 3 h. Cells were finally collected on polycarbonate filters (Millipore Merck; Darmstadt, Germany; 25 mm Ø, 3 mm pore-size) in a filter funnel, in which all subsequent washing and dehydration steps were carried out. A total of eight washing steps (2 mL MilliQ-deionised water each) were followed by a dehydration series in ethanol (30%, 50%, 70%, 80%, 95%, 100%; 10 min each). Filters were dehydrated with hexamethyldisilazane (HMDS), first in 1:1 HMDS:EtOH, followed by twice 100% HMDS, and then stored in a desiccator under gentle vacuum. Finally, filters were mounted on stubs, sputter coated (Emscope SC500; Ashford, UK) with gold-palladium and viewed under a SEM (FEI Quanta FEG 200; Eindhoven, The Netherlands). Micrographs were presented on a black background using Photoshop 6.0 (Adobe Systems; San Jose, USA).

4.2.3 Phylogenetic analysis

4.2.3.1 DNA extraction

Forty-five mL of exponentially growing culture was harvested and centrifuged at 3900 × g for 20 minutes. The cell pellet was stored at -80 °C. On the next day, DNA was extracted with a DNeasy Plant Mini kit (Qiagen, Hilden, Germany) according to the manufacturer's instructions. Disruption of cells was performed with a Mini-Bead Beater 24 (BioSpec Products, Bartlesville, United States) with two rounds at a speed of 6.0 m s^{-1} for 40 s, using 170 μm^3 of zirconium beads of 0.1 mm diameter. The DNA was resuspended in sterile Milli-Q water. The purity and concentration of DNA were measured by UV-

spectroscopy using a NanoDrop 2000 (Thermo Scientific, Wilmington, USA). The integrity of the DNA was verified using 1.2% agarose gel electrophoresis.

4.2.3.2 Polymerase Chain Reaction (PCR) amplification

The primers designed by D'Onofrio et al. (1999) were used to amplify the entire ITS1, 5.8S and ITS2 rDNA regions with an amplicon of 683 bp. The sequence of the forward primer ITS1 was 5'-TCCGTAGGTGAACCTGCGG-3' and 5'- TCCTCCGCTTATTGATATGC-3' for the reverse primer ITS4. The 28S rDNA (LSU D1- D2 region) amplification was performed with the forward DIR (5'-ACCCGCTGAATTTAAGCATA-3') and reverse D2C (5'-CCTTGGTCCGTGTTTCAAGA-3') primers that produced a DNA product of 764 bp (Edvardsen et al., 2003).

PCR reactions (30 μL) were conducted in a Veriti thermal cycler (Applied Biosystems, USA) using 80 ng of DNA. For ITS and 28S rDNA amplification, the master mix was prepared with the following concentrations: 0.4 mM of each dNTP, 0.12 μM of each primer, 4 mM of $MgCl_2$, 1 X GoTaq® Flexi buffer (Promega, Madison, WI, USA), and 1.25 U of GoTaq® DNA polymerase. The PCR was carried out at 94 °C for 4 min, followed by 40 cycles of 94 °C for 30 s, 55 or 60°C for 45 s (for ITS and 28S rDNA, respectively), 72 °C for 1 min, and a final extension step of 72 °C for 7 min. The PCR amplicons were analyzed on a 1.5% agarose gel electrophoresis and stained with GelRed.

4.2.3.3 Sequencing and phylogeny

The ITS and 28S rDNA PCR products were purified using a PureLink® Quick Gel Extraction Kit (Invitrogen) according to the manufacturer's protocol and sequenced by Sanger sequencing (SeqXcel, Inc., San Diego, CA). BLASTn (version NCBI-blast-2.7.1+) was used for the sequence homology analyses.

We used the species sequences reported by Tillmann et al. (2017c) for the phylogenetic analysis.

The alignment of 28S rDNA and ITS sequences were performed using CLUSTAL X software (Thompson et al., 1997), and MUSCLE software (Edgar, 2004), respectively. Phylogenetic trees were built with the

Maximum Likelihood method using the evolutionary model of Kimura 2-parameter for ITS rDNA and the Tamura-Nei (TN93) model for 28S rDNA, both with Gamma distribution. Initial trees for the heuristic search were obtained by Neighbor-Joining method to a matrix of pairwise distances estimated using the Maximum Composite Likelihood (MCL) approach. All positions containing gaps and missing data were eliminated. Nodal support was estimated by bootstrap analyses with 1000 replicates (Felsenstein, 1985) of the full heuristic algorithm, and the evolutionary analyses were performed in MEGA 7 software (Kumar et al., 2016). The species *Cochlodinium polykrikoides* and *C. strangulatum* were used as an outgroup in the 28S and ITS phylogenetic analysis, respectively.

Bayesian inferences (BI) were performed using MrBayes 3.1.2 (Ronquist and Huelsenbeck, 2003), using four chains of 1000 generation each by the Markov Chain Monte Carlo procedure. Sample frequency was 500, and the number of bur-in generations was 5000. The posterior probability (PP) values for the resulting 50% majority rule consensus tree were estimated after discarding the first 25% of the trees as burn-in.

4.2.4 Population growth characteristics

A stock culture of *H. calafianiensis*, A1-B5 strain in the exponential phase of growth (7.1 x 10^5 cell mL^{-1}) was used to inoculate three flasks with 250 mL of GSe medium. The inoculum was approximately 7.0 x 10^3 cell mL^{-1} for each flask. The cultures were maintained at 16 °C (sea surface water temperature when the specie was isolated) with an irradiance of 100 µmol quanta m^2 s^{-1} provided in a 12:12 hours light to dark cycle. Cell abundance was monitored every two days. A sample of each culture was fixed by Lugol-acetate solution and observed with an inverted light microscopy (Leica DM13000B, Leica Microsystems, Wetzlar, Germany). Cell counts were done in triplicate for each flask in a Neubauer chamber due to the small size of *Heterocapsa* (LeGresley and McDermott, 2010).

The growth rate (µ) was calculated from regression equation between natural log (ln) of cell abundance and time (Guillard, 1973) in the exponential growth phase.

4.2.5 Photosynthetic pigments analysis

For pigment analysis, 25 mL of *H. calafianiensis* (strain A1-B5) cultured at the same conditions detailed above were filtered through GF/F glass fiber filters (13 mm diameter) (Whatman, Kent, UK). The cells were harvested at the exponential phase of growth (day 5), with a cell abundance of 4.3 x 10^5 cell mL^{-1}. Filters were stored immediately at -80 °C. This analysis was performed in triplicate.

For pigment extraction, 1 mL of acetone was added to a 2 mL microcentrifuge tube containing the filter. Cells were disrupted using 170 μm^3 of zirconium beads of 0.1 mm diameter with one round of shaking in a Mini-Bead Beater 24 (BioSpec Products, Bartlesville, USA), at 6.0 m s^{-2} speed for 40 s. The samples were cleaned by two centrifugation steps at 13000 rpm for 8 min at 4 °C. Tetrabutylammonium acetate (TBAA) at 28 mM was added (30 µL of TBAA:100 µL of the sample) to the sample before injection to the high-performance liquid chromatography (HPLC) system.

Pigment analysis was carried out using the method described by Van Heukelem and Thomas (2001) modified by Almazan-Becerril and García-Mendoza (2008). The pigments were separated on a Zorbax XDB-C8 reverse-phase column (4.6 mm internal diameter and 150 mm in length, 3.5 µm particle size, Agilent Co, USA), using a 1260 Infinity II LC system (Agilent Co., USA). The binary solvent gradient consisted of two eluents with the following composition: methanol: TBAA 28 mM (70:30 v:v) as eluent A, and 100% methanol as eluent B. The solvent flow rate was 1 mL min^{-1}. The analytical gradient (% B, min) was: 5%, 0 min; 95%, 22 min; 95%, 27 min; 5%, 30 min. The pigments were detected (446 nm) by a photodiode array detector. The system was calibrated using fifteen pigment standards (DHI, Horsholm, Denmark). The identification of the pigments was performed by comparing the retention time of each peak with the commercial standards, and the calculation was done with the area value of each peak using the ChemStation software (Agilent, USA).

4.3 Results

4.3.1 Morphological description of *Heterocapsa calafianiensis* (Paredes-Banda, Hoppenrath García-Mendoza & Tillmann) sp. nov

Marine thecate photosynthetic dinophyte, elipsoid and slightly elongated in shape and scarcely dorso-ventrally compressed. Cells are between 16.6 to 19.6 µm long and 10.0 to 14.7 µm wide. Nucleus is positioned in the episome with one pyrenoid with starch sheath, and presumably one reticulate parietal chloroplast. Plate tabulation: APC (Po, cp?, X), 5', 3a, 7'', 6c, 5s, 5''', 2''''. Body scales are presented on cell surface with a triradiate basal plate with circular shape, inside a fine reticulation, and trefoil in the central basal plate. Body scales measure about 300 nm in diameter. Through the use of the TEM technique it was possible to see mature (long uprights) (A-D; Fig. 24) and immature scales (short uprights) (I – L; Fig. 24). Three-dimensional arrangement consisting in one central upright, six peripheral uprights and three radiated spines. Lacks the horizontal bars that interconnect the peripheral uprights, and some cells presented a central hole.

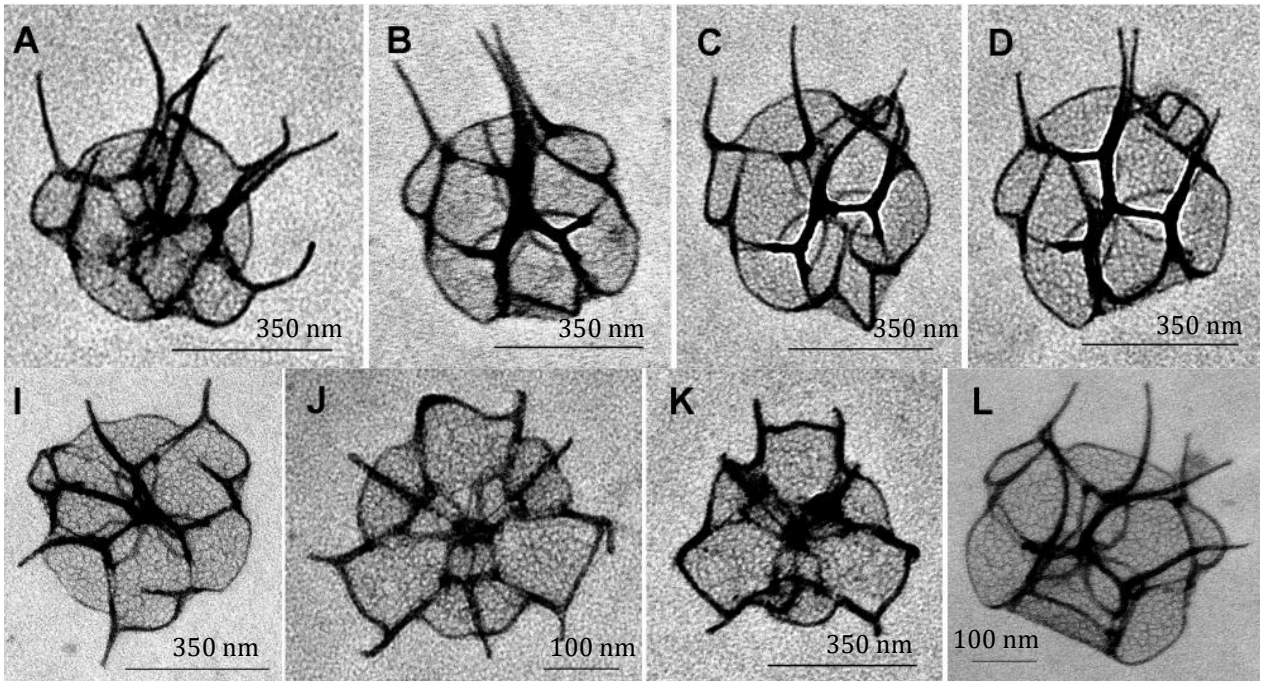

Figure. 24 Body scales of *Heterocapsa calafianiensis* sp. nov. (strain A1-B5): TEM micrographs (**A – D**) mature scales with long uprights. (**I – L**) immature scales with short uprights. The basal plate has a circular shape with fine reticulation. One central spine (**A, B, C**), six peripheral uprights (**J, K**) and three radiated spines (**J**).

HOLOTYPE: SEM stub CED (Urban Tillmann), prepared from clonal strain A1-B5 isolated from Punta Banda, Todos Santos Bay, Mexico. The stub is deposited at the Senckenberg Research Institute and Natural History Museum, Centre of Excellence for Dinophyte Taxonomy, Germany.

TYPE LOCALITY:

Todos Santos Bay (31° 48’ N and 116° 42’ W) is located in Northwest coast of Baja California Peninsula. It is a semi-enclosed body of water with two open sea entrances that are separated by Todos Santos Islands (Miranda Bojórquez, 2012).

HABITAT: marine coastal waters, planktonic

ETYMOLOGY: The species epithet *calafianiensis*, is to acknowledge the place where the species was isolated. Calafia was a queen of the mythical California Island described in a popular Spanish novel of the 14th century. When the Spaniards arrived at the peninsula they intertwined the legend of the mythical island of California, so they began with the denomination of California for these territories. This one of the theories of the origin of the name of the peninsula.

4.3.1.1 Detailed description

Using light and epifluorescence microscopy, all three clonal strains were identical in terms of size (Tab. 2) shape, and gross morphology. The selected strain A1-B5 were described and depicted in detail including SEM and TEM.

Motile cells were ellipsoid, slightly elongated, and had a conical episome and a hemispherial or slightly truncated hyposome. The episome ended in a pointed apical pore complex (Fig. 25B). The cells of strain A1-B5 have a mean average length of 16.7 µm and a width 11.7 µm. The mean length/width ratio was 1.43 (Tab. 2) and cells were slightly dorso-ventrally compressed (Fig. 23E). The cingulum was broad, incised, descending and displaced by almost its own width (Fig. 25C). Both cingulum and the broad sulcus were without prominent lists. A large and spherical nucleus was located in the episome (Fig. 25A, G, H). A single spherical pyrenoid surrounded by a starch sheath was located in the hyposome (Fig. 25A, B, E, F).

A presumably single chloroplast was reticulate and parietally arranged (Fig. 25D, H, I). No eyespot (stigma) or distinct accumulation body was visible with LM.

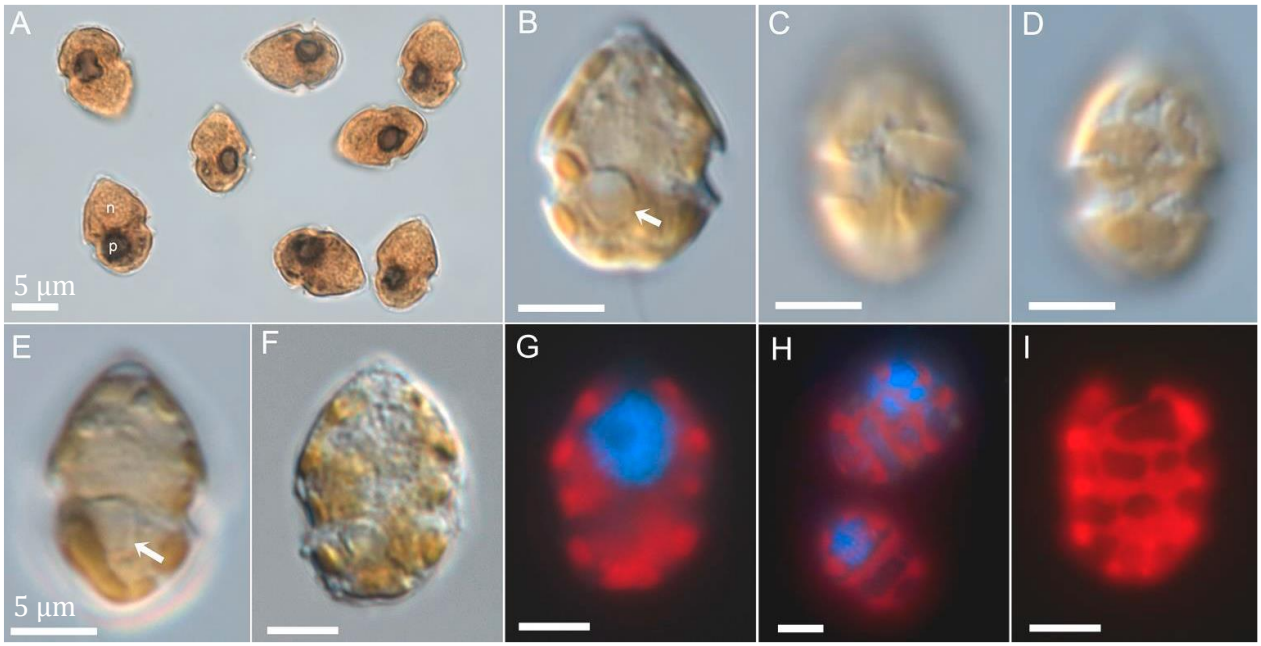

Figure. 25 *Heterocpsa calafianiensis* sp. nov. (strain A1-B5): LM of living and fixed cells. (**A**) Lugols iodine fixed cells. Note the large nucleus (n) in the episome and the dark stained pyrenoid (p) in the hyposome. (**B-E**) Living cells showing general size and shape. Note the pyrenoid (arrow) located in the hyposome. (**B-D**) The same cell in ventral view with three different focal planes. (**E**) Cell in lateral view. (**F,G**) The same formaldehyde fixed and DAPI stained cells in eplifluorescence view (UV excitation). (**I**) Cell in eplifluorescence view (blue light excitation) with chlorophyll autofluorescence to show the chloroplast structure. Scale bars = 5 µm.

Thecal plate were thin and difficult to observe using LM. The plate patter as resolved by detailed SEM (Figs 26 – 29) was APC (Po, cp?, X), 5', 3a, 7'', 6c, 5s, 5''', 2''''. The cells apex was surrounded by five apical plates and irregularly shaped small X-plate (Fig. 28B, C). The ventral (1') and both dorsal (3' and 4') apical plates were triangular at their distal end. The first two apical plates were hexagonal, both dorsal apical plate were pentagonal and the larger lateral plate 5' was octagonal. Three anterior intercalary plates were symmetrically arranged in dorsal position (Fig. 27). Within the clonal strain A1-B5 there was variability in the arrangement of epithecal intercalary plates. For the majority of cells (although not precisely quantified) both lateral intercalary plates 1a and 3a were 5-sided, whereas the central intercalary plate 2a was 7-sided an in contact with three postcingular plates (Fig. 27A–C). For a number of cells, plate 2a was slightly shifted to the left and in contact with two precingular plates (3'' and 4'') only, and thus both plates 2a and 3a were hexagonal (Fig. 27D–F). In the row of seven precingular plates,

the mid-dorsal plate 4'' was the smallest. On the ventral side, the precingular plate series was completed by the large anterior sulcal plate.

The apical pore complex consisted of a round pore, which was scattered with 6 – 10 thecal pores (Fig. 28D–G). Ventrally, and displaced to the cells right side, there was the irregularly shaped X-plate (or canal plate) which was in contact to the pore plate and the first (1') and last (5') apical plate (Fig. 26A, 28C). In the centre of the pore plate there was an oval rim (Fig. 28D, E) in whose centre there was a roundish pore visible from internal view (Fig. 28F, G). In external view, the pore was covered by a horseshoe-shaped plate (like the cover plate cp), which was invaded by another plate-like structure, which connected the cover plate and the X-plate (Fig. 28D–F). In internal view the pore plate was disconnected ventrally by a narrow slit in some cases (Fig. 26F) and continuous in other cases (Fig. 28G).

On the hypotheca there were five postcingular plates of roughly the same size, and two equally sized antapical plates (Fig. 29A, B). The cingulum (Fig. 29C, F) was composed of six cingular plates of comparable size. In the sulcal area, there were five sulcal plates (Fig. 29D–G). The large anterior sulcal plate (*sa*) extended into the epitheca and asymmetrically contacted apical plates 1' with a long, and apical plate 5' with a short suture (Fig. 26A, B; 28A). The centrally located posterior sulcal plate (*ps*) was large and extended into the hypotheca for more than 3/4 of its height (Fig. 26A, B). In the central sulcal area (Fig. 29D–G) the right sulcal plate extended the cingulum plate series. A left anterior (l*as*) and left posterior (*lps*) sulcal plate formed the left side of the sulcus. Plate *las* with its anterior part formed an inwardly directed pocket (Fig. 29D) where presumably both flagella emerged. In internal view of the central sulcal area there was an additional structure visible (Fig. 29F) with a more granular and wrinkled appearance different from the sulcal plates.

Thecal plates were smooth but had scattered thecal pores with a more or less pronounced and elevated outer rim (Fig. 26, 29A–C, H). Pores were irregularly distributed on most plates but were arranged in rows on postcingular plates, and to a lesser extent on precingular plates, towards the cingulum (Fig. 26, 29C). A number of pores were also present on the pore plate (Fig. 28D, E) and on the central sulcal plate (visible in internal view, Fig. 29G), whereas the X-plate was consistently free of pores (Fig. 28A–E).

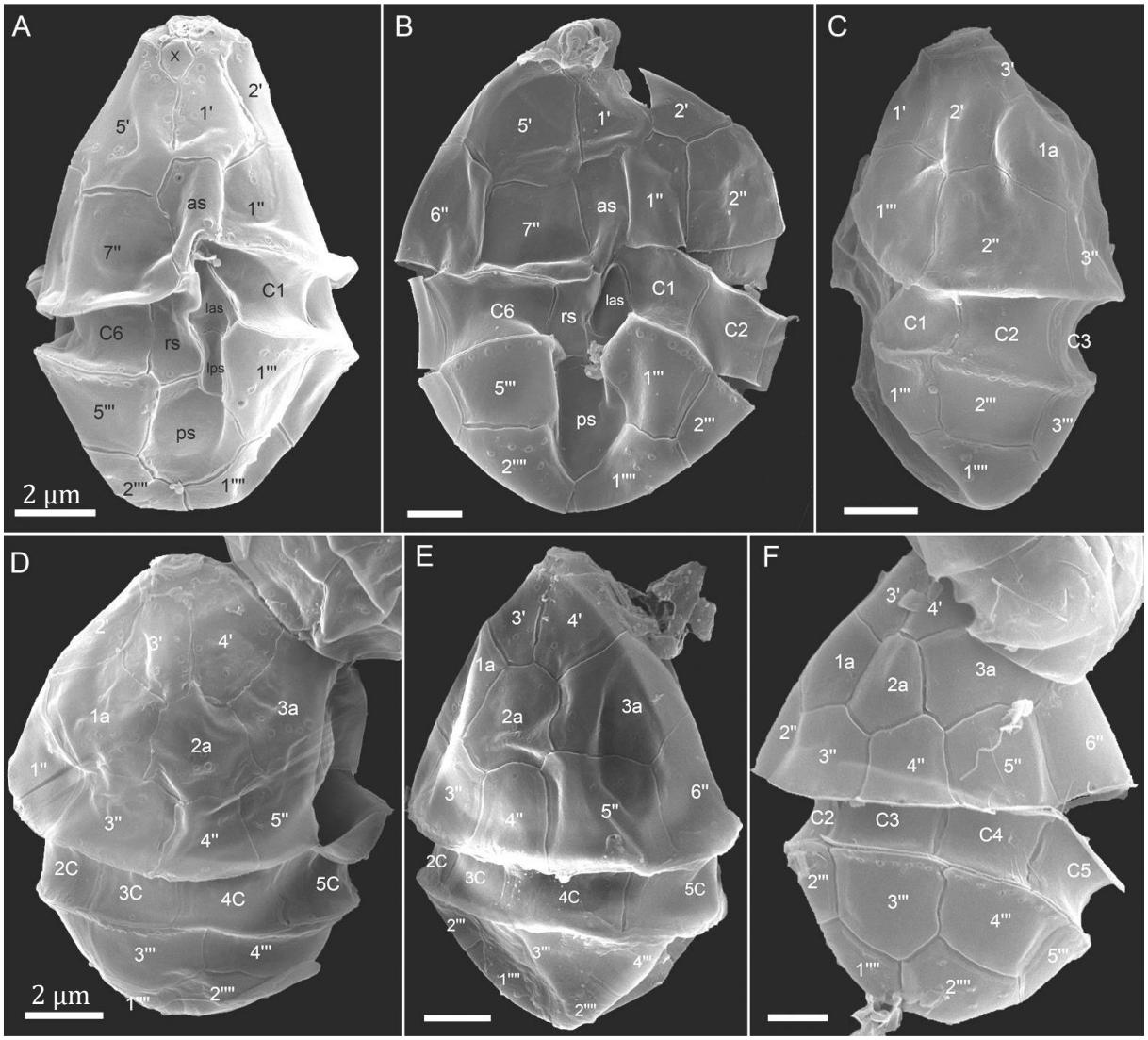

Figure 26. *Heterocapsa calafianiensis* sp. nov. (strain A1-B5): SEM micrographs of different cells in (**A, B**) ventral view, (**C**) left lateral view, and (**D – F**) in dorsal view. Note that the central epitheca intercalary plate 2a in **D** and **E** is heptagonal and in contact to three precingular plates, whereas in **F** this plate is hexagonal and in contact with two precingular plates only. Plate labels according to the Kofoidian system. Scale bars = 2 µm

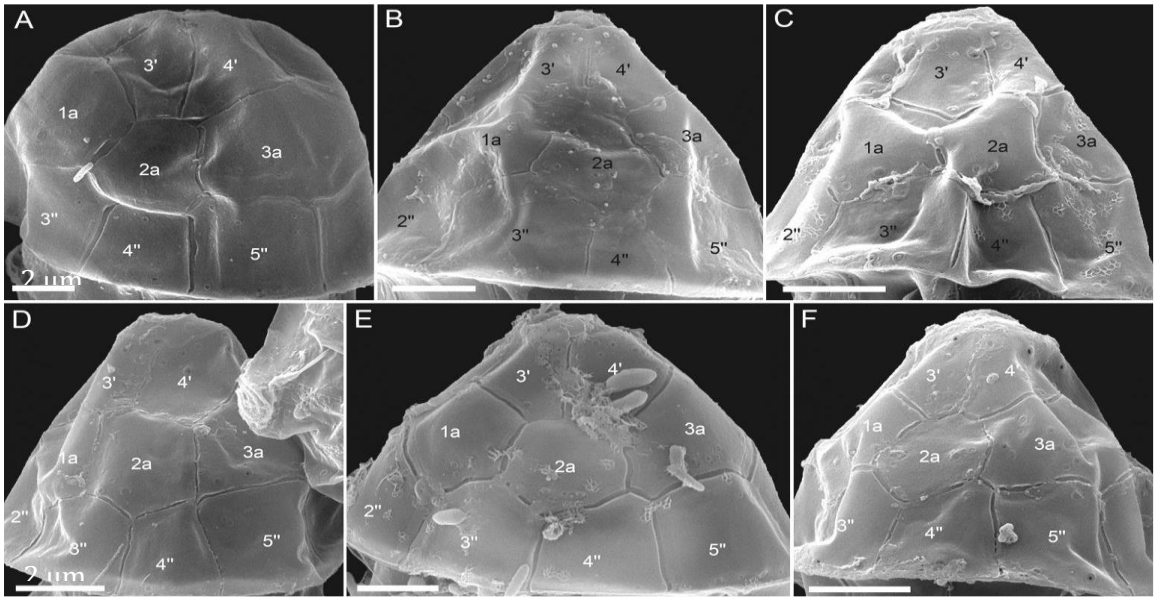

Figure. 27 *Heterocapsa calafianiensis* sp. nov. (strain A1-B5): SEM micrographs of epitheca of different cells in dorsal view. Note the heptagonal configuration of plate 2a in **A – C,** and the hexagonal configuration in **E** and **F.** For the cell in **D** the contact between 2a and 5 ' ' is just interrupted. Plate labels according to the Kofoidian system. Scale bars = 2 µm.

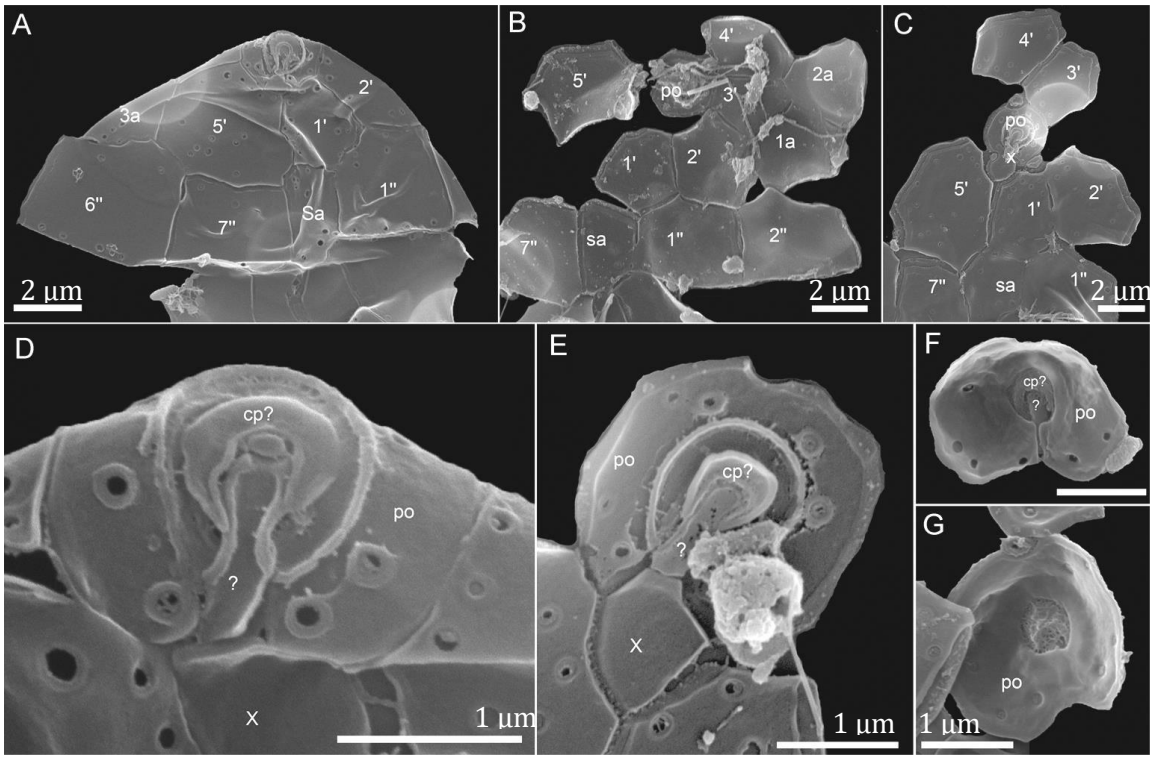

Figure. 28 *Heterocapsa calafianiensis* sp. nov. (strain A1-B5): SEM micrographs of epithecal details of different cells. (**A – C**) Epithecal plates in ventral (**A**) or apical (B, C) view. (**D – G**) Details of the apical pore complex (APC). Note that **F** and **G** represent internal views of the pore plate. Plate labels according to the Kofoidian system. Abbreviations: X: X-plate; *po*: pore plate; *cp*: cover plate; "?". unnamed structure between the cover plate and the X-plate. Scale bars = 2 µm (**A – C**) or 1 µm (**D – G**).

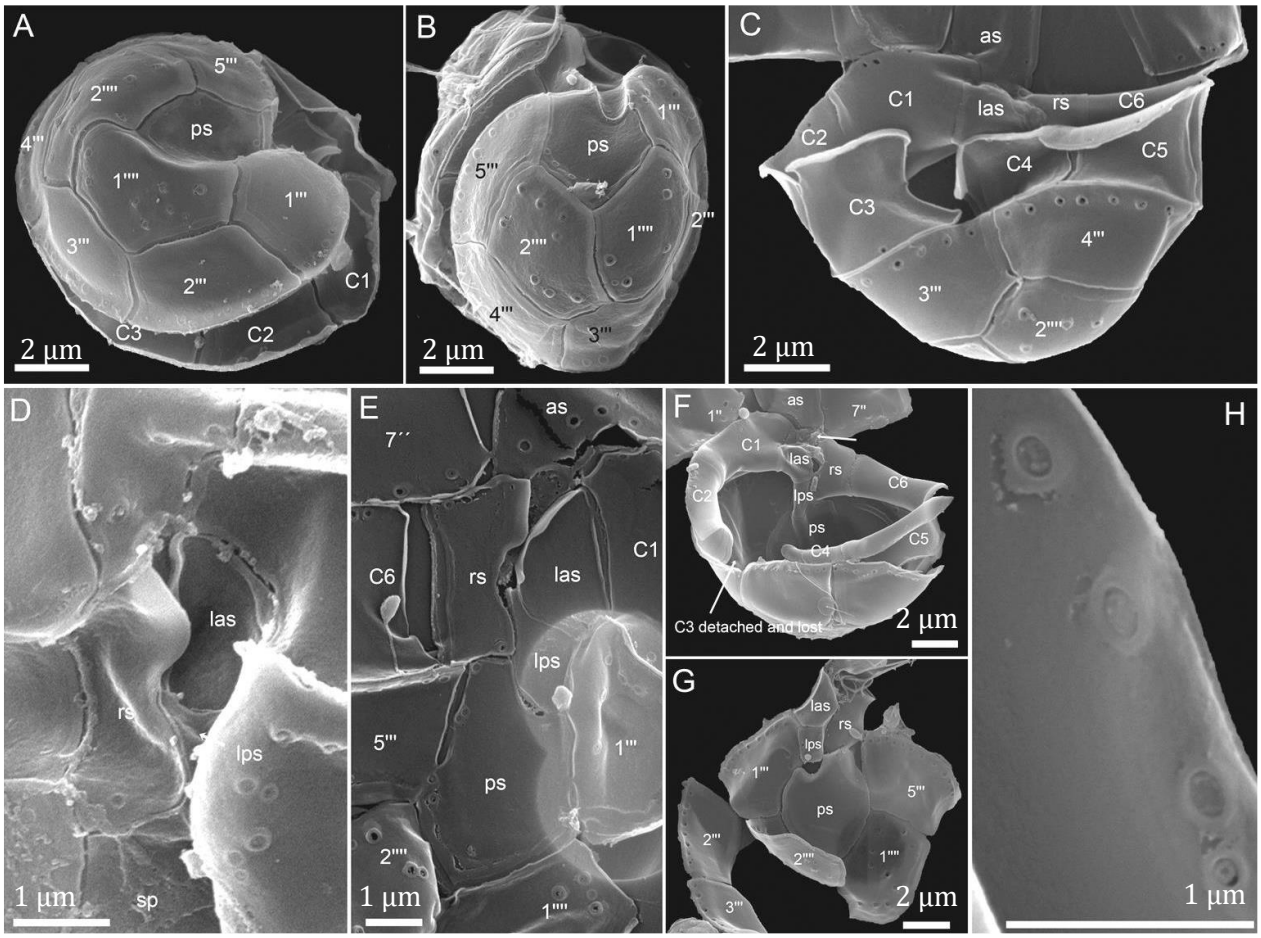

Figure. 29 *Heterocapsa calafianiensis* sp. nov. (strain A1-B5): SEM micrographs of hypothecal details of different cells. (**A, B**). Hypothecal plates in antapical view. (**C**) Cingular plates in dorsal view. (**D, E**) Detailed view of sulcal plates. (**F, G**) Detailed view of sulcal plate arrangement in internal view. (**H**) Detailed view of thecal pore structure. Plate labels according to the Kofoidian system. Abbreviations: *as*: anterior sulcal plate; *ps*: posterior sulcal plate; *rs*: right sulcal plate; *las*: Left anterior sulcal plate; *lps*: left posterior sulcal plate. Scale bars = 2 µm (**A – C, F, G**) or 1 µm (**D , E, H**).

Table 2. Cells size of three strains of *Heterocapsa calafianiensis* sp. nov.

Strain	**Length** **mean ± Std** **min – max**	**Width** **mean ± Std** **min – max**	**Length/width** **mean ± Std** **min – max**	**N**
A1-B5	16.7 ± 0.7 14.6 – 18.0	11.7 ± 0.7 10.1 – 12.8	1.43 ± 0.04 1.34 – 1.54	30
G3	16.0 ± 0.9 14.1 – 17.6	11.3 ± 0.6 10.0 – 12.2	1.42 ± 0.06 1.30 – 1.54	30
G8	17.1 ± 1.1 15.3 – 19.6	12.7 ± 0.9 10.9 – 14.7	1.35 ± 0.07 1.23 – 1.55	30

4.3.2 Phylogenetic analysis

The datasets generated from LSU (D1/D2 region) and ITS of the ribosomal rDNA operon showed that sequences of the A1-B5, G8 and G3 strains isolated from TSB are unique and clearly separated from all species within *Heterocapsa* for which sequence information is available.

4.3.2.1 Large Subunit (LSU) rDNA

A BLAST search was conducted on the obtained sequences to find the related sequences in the GenBank. The highest homology was a 94.81% identity with *Heterocapsa* sp. (EU165272) followed by a 94.36% identity with *H. niei* (JQ247713), now reclassified as *Heterocapsa* sp. by Tillmann et al. (2017c). In both cases, with 99% of sequence coverage and E value = 0. .

The phylogenetic tree of *Heterocapsa* species based on the LSU 28S rDNA molecular marker was built with 35 DNA sequences of 764 bp long. The best-scoring ML tree (- ln= 1388.95) is shown in Figure 30. There was a total of 231 positions in the final dataset. Seventeen distinct clades were obtained, including the one formed by the three LSU rDNA sequences from the strains isolated from the TSB (A1-B5, G8, and G3) (Fig. 30). The nodal support for the local strains was statistically low (65/0.70). In the genetic pairwise distance analysis *H. calafianiensis* was related with *Heterocapsa* sp. (as *Cachonina halii*) (AF033867) and *Heterocapsa* sp. (as *nei*) (JQ247713) with a *p*- value of 0.48. With a higher *p*-value of 0.057, another species related with *H. calafianiensis* was Heterocapsaceae sp. FIU 10 (EU165272) and *H.* cf. *pygmaea*. (EU165306, KT860562).

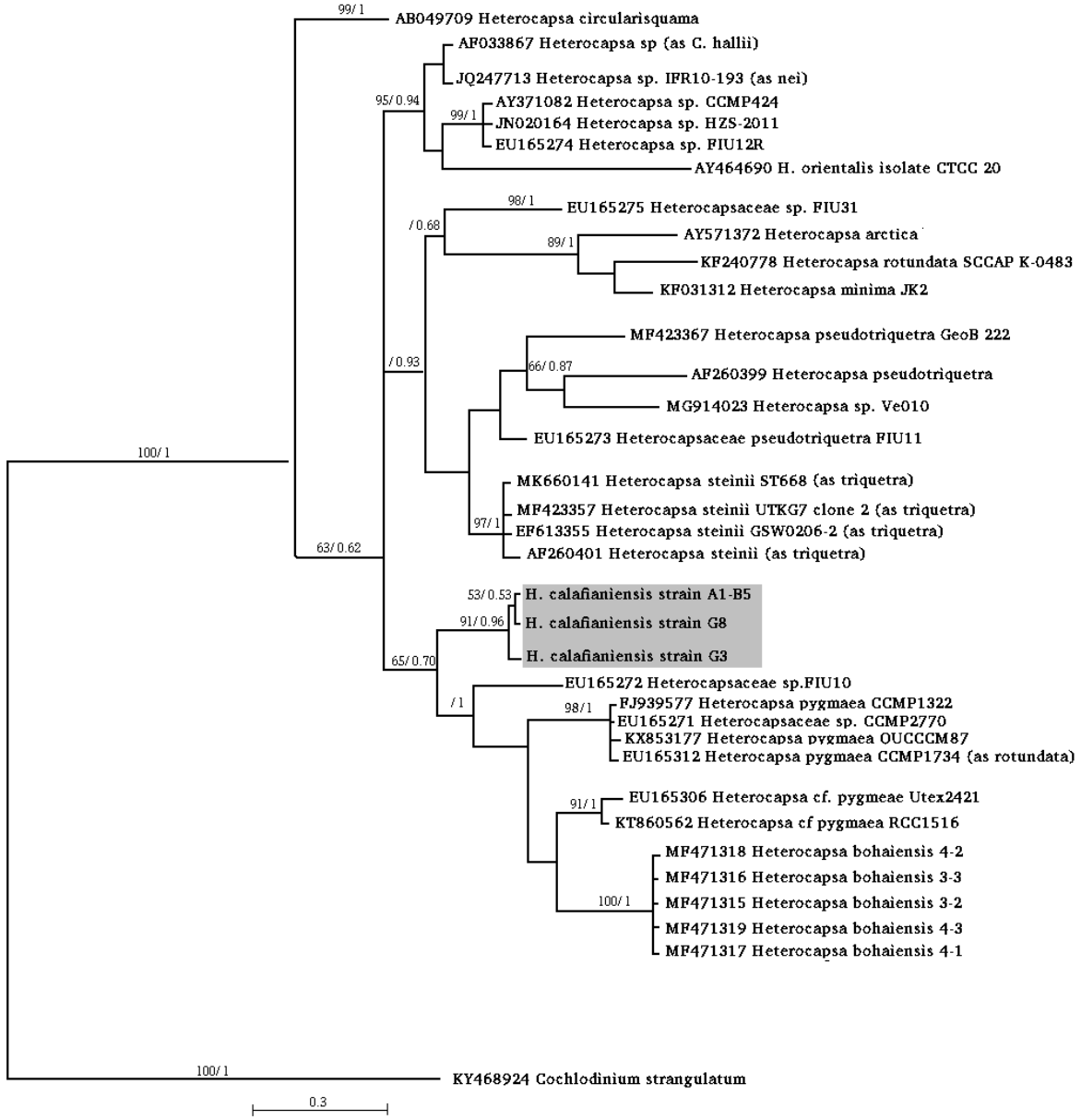

Figure 30. Phylogenetic tree of *Heterocapsa* species based on the maximum likelihood large ribosomal subunit) LSU 28S rDNA sequences. The numbers in the left of the branches are statistical support values (values < 50 are not shown) and next to slash are Bayesian inference *a posteriori* probabilities value. *Cochlodinium strangulatum* were used as outgroup. Bootstrap values (1000 replicates).

4.3.2.2 Internal Spacer Transcribed (ITS) rDNA

BLAST analysis with the ITS sequence resulted in a 90.67% identity of the BTS strains with *Heterocapsa* sp. (accession number: AB084099; AB084097), now identified by Tillmann et al. (2017c) as *H. horiguchii* with the 94% of coverage and E value = 0.

The phylogeny of *Heterocapsa* species based on the ITS molecular marker was built with 44 nucleotide sequences 683 bp long. The best-scoring ML tree (- ln= 772.26) is shown in Figure. 31. All positions containing gaps and missing data were eliminated. There was a total of 202 positions in the final dataset. Sixteen distinct clades were formed (Figure 31); the monophyletic clade, which corresponds to the local strains (A1-B5, G3, and G8) was clearly separated from other *Heterocapsa* species and had high nodal support of 90%. In the pairwise genetic distance analysis, the more related species was *H. horiguchii* (AB084099; AB084097) with *p*-value 0.062 and 0.066 respectively, the *p*-values for the sequences of all other *Heterocapsa* species analyzed were >0.13. The topologies for trees generated through ML and Bayesian inference were the same with similar bootstrap and posterior probability values.

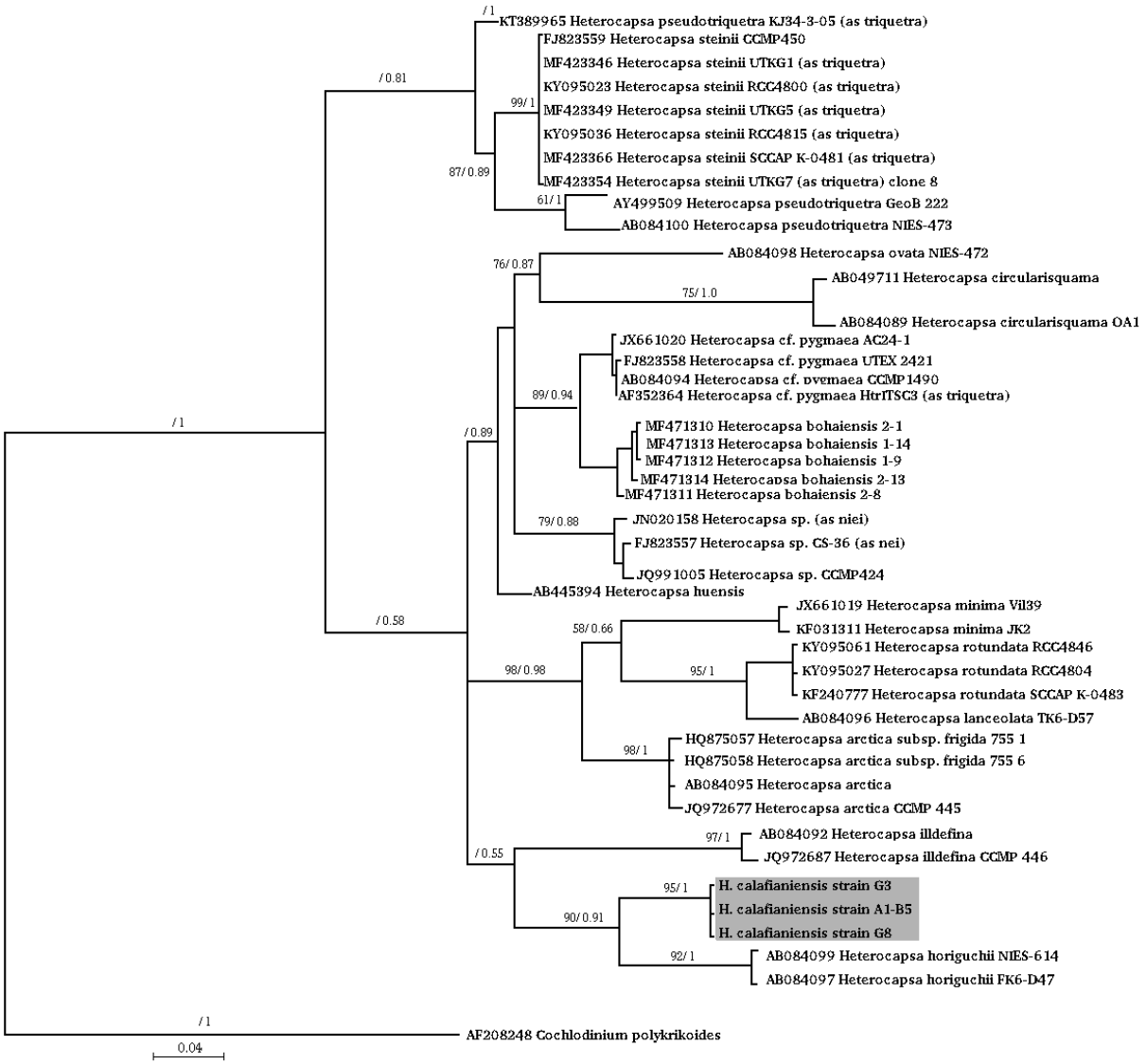

Figure 31. Phylogenetic tree of *Heterocapsa* species based on the maximum likelihood internal transcribed spacer (ITS) rDNA sequences. The numbers in the left of the branches are statistical support values (values < 50 are not shown) and next to slash are Bayesian inference posteriori probabilities value. *Cochlodinium polykrikoides* were used as outgroup. Bootstrap values (1000 replicates).

4.3.3 Characterization of growth population

The population growth of *H. calafianiensis* was characterized. Cell abundance was monitored for 17 days when the culture started to decay. Figure 30 shows that *H. calafianiensis* presented a short lag phase (< 2 days) when cultured at 16 °C with an irradiance of 100 µmol quanta m^{-2} s^{-1}. The exponential phase started on the third day, and was relatively short (8 days), and the highest cell density of 118 x 10^3 cells mL^{-1} was reached on day 11 (Fig. 32). Therefore, the stationary phase was registered 13 days after inoculation. The maximum growth rate was 0.63 d^{-1}.

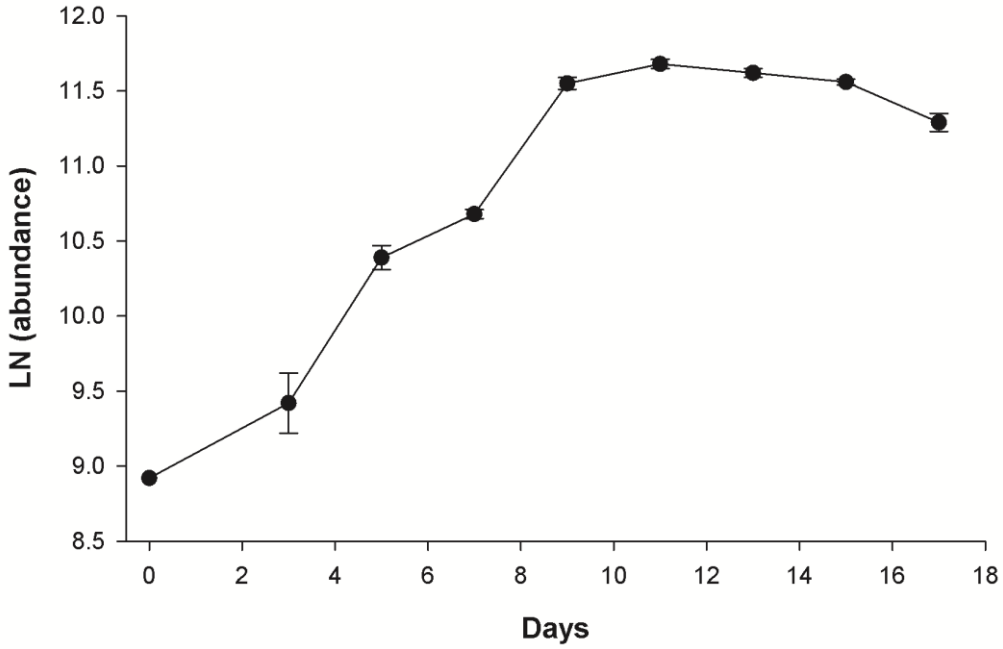

Figure 32. Population growth characteristics of *H. calafianiensis* strain A1-B5 maintained at 16 °C with an irradiance of 100 µmol quanta m^{-2} s^{-1}. The Log of the cell abundance over time is presented.

4.3.4 Pigments analysis

Pigments detected in the HPLC analysis of *H. calafianiensis* (strain A1-B5) are shown in Figure 33. Peridinin was the major accessory pigments followed by the carotenoid dinoxanthin and Chl c_2. Other carotenoids detected were diadinoxanthin, iso-peridinin and β,β-carotene. Chl *a* was the principal photosynthetic pigment. The identity of absorbance peak with the retention time of 11.72 min could not be confirmed. The concentration of each pigment in cells sampled during the exponential phase of growth is presented in Table 3.

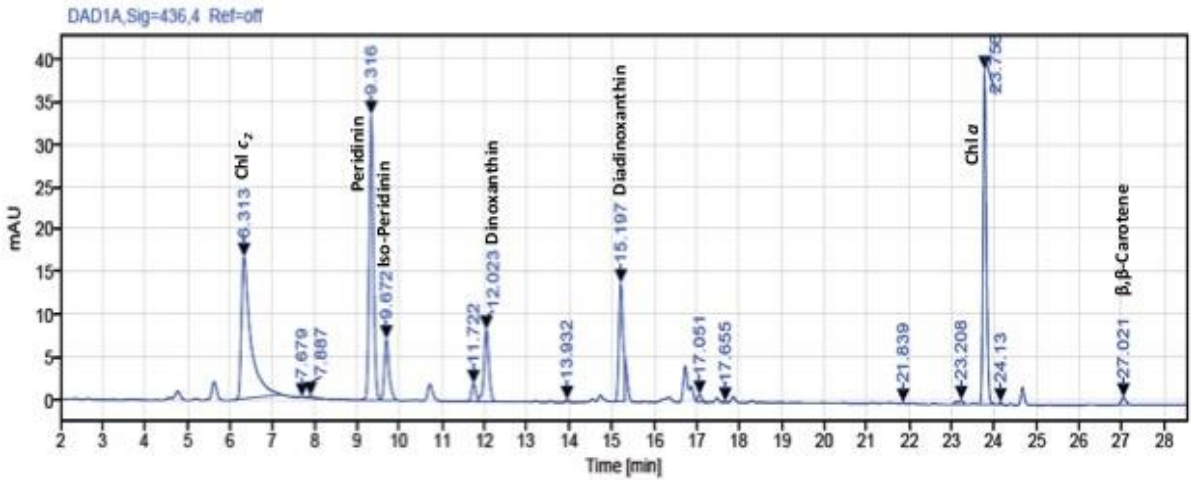

Figure 33. Chromatogram of pigments of *H. calafianiensis* in cells sampled on cultures at exponential phase of growth. The pigments were detected at 436.4 nm.

Table 3. Cellular pigment concentration of *H. calafianiensis* in exponential phase of growth. The mean +/- standard deviation of three replicates is presented.

Chl c_2	**Peridinin**	**Iso Peridinin**	**Diadinoxanthin**	**Dinoxanthin**	**Alomers Chl *a***	**Chl *a***	**β,β carotene**
pg cell^{-1}	pg cell^{-1}	pg cell^{-1}	pg cell^{-1}	pg cell^{-1}	pg cell^{-1}	pg cell^{-1}	pg cell^{-1}
1.325 ± 0.12	2.105 ± 0.19	0.509 ± 0.04	0.755 ± 0.08	0.558± 0.055	0.090 ± 0.01	5.043 ± 0.863	0.060 ± 0.01

4.4 Discussion

4.4.1 Morphology

The taxonomic criteria for the identification of *Heterocapsa* genus at the beginning were the cell shape and the presence of sutures only on the epitheca (with the type species *H. triquetra*: Stein 1883) to establish the genus. Later the plate pattern of whole cell and size became important characters for the species description (Loeblich 1969; Herman and Sweeney, 1976 in Iwataki et al., 2002). Recently the ultrastructure of triradiate body scales had been recognized as essential requirement for the establishment of a new *Heterocapsa* taxon (Iwataki et al., 2002). The plate tabulation: APC (Po, cp?, X), 5', 3a, 7'', 6c, 5s, 5''', 2'''', the reticulated parietal chloroplast, and the

body scales situated immediately above the plasma membrane are the congruous morphological characters that place a *H. calafianiensis* within the *Heterocapsa* genus (Iwataki, 2008).

The cell morphology and thecal plate arrangement of *H. calafianiensis* shown a similar morphology with *H. horiguchii* both are ellipsoid cells (about average of 16.7 – 17.2 µm in length) although the size of the epitheca is relatively larger than hypoyheca in *H. calafianiensis* and in *H. horiguchii* both have almost equal size (Iwataki et al., 2002). Also the body scales are similar between *H. calafianiensis* and *H. horiguchii*; in both the scales consist of a basal circular plate with a central upright and six peripheral uprights, three radiating spines, six ridges radiate across the basal plate and measures about 300 nm (Iwataki et al., 2002). The difference is the absence of the three radial bars in *H. calafianiensis* and the presence of a central hole as in *H. rotundata* (Hansen, 1995). The body scales of *H. laceolata* also posses a central hole but the cell shape of *H. laceolata* is very different from *H. calafianiensis* with a large ephiteca, which is almost twice the length of the hypotheca and is unique within the genus (Iwataki et al., 2002). The difference in the cell shape, size, nucleus and pyrenoides position is described among the Heterocapsa species is described in table 3.

Some intraspecific variations in the thecal plate arrangement of *H. calafianiensis* had been observed. The apical pore complex (APC) comprises an apical pore plate (Po), and a canal plate (X) covered by a cover plate (cp). The Po has between 6 to 10 thecal pores, in *H. minima* the presence of only 6 thecal pores around the Po plate has been observed (Salas et al 2014). An extra structure acting as connection (?) (nameless structure) between X and cp was recorded in *H. minima* (Salas et al., 2014) and in *H. niei* (Steidinger y Tangen, 1996), this (?) was the same structure observed in *H. calafianiensis*.

H. calafianiensis, like all other species of the genus, has 6 cingular plates.

The fourth and third precingular plates are the keystone plates in *H. calafianiensis*, instead in *H. triquetra* only the fourth precingular plate is the keystone plate (Tillmann et al., 2017c).

Table 4. Morphological characteristics of species of genus *Heterocapsa* (Iwataki et al., 2002; Xiao et al., 2018) and modified in this study.

Species	Lenght (µm)	Cell shape	Nucleus/ Position	Pyrenoid number/ position	Body scales/ size/spines
H. artica	22.5 – 37.5	Ellipsoidal, larger epitheca	Ellipsoidal/ middle	1/ hypotheca	Triangular/ 350-400 nm/9-12
H. circularisquama	20.0 – 28.8	Ellipsoidal, equal size (epi and hypotheca)	Ellipsoidal/ left side	1/ middle	Circular/ 400 nm/ 6
H. horiguchii	13.2 – 20.8	Ellipsoidal, equal size (epi and hypotheca)	Spherical/ epitheca	1/ hypotheca	Circular/ 310 nm/ 6
H. huensis	13.0 - 25	Ellipsoidal, equal size (epi and hypotheca)	Spherical	Multiple/ above nucleus	Triangular/550 nm/ 9
H. illdefina	22.0 – 25.0	Ellipsoidal, equal size (epi and hypotheca)	Ellipsoidal/ middle	1/ middle	Triangular/ 430 nm/ 9
H. minima	7.4 – 10.0	Ellipsoidal, larger epitheca	Spherical/ hypotheca	1/ above nucleus	Circular/ 400 nm/ 6
H. niei	17.0 – 20.0	Ellipsoidal, equal size (epi and hypotheca)	Ellipsoidal/ right side	1/ epitheca	Triangular/ 300 nm/15
H. orientalis	18.0 – 35.0	Spherical, equal size (epi and hypotheca)	Spherical/ posterior	1/ above nucleus	Triangular/ 300 nm/9
H. ovata	23.0 – 24.0	Spherical, equal size (epi and hypotheca)	Spherical/ anterior	1/ below nucleus	Triangular/ 220 nm/6
H. pygmaea	13.3	Ellipsoidal, equal size (epi and hypotheca)	Spherical/ posterior	1/ epitheca	Circular/ 400 nm/ 6
H. rotundata	9.0 – 11.7	Bullet-like, larger epitheca	Ellipsoidal/ dorsal	1/ epitheca	Triangular/ 350 nm/9
H. triquetra	19.0 – 30.0	Rhomboidal, equal size (epi and hypotheca)	Spherical/ ephiteca	1/ hypotheca	Triangular/ 250 nm/9

Species	Lenght (µm)	Cell shape	Nucleus/ Position	Pyrenoid number/ position	Body scales/ size/spines
H. pseudotriquetra	18.0 – 28.0	Spherical, equal size (epi and hypotheca)	Spherical/ anterior	1/ below nucleus	Triangular/ 240 nm/9
H. lanceolata	16.4 – 25.0	Lanceolate, larger epitheca	Ellipsoidal/ middle	1/ epitheca	Hexagonal/ 500 nm/9
H. pacifica	45.0	Rhomboidal, equal size (epi and hypotheca)	Elliptical/ right side	1/ above nucleus	n.d
H. bohaiensis	9.9 – 16.5	Ellipsoidal, larger epitheca	Oval to ellipsoid/ middle	1 – 3/ above or aside nucleus	Triangular/ 300-350 nm/9
H. calafianiensis	16.6 – 19.6	Ellipsoidal, larger epitheca	Spherical/epitheca	1/ hypotheca	Circular/ 300 nm/9

4.4.2 Phylogenetic taxonomy

In this study, we presented the phylogenetic analysis of *H. calafianensis* sequence of the ITS1, 5.8S, and ITS2 regions and LSU D1-D2 regions. In both cases, we found a monophylogenetic group for *H. calafianiensis* isolated from TSB, which differs from other *Heterocapsa* species that have been described before in the GenBank database. The morphological identification and the molecular phylogenetic analysis support the new record for this genus.

Dinoflagellates classification is difficult due to its wide variety of forms and evolutionary diversity. Around 2000 species of dinoflagellates have been described; the use of molecular markers to the specific identification of the species has been implemented (Smayda and Reynolds, 2003). There have been attempts to develop DNA barcoding that helps the species identification, especially in field samples. Two mitochondrial markers were tested, the cytochrome oxidase I (COI) (Stern et al., 2010) and the oxidase B (COB) (Lin et al., 2009). However, they had a variable success because they could not amplify all dinoflagellates strains or could not resolve ambiguous genus to species level (Stern et al., 2012). In this study, we used the intergenic regions (ITS), because the database has a lot of sequences to compare, also it has been shown that it can differentiate cryptic/ pseudo-cryptic species (Hariganeya et al., 2013; Vandersea et al., 2012) and is useful because it diverges faster during speciation, providing a better resolution between recently diverged taxa (Litaker et al., 2007).

The closely related species with the ITS marker was *H. horiguchii*, with *a p-value* of 0.06. Therefore, their OTUs (Operational Taxonomic Units) are related to being sister taxa with *H. calafianiensis* in the phylogenetic tree. Litaker et al. (2007) mention that a *p-value* > 0.04 could be used to delineate the most free-living dinoflagellate species using the ITS region, the *p-value* calculated in this study support the speciation of *H. calafianiensis* and our results are in line with the author. In another study, Stern et al. (2012) suggest the use of the cut-off value of 0.02 for some conspecific strains of dinoflagellates. Still, the author mentions that in the case of *Heterocapsa*, a higher *p-value* between 0.032 to 0.094 is useful because it reflects the cryptic diversity of the genus.

The LSU rDNA phylogenetic tree had less resolution, with low statistical nodal support (LBS 65, BPP 0.7). Notwithstanding, an independent clade was formed for *H. calafianiensis* as in the ITS, this less resolution is related to the characteristics of this molecular marker, which has highly variable regions intermixed with very conservative areas (Hillis and Dixon, 1991). The D domains are useful to reconstruct relatively

recent evolutionary events (Lenaers et al., 1991). The combination of different molecular markers ensure the identification of species (Salas et al., 2014; Tillman et al., 2017; Xiao et al., 2018).

The pairwise genetic distance of the LSU genes is different from the ITS; this is because there are not LSU 28S rDNA sequences available for *H. horiguchii*. The closely related species with *H. calafianiensis* was *Heterocapsa* sp. (as *H. nei* and as *Cachonina halii*) not yet identified.

The history of the description of this genus has been confusing, and some misidentifications of the species have occurred (Gottschling et al., 2018; Tillmann et al., 2017c; Yoshida et al., 2003). Therefore, some sequences deposited in the GenBank are misidentified. Stern et al. (2012), tried to make a phylogenetic identification of *Heterocapsa* species, but found that the genus has multiple name synonyms. In the same way *H. pygmeae* (CCMP1322) (Iwataki et al., 2004) that is identical to *Glenodinium halii* (CCMP2770), which was changed to *C. halii* and then to *H. halli*. This last name is recognized as a heterotypic synonym of *H. illdefina* (Morrill and Loeblich, 1981). These complicate establishing phylogenetic relationships.

4.4.3 Growth characteristics

In the ocean environment, the structure and composition of the dinoflagellates population are driven by a combination of biological, chemical, and physical factors. Light energy, temperature, the availability of nutrients, as well as genotype, are key factors in growth patterns for dinoflagellates (Smayda and Reynolds, 2003).

In this study, the µ*max* for *H. calafianiensis* was 0.63 d^{-1} during the culture exponential phase until day 11 and a maximum cell density of 118 x 10^3 cells mL^{-1}. The growth rate seems to be higher compared to other dinoflagellates. For example, *A. ostenfeldii* was cultured for 20 days at 16 °C with 12 h light: 12h dark and 155 µmol quanta m^{-2} s^{-1} and had a maximum growth rate of 0.14 d^{-1} with a cell density of 146 x 10^2 cells mL^{-1} (Medhioub et al., 2011). This difference in the growth rate could be explained by the difference of the cellular diameter of each species. Algal ecologist has established that the growth rate in an algal population (µ in divisions per day) decreases with increasing cell size (Mizuno, 1991; Niklas, 1994). Otherwise, Banse (1977) suggested that a low growth rate is directly related to a low photosynthetic capacity, which means low chlorophyll *a* ratios between the carbon (Chl *a*: C). In the

study of Medhioub et al. (2011), the cell diameter of *A. ostenfeldii* was 26-27 µm, while the cell size of *H. calafianiensis* is 16.0-17.1 µm in length.

Otherwise, *Azadinium. spinosum* is a small photosynthetic dinoflagellate with a length between 12.0 – 16.0 µm (Tillmann et al., 2009a). In a study conducted by Kilcoyne et al. (2019) with *Az. spinosum* at cultured conditions of 18 °C with 12 h light: 12h dark and 32 µmol quanta m^{-2} s^{-1}, the maximum growth rate was 0.22 d^{-1}. This growth continues to be less than our study. The temperature and light intensity are two determining parameters that influence the growth kinetics in dinoflagellates (Garcés and Masó, 2001). Then, it is possible that the low experimental irradiance in *Az. spinosum* reduces its growth rate.

There are a few studies about the growth rate of *Heterocapsa*, Tarutani et al. (2001) characterized the growth of *H. circularisquama* (20.0 – 28.8 length) in the following experimental conditions (20 °C with 12 h light: 12h dark and 50 µmol quanta m^{-2} s^{-1}), the author recorded a µ*max* between 0.69 – 0.72 d^{-1}, which were similar to our study. *H. triquetra* (19.0 – 30.0 length) was grown with low turbulence at 15 °C with 16 h light: 8h dark and 90 µmol quanta m^{-2} s^{-1}, under these conditions a mean growth rate of 0.42 d^{-1} were registered (Havskum and Hansen, 2006). It is difficult to compare growth rates because each culture condition influences the physiology of the cells; however, apparently, *Heterocapsa* genus has a higher growth rate compared to other dinoflagellates.

4.4.4 Pigment profile

H. calafianiensis has a dinoflagellate Type-1 pigment profile. Peridinin, dinoxanthin, and Chl c_2 are the main pigments that define this group (Zapata et al., 2012). The types of chloroplast correspond with the evolutionary lineages within dinoflagellates; those of Type-1 were acquired through a secondary endosymbiosis. According to the type of the chloroplast are six different types; most dinoflagellates species correspond to the Type-1 (71% species, 51% strains) (Zapata et al., 2012).

The toxin profile that we found coincides with that described for *H. triquetra* by Haguet et al. (2017). They analyzed the pigment composition by reverse-phase HPLC and did a thorough search finding also carotenoids P457, pyrrohoxanthin, 2,4 magnesium divinyl phaeoporphyrin a*5* monomethyl ester (MgDVP), peridininol, and diadinochrome. *Scrippsiella* genus has chloroplasts Type-1 and their pigment profile is the same as *H. calafinianiensis;* however, the author also detected MgDVP and peridininol

(Fagín et al., 2019). The peak with the retention time of 11.72 min of this study might be MgDVP, which has a retention time of 10.83 – 11.0 min in the method standardized by Zapata et al. (2000), but it needs to be confirmed with a standard.

Under the culture conditions in which *H. calafianiensis* was maintained, a lower pigment concentration was recorded compared to those reported for *H. pygmaea* that was 7.05 pg cell^{-1} of peridinin (at 35 µmol quanta m^{-2} s^{-1}) (Johnsen et al., 1994). Meanwhile for *H. calafianiensis* we registered 2.10 pg cell^{-1}. This difference could be related with the low irradiance used for *H. pygmaea* culture. The peridinin has a carbonyl group in their molecular structure to fulfill the light-harvesting function during photosynthesis (Di Valentin et al., 2008); then at low irradiance more pigment is needed.

4.5 Conclusions

In this study by morphological characterization and phylogenetic analysis, conclusive results were obtained to make the description of a new *Heterocapsa* species. A monophyletic group of *H. calafianiensis* was formed with an independent clade by the analysis of the ITS and LSU sequences. The phylogenetic tree showed statistical support, and the *p*-value of the ITS region confirmed the speciation of *H. calafianiensis*. In the morphological description the plate tabulation was like the typical one described for genus: APC (Po, cp ?, X), 5 ', 3a, 7' ', 6c, 5s, 5' '', 2 '' ''. With the observation of the plate (?) (namless structure) like in other two species (*H. minima* and *H. niei*), the keystone plates to *H. calafianiensis* was the third and fourth precingular plates unique in this species and the presence of the body scales composed by one central upright, six peripheral uprights, and three radiating spines. The pigment profile was typical for the majority of the dinoflagellates that was the Type-1 with Peridinin as the main accessory pigment. And the growth rate of *H. calafianiensis* was higher compare with other dinoflagellates; this suggests a high potential for the formation of blooms in the region.

Chapter 5. General discussion

Baja California State contributed with 9% of the aquaculture and fisheries production equivalent to 1,612.5 millions MXN of the overall Mexican production in 2014 (Moreno-Moreno et al., 2016). The aquaculture brings social and economic benefits, but principally is an important source of nutritious, low-cost food for the population. Todos Santos Bay, located on the Northwest Pacific coast, is an important site for the development of mariculture activities (e.g., the culture of bivalves mollusks and tuna fattening). To prevent economic losses and health risks it is necessary to monitor the phytoplanktonic species, especially those with toxic potential. In this study, *A. ostenfeldii* was identified for the first time in the Pacific Northwest; the closest record was on the coast of Nova Scotia (Cembella et al., 2009).

Due to the small size of *Az. spinosum*, its identification was possible employing specific primers, amplified by PCR, the morphological characterization was not clear, this species was previously recorded in Puget Sound, Washington State (Kim et al., 2017). With our study, its distribution was extended to the northwest coast of Mexico. As in this study, also Kim et al. (2017) could only record the species using specific primers by qPCR technique, but the morphological identification was not possible.

We achieve to culture and register a new species of the genus *Heterocaspsa*; this is a significant contribution since experimental bioassays can be done to know the toxic potential of *H. calafianiensis*. The knowledge of this genus is limited on the Mexican coast, only in the Yucatán Peninsula, the toxigenic *H. circularisquama* was recorded as a potential risk (Herrera Silveira et al., 2010).

There is increasing concern about the expansion of HABs over recent decades. It has been linked to climate change producing an ocean acidification, precipitation, nutrient stress or availability and the physical structure of the water column. All of these changes influence the productivity, composition and global range of the phytoplankton assembles (Griffith and Gobler, in print). In TSB the change of the phytoplankton community caused by the increase of the superficial water temperature was evident, registering a low abundance of diatoms and dinoflagellates during the last years. The abnormally warm conditions began on 2015 associated to the “El Niño” event and in the region; a high abundance of the Rhodophyta *Chatonella* spp. was recorded on 2016 causing a massive death of tuna representing one of the most important economic losses in the mariculture of Mexico (García-Mendoza et al., 2018). An expansion of the range of warm-water species distribution and species-specific changes in the abundance is expected (Gerssen and Gago-Martínez, 2019). As in other coast of the world, in the Bay we also have clearly seen the effect of the change of environmental conditions on the phytoplanktonic

community and the increase of HABs. In the case of our interested species, the abundance of *A. ostenfeldii* in the region was lower from 2014 to 2016, associated to a strong stratification in the water column (decrease of 8.5 °C from the surface to 10 m depth) due to the high surface temperatures (22.9 °C in August 2016). During 2016, an abundance <500 cells L^{-1} of *A. ostenfeldii* were recorded. For the first time *Az. spinosum* was monitored in the Bay and related environmental conditions with its presence. The seasonality of the *Az. spinosum* species was related with a homogeneous water column and low concentrations of nitrates and nitrites (about 3.60 to 4 µM) in the 2016 – 2017 period. I had not data to do a timeline to compare the conditions between years in the Bay, but the conditions during 2016-2017 monitoring were similar to those reported in other regions when *Az. spinosum* is present (Akselman and Negri, 2012; Tillmann et al., 2014a).

Establishing ecological interactions between the phytoplankton communities is complicated since monitoring is needed over the years that allow observing trends. And it is necessary to add the physical-chemical requirements that each species has; all of these are complex mechanisms. However, during this study, we could observe the seasonality of *Az. spinosum* in the winter months, but also, *Heterocapsa* was present during the same season. Both species were successful at a time that other dinoflagellates or diatoms were not. In one study during of three wintertime blooms of *H. triquetra* in Newport River estuary, Litaker et al. (2002) determined that the runoff following the rainfall events supplied inorganic nutrients critical for bloom initiation and development.

On the other hand, Millette et al. (2017) found the success of *H. rotundata* to formed bloom in the Chesapeake Bay was related to the switching from phototrophy to phagotrophy when the irradiance decreased, giving an advantage over other phytoplankton in winter. The maximum bacterial ingestion rate has been calculated to be 11.2 bacteria *H. rotundata* $^{-1}$ h^{-1}, which was equivalent to the ingestion of 76% of their body carbon per day (Seong et al., 2006). In the TSB during the winter, the rainfall-runoff transport the nutrients from the land to the coast, which promotes a greater concentration of bacteria that would be linked to the presence of *Heterocapsa*. Although there are no reports until the moment of this switching in *Azadinium*, probably the phagotrophy is the same strategy to survive during the winter.

The term “emerging toxin” could be ambiguous, because it may be associated with the concept of new toxin, and this is not the case. Emerging toxins identify those toxins that might be increasing their presence in a certain area. However, they are known in other geographical zones of the world, are new to an area, or increasing their presence with time due to the environmental conditions (EFSA, 2010). Then in the TSB, the azaspiracids can be considered as emerging toxins because it is detected

consistently every year during the winter months; the concentrations recorded in the cultured mussels were similar in the two sampling periods (February 2014 with 15.29 µg Kg^{-1} and November 2016 with 14 µg Kg^{-1}). However, in 2016, the sampling sites were expanded, and a sample of non-commercial mussels was obtained, and the highest concentration of azaspiracids (23 µg Kg^{-1} and) was detected. This extra mussel sample gives us a hint that it is necessary to monitor the azaspiracids in other parts of TSB to have a better understanding of *Az. spinosum* distribution. Apparently it is an oceanic species that enter in the Bay through the North entrance and in front of Punta Banda. Due to the low permissible limit for the consumption of this toxin, environmental changes can become a health hazard; then it is necessary to continue monitoring the azaspiracids. Besides, the spirolides are not emerging toxins because the accumulation of this toxin in the mussel is very low, even below the detection limit, then it does not a risk for health.

Harmful algal blooms (HABs) are a natural phenomenon, whose impacts on aquaculture, fisheries and public health has increased worldwide (Salcedo-Garduño et al., 2018). It is not easy to quantify the real cost of the HABs because not only does it involve direct losses to the fisheries sector, tourism, or health care, but also the cost of monitoring as mitigation or prevention programs should be added (Kudela et al., 2015). The annual cost of the HABs in the United States was estimated in ± USD 95 million (Hoagland and Scatasta, 2006), in Europe > € 800 million (Scatasta, 2003 in Berdalet et al., 2016), and in Japan > USD 1 billion (Kim, 2006 in Berdalet et al., 2016). In Mexico, this estimation has not been calculated; some events have been reported with the losses in the fisheries. For example, in Oaxaca during the period 1989 to 2014, 14 HABs related to paralytic toxin were recognized with 139 intoxications, nine deaths, and > USD 500.000 in losses with 708 days of sanitary closures (Alonso-Rodríguez et al., 2015). In the northeast of Ensenada in 2007, a bloom of *Ceratium divaricatum* caused anoxic conditions that produced and ecological catastrophe in benthic organisms such as lobsters, starfish, and crabs, the lobster population with dead biomass more than five tons was the most affected (Orellana-Cepeda et al., 2007). Due to the implications and impacts of the HABs, it is necessary to implement efficient analytical methods for toxin detection as well as new technologies to the identification of toxic species. In the official Mexican norm (NOM-242-SSA1-2009), the method to detect the toxins is the mouse bioassay, this method has deficiencies because cannot distinguish different types of toxins and analogs, with this limitation toxins such as azaspiracids, palytoxins, among others are not be considered in the norm and are not monitored (COFEPRIS, 2008). This would have to be modified, in this study, through a timeline, it is shown that azaspiracids are not only being accumulated in the mussels but should be considered as emerging toxins in the TSB. On the other hand, it is also necessary to implement new techniques for the identification of phytoplankton species. While it is true that the

morphological description through the microscopy should not be replaced, adding the use of molecular techniques with specific markers is a very useful tool for the detection of cryptic or very small size species. In this study, the effectiveness of the use of molecular markers is verified, which allowed me to identify *Az. spinosum* in field samples, which through microscopy, was not possible.

Molecular techniques to detect HABs species are being gradually considered as an attractive alternative to standard laboratory methods. They offer faster and more accurate means of detecting and monitoring species, with respect to their traditional homologues based on isolating the species to culturing and microscopic identification. Molecular techniques are particularly attractive when multiple species need to be detected and/or are in very low abundance (Medlin and Orozco, 2017). Also, allow to differenciate cryptic species which morphological chracterization is ambiguos and require a high microscopy technique resolution and extensive training to distinguish similar species as the case of the *Alexandrium* or *Azadinium* genus. Another consideration to implement these techniques in the regulatory monitoring programs is the co-occurrence of morphologically identical toxic and nontoxic ribotypes that the only way to differentiate them is using molecular techniques as qPCR or the use of random amplified polymorphic DNA (RAPD) allowing early and accurate alerts of HABs events (Eckford-Soper et al., 2013; Toebe, et al., 2013b). In the present study, the PCR technique allowed the identification of *Az. spinosum* in water samples that by microscopy could not be achieved. Since this is a small species (12-16 µm) with low abundances in TSB, which could not be isolated. I picked the cells one by one from water field samples to prepare them for SEM microscope making it a very laborious and long process without success. However the limitation to implement the molecular techniques to the regular monitoring programs are the cost of the equiments, reactives and supplies.

The TSB is influenced mainly by the California Current System (CCS However two important ocean currents are present in the region. A seasonal coastal jet towards the equator transports water of low salinity, low temperature, and high oxygen content (Subarctic water) (Strub and James, 2000). The other is the subsurface countercurrent (SC) that flows along the continental slope (~ 200 to 400 m) towards the pole and carries subsurface equatorial water (relatively warm and saline waters) (Pérez-Brunius et al., 2006). Interannual variability indicates that the bay is also influenced by local and regional processes, with which different hydrological conditions are generated and affects the physical properties and ecosystem processes in the area (De la Cruz-Orozco et al., 2017). The present study was carried out during anomalous years. Abnormally warm waters were registered from 2013-2014 in the region associated with the phenomenon is known as " The Blob" in addition, during the 2016-2017 period, "El Niño" caused elevated SST in the region (Cruz-Rico y Rivas, 2018; García-Mendoza et al., 2018). In this

study, low diversity and low concentrations of phytoplankton were recorded especially during the 2016-2017 period associated with the abnormal conditions and was in agreement with the records for the northern regions of California System (Durazo et al., 2017; Wells et al., 2017) .The high temperatures that occurred in the region should not have been a limitation for the growth of *A. ostenfeldii*. This species has been recorded in areas with temperatures up to 19 °C (Anderson et al., 2012a; Hakanen et al., 2012; Van de Waal et al., 2015). However, during 2016- 2017, the species could not be detected or was at low abundance (< 500 cells L^{-1}). In the present study, a strong stratification related to the high surface water (8.5 °C difference between surface and thermocline) was recorded. This was higher compared to previous years (5 °C of difference) (Peña Manjarrez et al., 2009). Inorganic nutrients generally are not a limiting factor for *A. ostenfeldii* since this dinoflagellate is a mixotrophy species (Anderson et al., 2012a; Hakanen et al., 2012). Apparently, the strong stratification was the variable that influenced the presence of the species in TSB, which may be related to the effects on the mobility behavior of the species. *A. ostenfeldii* has well-established migration patterns due to the need for greater energy for its displacement to cross the warm layer to move to the surface, which is energetically expensive (Raven y Richardson, 1984), the species in the region could be encysting as a survival strategy. But, it is necessary to analyze the sediments to verify this besides the sediments will be the best way to know if the species has a potential to form blooms in the region.

On the other hand, *Az. spinosum* was present in TSB during winter months the water column is homogeneous; this characteristic is typical of the season (Espinosa-Carreón et al., 2001). The abundance of *Az. spinosum* was determined only in the second sampling period (2016-2017) but the toxin register is a good indicator of the presence of the species (Tillmann et al., 2014a), so the seasonality of *Az. spinosum* has been consistent since 2012 (García-Mendoza et al., 2014) until now in TSB. Probably, this species proliferates in more oceanic waters and it is transported into the bay. In winter there is a horizontal advection of the surface current from the North entrance of the TSB with southeast direction and causes cyclonic circulation with variable winds in the winter (Cervantes-Audelo, 2013). *Az. spinosum* was registered principally on the surface. This oceanic distribution was described by Blanco et al. (2017) and Tillmann et al. (2014a). However, the specific environmental or biological factors associated with this distribution are not known. In the ACP analysis performed in this study, the abundance of *Az. spinosum* was not correlated to the low-temperature of the seawater during the winter as expected, but rather to the low nitrate and nitrite concentration detected in this season, which not change significantly during the study. Another variable that it is probably associated with presence of *Az. spinosum* is the low irradiance prevalent in the winter. In experimental conditions high irradiance limits the growth of *Azadinium* species (Kilcoyne et al., 2019; Tillmann et al., 2014b) and when they were isolated the

irradiance was between 20 to 40 µmol.m^{-2}.s^{-1} (Potvin, et al., 2012; Tillmann et al., 2009a). Therefore the cloudy days of the winter and fewer hours of light could favor the species in TSB.

Chapter 6. General conclusions

The PCR (using 28S and ITS rDNA primers), in combination with epifluorescence microscopy techniques, allowed the identification of *A. ostenfeldii*, confirming that this is the producer species of spirolides detected in cultured mussels in the BTS. The presence of this species and the spirolide concentration did not presented clear temporality of appearance. The only analog detected by LC-MS/MS in mussels was the 13 desm-SPXC. The toxin profile and the phylogenetic analysis, cluster the strain of TSB with the Pacific strains, which corresponds to the group 1 of the *A. ostenfeldii* toxigenic species.

The distribution of *A. ostenfeldii* is heterogeneous in the TSB and it was detected in Salsipuedes Bay and Punta Banda. The abundance of this species was low during the sampling period of 2016 to 2017 related to positive anomalies and the strong stratification present in the water column. *A. ostenfeldii* is a common component of the phytoplankton community in the region.

The use of specific primers (18S rDNA) allowed the molecular identification of *Az. spinosum* as the producer species of the azaspiracid AZA-1 detected in the cultured mussels. This species has so far been reported as the only producer of AZA-1. The toxin and the species were consistently detected during winter months. The detection of the toxin in mollusks is a good indicator of the presence of *Az. spinosum* in the TSB.

Az. spinosum apparently has an oceanic distribution. Higher abundances for the species was recorded in Salsipuedes Bay than inside TSB. Through of surface current from the North entrance of TSB, the cells could be transported into the bay. The environmental conditions that favored the presence of the species were the homogeneity in the water column with a low concentration of nitrates and nitrites. The temperature was not correlated with the abundance of the species, but the species was present in a temperature range of 14–16 °C.

A new species with the potential to form blooms was identified. *H. calafianiensis* presented a typical tabulation plate for the genus: APC (Po, cp?, X), 5', 3a, 7'', 6c, 5s, 5''', 2'''' and also the presence tridimensiomal body scales. This species was isolated in the winter season.

Todos Santos Bay is a complex ecosystem with a clear seasonal environmental variability and also is affected importantly by mesoscales of global environmental phenomena. The presence of abnormally high water temperatures affected the phytoplankton community with an overall decrease in the

abundance and diversity of phytoplankton species. Although *A. ostenfeldii* and *Az. spinosum* are in TSB, the environmental conditions that favor the presence of each species are different. The highest abundances for *A. ostenfeldii* were recorded in warm waters (17 - 20 °C) without strong stratification; conversely, *Azadinium spinosum* and *Heterocapsa calafianiensis* were recorded in homogeneous waters with a low temperature (14 – 16 °C).

Bibliographic references

Aké-Castillo, J. A., Rodríguez-Gómez, C. F., Perales-Valdivia, H., Sanay-González, R. 2016. Florecimiento de *Heterocapsa rotundata* (Dinophyta) en el estuario río Jamapa, Veracruz. En E. García-Mendoza, S. L. Quijano-Scheggia, A. Olivos-Ortiz, & E. J. Vásquez-Núñez (Eds.), Florecimientos Algales Nocivos. CICESE. pp. 1–16.

Akselman, R., Negri, R. M. 2012. Blooms of *Azadinium* cf *spinosum* in northern shelf waters of Argentina, Southwestern Atlantic. Harmful Algae, 19, 30–38.

Alexander, J., Benford, D., Cockburn, A., Cravedi, J., Dogliotti, E., Domenico, A. Di, Fernández-Cruz, M. L., Fink-Gremmels, J., Fürst, P., Galli Corrado, Grandjean, P., Gzyl, J., Heinemeyer, G., Johansson, N., Mutti, A., Schlatter, J., Leeuwen, R. Van, Van Peteghem, C., Verger, P. 2008. Marine biotoxins in shellfish – Azaspiracid group Scientific Opinion of the Panel on Contaminants in the Food Chain Adopted on 9 June 2008. The EFSA Journal, 723(June), 1–52. doi:10.2903/j.efsa.2008.723

Almandoz, G. O., Montoya, N. G., Hernando, M. P., Benavides, H. R., Carignan, M. O., Ferrario, M. E. 2014. Toxic strains of the Alexandrium ostenfeldii complex in southern South America (Beagle Channel, Argentina). Harmful Algae, 37, 100–109. doi:10.1016/j.hal.2014.05.011

Almazan-Becerril, A., García-Mendoza, E. 2008. Maximum efficiency of charge separation of photosystem II of the phytoplankton community in the Eastern Tropical North Pacific off Mexico: A nutrient stress diagnostic tool? Ciencias Marinas, 34(1), 29–43. doi:10.7773/cm.v34i1.1151

Alonso-Rodríguez, R., Mendoza-Amézquita, E., Velásquez-López, S. A., Seim, J. A., Martínez-Rodríguez, V. M. 2015. Florecimientos algales nocivos producidos por *Pyrodinium bahamense* en Oaxaca, México (2009-2010). Salud Pública de México, 57(4), 343. doi:10.21149/spm.v57i4.7578

Anderson, D. 2007. The ecology and oceanography of harmful algal blooms: multidisciplinary approaches to research and management. IOC Technical Series, (June), 38. doi:IOC/2007/TS/74

Anderson, D. M., Alpermann, T. J., Cembella, A. D., Collos, Y., Masseret, E., Montresor, M. 2012a. The globally distributed genus *Alexandrium*: Multifaceted roles in marine ecosystems and impacts on human health. Harmful Algae, 14, 10–35. doi:10.1016/j.hal.2011.10.012

Anderson, D. M., Cembella, A. D., Hallegraeff, G. M. 2012b. Progress in understanding Harmful Algal Blooms: Paradigm shifts and new technologies for research, monitoring, and management. Annual Review of Marine Science, 4(1), 143–176. doi:10.1146/annurev-marine-120308-081121

Anderson, D. M., Glibert, P. M., Burkholder, J. M. 2002. Harmful algal blooms and eutrophication: nutrient sources, composition, and consequences. Estuaries, 25(4), 704–726. doi:10.1007/BF02804901

Anderson, D.M. 1998. Physiology and bloom dynamics of toxic *Alexandrium* species, with emphasis on life cycle transitions. In: Anderson, D.M., Cembella, A.D., Hallegraeff, G.M, eds. Physiological Ecology of Harmful Algal Blooms. Springer-Verlag, Heidelberg, 29–40pp

Argote Espinosa, M., Gavidia Medina, F., Amador Buenrostro, A. 1991. Wind-induced circulation in Todos Santos Bay, B. C., Mexico. Atmosfera, 4(2), 101–115.

Attaran-Fariman, G., Javid, P. 2013. The phylogeny of *Heterocapsa* sp. (Dinophyceae) isolated from the south coast of Iran during a *Cochlodinium polykrikoides* bloom. Turkish Journal of Botany, 37(4), 778–783. doi:10.3906/bot-1206-40

Balech, E., and Tangen, K. 1985. Morphology and taxonomy of toxic species in the Tamarensis group (Dinophyceae): *Alexandrium excavatum* (Braarud) comb. nov. and *Alexandrium ostenfeldii* (Paulsen) comb. nov. Sarsia. 70 (4), 333–343.

Balech, E. 1995. The Genus *Alexandrium* Halim (Dinoflagellata). Sherkin Island Marine Station, Sherkin Island, Co., Cork, Ireland. 151pp.

Banse, K. 1977. Determining the carbon-to-chlorophyll ratio of natural phytoplankton. Marine Biology, 41(3), 199–212.

Berdalet, E., Fleming, L. E., Gowen, R., Davidson, K., Hess, P., Backer, L. C., Moore, S. K., Hoagland, P., Enevoldsen, H. 2016. Marine harmful algal blooms, human health and wellbeing: challenges and opportunities in the 21st century. Journal of the Marine Biological Association of the United Kingdom, 96(1), 61–91. doi:10.1017/S0025315415001733

Blackburn, S. I., Bolch, C. J. S., Haskard, K. A., Hallegraeff, G. M. 2001. Reproductive compatibility among four global populations of the toxic dinoflagellate *Gymnodinium catenatum* (Dinophyceae). Phycologia, 40(1), 78–87. doi:10.2216/i0031-8884-40-1-78.1

Blanco, J., Arévalo, F., Moroño, Á., Correa, J., Muñíz, S., Mariño, C., Martín, H. 2017. Presence of azaspiracids in bivalve molluscs from Northern Spain. Toxicon, 137(September), 135–143. doi:10.1016/j.toxicon.2017.07.025

Botana, L. M. 2014. Seafood and freshwater toxins (Third edit; Luis M. Botana, Ed.). CRC Press.

Boczar, B., Beitler, M., Liston, J., Sullivan, J., Cattolico, R. 1998. Paralytic shellfish toxins in *Protogonyaulax tamarensis* and *Protogonyaulax catenella* in axenic culture. Plant Physiology. 88, 1285–1290.

Borkman, D.G., Smayda, T.J., Tomas, C.R., York, R., Strangman, W., Wright, J. 2012. Toxic *Alexandrium peruvianum* (Balech and de Mendiola) Balech and Tangen in Narragansett Bay, Rhode Island (USA). Harmful Algae. 19: 92–100. doi: 10.1016/j.hal.2012.06.004

Braña Magdalena, A., Lehane, M., Krys, S., Fernández, M. L., Furey, A., James, K. J. 2003. The first identification of azaspiracids in shellfish from France and Spain. Toxicon, 42(1), 105–108. doi:10.1016/S0041-0101(03)00105-3

Brown, E. R., Cepeda, M. R., Mascuch, S. J., Poulson-Ellestad, K. L., Kubanek, J. 2019. Chemical ecology of the marine plankton. Natural Product Reports, 36(8), 1093–1116. doi:10.1039/C8NP00085A

Burkholder, J. M., Glibert, P. M., Skelton, H. M. 2008. Mixotrophy, a major mode of nutrition for harmful algal species in eutrophic waters. Harmful Algae, 8(1), 77–93. doi:10.1016/j.hal.2008.08.010

Burkholder, J. M., Hallegraeff, G. M., Melia, G., Cohen, A., Bowers, H. A., Oldach, D. W., Parrow, M. W., Sullivan, M. J., Zimba, P. V., Allen, E. H., Kinder, C. A., Mallin, M. A. 2007. Phytoplankton and bacterial assemblages in ballast water of U.S. military ships as a function of port of origin, voyage time, and ocean exchange practices. Harmful Algae, 6(4), 486–518. doi:10.1016/j.hal.2006.11.006

Butterwick, C., Heaney, S.I., Talling, J.F. 2005. Diversity in the influence of temperature on the growth rates of freshwater algae, and its ecological relevance. Freshwat. Biol. 50, 29 –300. doi: 10.1111/j.1365-2427.2004.01317.x

Cáceres-Martínez, J. 1997. Mussel fishery and culture in Baja California, México: history, present status, and future. In: Mackenzie, I., Burrell, V., Rosenfield, A., Hobart,W (Eds.), The History, Present Condition and Future of the Molluscan Fisheries of North America and Europe. National Oceanic and Atmospheric Administration (NOAA). pp. 41–55.

Calva-Chávez, M. 2014. Variación estacional y sinóptica de la trampa de surgencia en la Bahía de Todos Santos, B.C. Centro de Investigación Científica y de Educación Superior de Ensenada, Baja California. 47 pp.

Camacho, F. ., Rodríguez, J. ., Mirón, A. ., García, M. C., Belarbi, E. H., Chisti, Y., Grima, E. M. 2007. Biotechnological significance of toxic marine dinoflagellates. Biotechnology Advances, 25(2), 176–194. doi:10.1016/j.biotechadv.2006.11.008

Casiraghi, M., Labra, M., Ferri, E., Galimberti, A., De Mattia, F. 2010. DNA barcoding: theoretical aspects and practical applications. In: Nimis, P., Vignes, R (Eds.), Tools for Identifying Biodiversity: Progress and Problems (first). Edizioni Università di Trieste: Venezia. pp. 269–273.

Cembella, A. D. 2018. Chapter 16 Harmful Algal Species Fact Sheets: *Alexandrium*. S. Shumway, J. Burkholder , S. Morton, eds. Harmful Algal Blooms: A Compendium Desk Reference, Wiley-Blackwell, 12 p.

Cembella, A.D., Bauder, A.G., Lewis, N.I., Quilliam, M.A. 2001. Association of the gonyaulacoid dinoflagellate *Alexandrium ostenfeldii* with spirolide toxins in size-fractionated plankton. Journal of Plankton Research. 23, 1413–1419. doi: 10.1093/plankt/23.12.1413

Cembella, A., Lewis, N., Quilliam, M. 2000a. The marine dinoflagellate *Alexandrium ostenfeldii* (Dinophyceae) as the causative organism of spirolide shellfish toxins. Phycologia, 39, 67–74. doi: 10.2216/i0031-8884-39-1-67.1

Cembella, A.D., Bauder, A.G., Lewis, N.I., Quilliam, M.A. 2000b. Population dynamics and spirolide composition of the toxigenic dinoflagellate *Alexandrium ostenfeldii* in coastal embayments of Nova Scotia. In: Hallegraeff, G.M., Blackburn, S.I., Bolch, J.S., Lewis, R.J, eds. IX International Conference on Harmful Algal Blooms. Intergovernmental Oceanographic Commission, Hobart, Australia, 173–176 p

Cembella, A. D., Lewis, N. I. Quilliam, M. A. 1999. Spirolide composition in micro-extracted pooled cells isolated from natural plankton assemblages and from cultures of the dinoflagellate *Alexandrium ostenfeldii*. Natural. Toxins. 8, 197–206. doi.10.1/15227189(200009/10)002

Cervantes-Audelo, I. 2013. Análisis de circulación y dispersión en la Bahía de Todos Santos, Baja California. Universidad del Mar. 61 pp.

COFEPRIS. 2008. Guía técnica para el control sanitario de moluscos bivalvos. En Programa de Sanidad de Moluscos Bivalvos. doi:10.1017/CBO9781107415324.004

COFEPRIS. 2018. Ocurrencia de Florecimientos Algales Ocurridos en el Territorio Nacional de 2003 a 2014.

Colin, S., Dam, H. 2003. Effects of the toxic dinoflagellate *Alexandrium fundyense* on the copepod *Acartia hudsonica*: a test of the mechanisms that reduce ingestion rates. Marine Ecology Progress Series, 248, 55–65. doi:10.3354/meps248055

Collos, Y., Vaquer, A., Laabir, M., Abadie, E., Laugier, T., Pastoureaud, A., Souchu, P. 2007. Contribution of several nitrogen sources to growth of *Alexandrium catenella* during blooms in Thau lagoon, southern France. Harmful Algae. 6, 781–789. doi: 10.1016/j.hal.20004.0037.

CONAPESCA. 2008. Diagnóstico y planificación regional de la pesca y acuacultura en México, Resumen Ejecutivo.

Cruz-Rico, J., Rivas, D. 2018. Physical and biogeochemical variability in Todos Santos Bay, northwestern Baja California, derived from a numerical NPZD model. Journal of Marine Systems, 183, 63–75. doi:10.1016/j.jmarsys.2018.04.001

Cuellar-Martinez, T., Ruiz-Fernández, A. C., Alonso-Hernández, C., Amaya-Monterrosa, O., Quintanilla, R., Carrillo-Ovalle, H. L., Arbeláez M, N., Díaz-Asencio, L., Méndez, S. M., Vargas, M., Chow-Wong, N. F., Valerio-Gonzalez, L. R., Enevoldsen, H., Dechraoui Bottein, M.-Y. 2018. Addressing the problem of Harmful Algal Blooms in Latin America and the Caribbean- A regional network for early warning and response. Frontiers in Marine Science, 5. doi:10.3389/fmars.2018.00409

Culverhouse, P., Williams, R., Reguera, B., Herry, V., González-Gil, S. 2003. Do experts make mistakes? A comparison of human and machine identification of dinoflagellates. Marine Ecology Progress Series, 247, 17–25. doi:10.3354/meps247017

D'Onofrio, G., Marino, D., Bianco, L., Busico, E., Montresor, M. 1999. Toward an assessment on the taxonomy of dinoflagellates that produce calcareous cysts (Calciodinelloideae, Dinophyceae): A morphological and molecular approach. Journal of Phycology, 35(5), 1063–1078. doi:10.1046/j.1529-8817.1999.3551063.x

Dagenais-Bellefeuille, S., Morse, D. 2013. Putting the N in dinoflagellates. Frontiers in Microbiology, 4(DEC), 1–14. doi:10.3389/fmicb.2013.00369

De la Cruz-Orozco, M. E., Gómez-Ocampo, E., Miranda-Bojórquez, L. E., Cepeda-Morales, J., Durazo, R., Lavaniegos, B. E., Espinosa-Carreón, T. L., Sosa-Ávalos, R., Aguirre-Hernández, E., Gaxiola-Castro, G. 2017. Biomasa y producción del fitoplancton frente a la Península de Baja California: 1997–2016. Ciencias Marinas, 43(4), 217–228. doi:10.7773/cm.v43i4.2793

Di Valentin, M., Ceola, S., Salvadori, E., Agostini, G., Carbonera, D. 2008. Identification by time-resolved EPR of the peridinins directly involved in chlorophyll triplet quenching in the peridinin–chlorophyll a–protein from Amphidinium carterae. Biochimica et Biophysica Acta (BBA) - Bioenergetics, 1777(2), 186–195. doi:10.1016/j.bbabio.2007.09.002

Durazo, R. 2015. Seasonality of the transitional region of the California Current Sistem off Baja California. Journal of Geophysical Research: Oceans, 120, 1173–1196. doi:10.1002/2014JC010405

Durazo, R., Castro, R., Miranda, L. E., Delgadillo-Hinojosa, F., Mejía-Trejo, A. 2017. Anomalous hydrographic conditions off the northwestern coast of the Baja California Peninsula during 2013-2016. Ciencias Marinas, 43(2), 81–92. doi:10.7773/cm.v43i2.2754

Eckford-Soper, L. K., Davidson, K., Bresnan, E. 2013. Identification and quantification of toxic and nontoxic strains of the harmful dinoflagellate Alexandrium tamarense using fluorescence in situ hybridization and flow cytometry. Limnology and Oceanography: Methods, 11, 540–548. doi:10.4319/lom.2013.11.540

Edgar, R. . 2004. MUSCLE: Multiple sequence alignment with high accuracy and high throughput. Nucleic Acids Research, 32(5), 1792–1797. doi:10.1093/nar/gkh340

Edler, L., and Elbrächter, M. 2010. The Utermöhl method for quantitative phytoplankton analysis. In: Karlson, B., Cusack, C., Bresnan, E, eds. Microscopic and molecular methods for quantitative phytoplankton analysis, UNESCO, Paris, 110 p.

Edvardsen, B., Shalchian-Tabrizi, K., Jakobsen, K. S., Medlin, L. K., Dahl, E., Brubak, S., Paasche, E. 2003. Genetic variability and molecular phylogeny of Dinophysis species (Dinophyceae) from Norwegian waters inferred from single cell analyses of rDNA. Journal of Phycology, 39(2), 395–408. doi:10.1046/j.1529-8817.2003.01252.x

Elferink, S., Neuhaus, S., Wohlrab, S., Toebe, K., Voß, D. Gottschling, M., Lundholm, N., Krock, B., Koch, B.P., Zielinski, O., Cembella, A., Uwe, J. 2017. Molecular diversity patterns among various phytoplankton size-fractions in West Greenland in late summer. Deep-Sea Research Part I: Oceanographic Research Papers, 121, 54-69. doi: 10.1016/j.dsr.2016.11.002

European Union Reference Laboratory for Marine Biotoxins (EURLMB). 2015. EU Harmonized Standard Operating Procedure for Determination of Lipophilic Marine Biotoxins in Molluscs by LC-MS/MS. Version 5. Available at: http://www.aecosan.msssi.gob.es/CRLMB/docs/docs/metodos_analiticos_de_desarrollo/EU-Harmonised-SOP-LIPO-LCMSMS_Version5.pdf

EFSA. 2010. Scientific Opinion on marine biotoxins in shellfish - Cyclic imines (spirolides, gymnodimines, pinnatoxins and pteriatoxins). En EFSA Journal (Vol. 8). doi:10.2903/j.efsa.2010.1628

Epstein, P. . 1998. Marine Ecosystems: Emerging diseases as indicators of change (First edit). Health Ecological and Economic Dimensions (HEED) of Global Change Program: Boston.

Espinosa-Carreón, T. L., Gaxiola-Castro, G., Robles-Pacheco, J. M., Nájera-Martínez, S. 2001. Temperatura, salinidad, nutrientes y clorofila a en aguas costeras de la Ensenada del Sur de California. Ciencias Marinas, 27(3), 397–422. doi:10.7773/cm.v27i3.490

Fagín, E., Bravo, I., Garrido, J. L., Rodríguez, F., Figueroa, R. I. 2019. *Scrippsiella acuminata* versus *Scrippsiella ramonii*: A Physiological Comparison. Cytometry Part A, 95(9), 985–996. doi:10.1002/cyto.a.23849

FAO. 2011. Assessment and management of biotoxin risks in bivalve molluscs. En J. Lawrence, H. Loreal, H. Toyofuku, P. Hess, I. Karunasagar, & L. Ababouch (Eds.), FAO Fisheries and Aquaculture Technical Paper No 551. Rome, Italy.

Farfán Mateos, E. 2010. Modelación de la circulación costera estacional en la región de Baja California y sur de California y de la Bahía de Todos Santos. Centro de Investigación Científica y de Educación de Ensenada Baja California. 4–31 pp.

Felsenstein, J. 1985. Confidence limits on phylogenies: An approach using the bootstrap. Evolution, 39(4), 783–791. doi:10.1111/j.1558-5646.1985.tb00420.x

Fensome, R. A., Saldarriaga, J. F., Taylor, Max, F. J. 1999. Dinoflagellate phylogeny revisited: reconciling morphological and molecular based phylogenies. Grana, 38(2–3), 66–80. doi:10.1080/00173139908559216

Fimbres Martínez, M. 2019. Distribución y abundancia de microalgas ictiotóxicas en la costa noroeste de Baja California, México. Centro de investigación Científica y de Educación Superior de Ensenada, Baja California. 80 pp.

Franco, J. M., Paz, B., Riobo, P., Pizarro, G., Figueroa, R., Fraga, S., Bravo, I. 2006. First report of the production of spirolides by *Alexandrium peruvianum* (Dinophyceae) from the Mediterranean Sea. Abstracts 12th International Conference on Harmful Algae, Copenhagen, Denmark, 397 pp.

Fritz, L., and Triemer, R. E. 1985. A rapid simple technique utilizing Calcofluor White M2R for the visualization of dinoflagellate thecal plates. J. Phycol. 21, 662-664. doi: 10.1111/j.0022-3646.1985.00662.x

Fujiki, H., Suganuma, M. 1993. Tumor promotion by inhibitors of protein phosphatases 1 and 2A: the okadaic acid class of compounds. Adv Cancer Res., 61, 143–194.

Furey, A., Moroney, C., Braña Magdalena, A., Fidalgo Saez, M. J., Lehane, M., James, K. J. 2003. Geographical, temporal, and species variation of the polyether toxins, azaspiracids, in shellfish. Environmental Science and Technology, 37(14), 3078–3084. doi:10.1021/es020246z

Furey, A., O'Doherty, S., O'Callaghan, K., Lehane, M., James, K. J. 2010. Azaspiracid poisoning (AZP) toxins in shellfish: Toxicological and health considerations. Toxicon, 56(2), 173–190. doi:10.1016/j.toxicon.2009.09.009

Garcés, E., Masó, M. 2001. Phytoplankton potential growth rate versus increase in cell numbers: estimation of cell lysis. Marine Ecology Progress Series, 212, 297–300. doi:10.3354/meps212297

García–Altarez. M., Casanova, A., Bane, V., Diogène, J., Furey, A., De la Iglesia, P. 2014. Confirmation of pinnatoxins and.spirolides in shellfish and passive samplers from Catalonia (Spain) by liquid chromatography coupled with tripe quadrupole and high resolution hybrid tandem mass spectrometry. Mar. Drugs. 12, 3706–3732. doi: 0.3390/md12063706

García-Mendoza, E., Cáceres-Martínez, J., Rivas, D., Fimbres-Martinez, M., Sánchez-Bravo, Y., Vásquez-Yeomans, R., Medina-Elizalde, J. 2018. Mass mortality of cultivated Northern bluefin tuna (*Thunnus thynnus orientalis*) associated with *Chattonella* species in Baja California, Mexico. Frontiers in Marine Science, 5(454), 1–16. doi:10.3389/fmars.2018.00454

García-Mendoza, E., Rivas, D., Olivos-Ortiz, A., Almazán-Becerril, A., Castañeda-Vega, C., Peña-Manjarrez, J. L. 2009. A toxic Pseudo-nitzschia bloom in Todos Santos Bay, northwestern Baja California, Mexico. Harmful Algae, 8(3), 493–503. doi:10.1016/j.hal.2008.10.002

García-Mendoza, E., Sánchez-Bravo, Y. A., Turner, A., Blanco, J., O'Neil, A., Mancera-Flores, J., Pérez-Brunius, P., Rivas, D., Almazán-Becerril, A., Peña-Manjarrez, J. L. 2014. Lipophilic toxins in cultivated mussels (*Mytilus galloprovincialis*) from Baja California, Mexico. Toxicon, 90, 111–123. doi:10.1016/j.toxicon.2014.07.017

Garneau, M.E., Schnetzer, A., Counway, P.D., Jones, A.C., Seubert, E.L., Caron, D.A. 2011. Examination of seasonal dynamic of the toxic dinoflagellate *Alexandrium catenella* at Redondo Beach, California by quantitative PCR. Appl. Environ. Microbiol. 77 (21), 7669–7680. doi: 10.1128/AEM.06174-1

Gárrate-Lizárraga, I., Muñetón-Gómez, M., Maldonado-López, V. 2006. Florecimiento del dinoflagelado *Gonyaulax polygramma* frente a la isla Espítitu Santo, Golfo de California, México. Rev. Invest. Mar, 27(1), 31–39.

Gerssen, A., Gago-Martínez, A. 2019. Emerging marine biotoxins. Toxins, 11(6), 11–13. doi:10.3390/toxins11060314

Gerssen, A., P.J. Mulder, P., A. Mairead, M., Boer, J. 2009. Liquid chromatography-tandem mass spectrometry method for the detection of marine lipophilic toxins under alkaline conditions. Journal of Chromatography A. Vol. 1216 (9), 421-430. doi: 10.1016/j.chroma.2008.12.099 ·

Gill, S., Murphy, M., Clausen, J., Richard, D., Quilliam, M., MacKinnon, S., LaBlanc, P., Mueller, R., Pulido, O. 2003. Neural injury biomarkers of novel shellfish toxins, spirolides: A pilot study using immunochemical and transcriptional analysis. Neurotoxicology. 24:593–604. doi: 10.1016/S0161-813X(03)00014-7

Gribble, K., Keafer, B., Quilliam, M., Cembella, A., Kulis, D., Manahan, A., Anderson, D. 2005. Distribution and toxicity of *Alexandrium ostenfeldii* (Dinophyceae) in the Gulf of Maine, USA. Deep Sea Research Part II: Topical Studies in Oceanography. 52, 2745–2763. doi: 10.1016/j.dsr2.2005.06.018

Godhe, A. 2001. Relationship between planktonic dinoflagellate abundance, cysts recovered in sediment traps and environmental factors in the Gullmar Fjord, Sweden. Journal of Plankton Research, 23(9), 923–938. doi:10.1093/plankt/23.9.923

Gómez, F. 2012. A checklist and classification of living dinoflagellates (Dinoflagellata, Alveolata). CICIMAR Oceánides, 27(1), 65–140.

Gottschling, M., Tillmann, U., Kusber, W. H., Hoppenrath, M., Elbrächter, M. 2018. (2607) Proposal to conserve the name *Heterocapsa* (Dinophyceae) with a conserved type. Taxon, 67(3), 632–633. doi:10.12705/673.16

Grassoff, K., Ehrhardt, M., Kremling, K., Almgren, T. 1983. Methods of seawater analysis (K. Grassoff, M. Ehrhardt, K. Kremling, Eds.). Verlag Chemie: Weinheim.

Griffith, A. W., Gobler, C. J. Harmful algal blooms: A climate change co-stressor in marine and freshwater ecosystems. Harmful Algae. doi:10.1016/j.hal.2019.03.008

Gruber, N. 2008. The marine Nitrogen cycle: Overview and challenges. En D. Capone, D. Bronk, & M. Mulholland (Eds.), Nitrogen in the Marine Environment (2nd Editio). doi:10.1016/B978-0-12-372522-6.00001-3

Guillard, R. R. L. 1973. Division rates. En J. R. Stein (Ed.), Culture Methods and Growth Measurements. Handbook of Phycological Methods. Cambridge University Press: Cambridge. pp. 289–313.

Hackett, J. D., Anderson, D. M., Erdner, D. L., Bhattacharya, D. 2004. Dinoflagellates: a remarkable evolutionary experiment. American Journal of Botany, 91(10), 1523–1534. doi:10.3732/ajb.91.10.1523

Haguet, Q., Bonnet, A., Bérard, J.-B., Goldberg, J., Joguet, N., Fleury, A., Thiéry, V., Picot, L. 2017. Antimelanoma activity of *Heterocapsa triquetra* pigments. Algal Research, 25(July), 207–215. doi:10.1016/j.algal.2017.04.034

Hakanen, P., Suikkanen, S., Franzén, J., Franzén, H., Kankaanpää, H., Kremp, A. 2012. Bloom and toxin dynamics of *Alexandrium ostenfeldii* in a shallow embayment at the SW coast of Finland, northern Baltic Sea. Harmful Algae, 15, 91–99. doi:10.1016/j.hal.2011.12.002

Hall, T. 1999. BioEdit: A user-friendly biological sequence alignment editor and analysis program for Windows 95/98/NT. Nucleic Acids Symposium Series 41, 95–98.

Hallegraeff, G. M. 1993. A review of harmful algal blooms and their apparent global increase. Phycologia, 32(2), 79–99. doi:10.2216/i0031-8884-32-2-79.1

Hansen, P. J. 2011. The Role of Photosynthesis and Food Uptake for the Growth of Marine Mixotrophic Dinoflagellates1. Journal of Eukaryotic Microbiology, 58(3), 203–214. doi:10.1111/j.1550-7408.2011.00537.x

Hansen, P. J., Cembella, A. D., Moestrup, O. 1992. The marine dinoflagellate *Alexandrium ostenfeldii*: Paralytic shellfish toxin concentration, composition, and toxicity to a tintinnid ciliate. Journal of Phycology, 28(5), 597–603. doi:10.1111/j.0022-3646.1992.00597.x

Hariganeya, N., Tanimoto, Y., Yamaguchi, H., Nishimura, T., Tawong, W., Sakanari, H., Yoshimatsu, T., Sato, S., Preston, C. M., Adachi, M. 2013. Quantitative PCR method for enumeration of cells of cryptic species of the toxic marine Dinoflagellate *Ostreopsis* spp. in coastal waters of Japan. PLoS ONE, 8(3), e57627. doi:10.1371/journal.pone.0057627

Hargraves, P.E., Maranda, L. 2002. Potentially Toxic of Harmful Microalgae from the Northeast Coast. Northeastern Naturalist. 9(1), 81–120. doi.org/10.1656/1092-6194(2002)009

Havskum, H., Hansen, P. J. 2006. Net growth of the bloom-forming dinoflagellate *Heterocapsa triquetra* and pH: Why turbulence matters. Aquatic Microbial Ecology, 42(1), 55–62. doi:10.3354/ame042055

Hernández-Becerril, D. U., Barón-Campis, S. A., Escobar-Morales, S. 2012. Un nuevo registro de *Azadinium spinosum* (Dinoflagellata) en el Pacífico tropical Mexicano. Revista de Biologia Marina y Oceanografia, 47(3), 553–557. doi:10.4067/S0718-19572012000300016

Herrera Silveira, J., Álvarez Góngora, C., Merino Virgilio, F., Aguilar Trujillo, A. 2010. Mareas rojas en las costas de Yucatán. Biodiversidad, 320–321.

Hillis, D. M., Dixon, M. T. 1991. Ribosomal DNA: Molecular evolution and phylogenetic inference. The Quarterly Review of Biology, 66(4), 411–453. doi:10.1086/417338

Hoagland, P., Scatasta, S. 2006. The Economic Effects of Harmful Algal Blooms. In E. Granéli., J. . Turner (Eds.), Ecology of Harmful Algae. doi:10.1007/978-3-540-32210-8_30

Holmes, M. ., Lewis, R. 2002. Toxin-producing dinoflagellates. En A. Ménez (Ed.), Perspectives in Molecular Toxicology. Wiley and Sons. pp. 39–65.

Hoppenrath, M., Saldarriaga, J. F. 2008. Tabulation in Diniflagellates. Consultado el 5 de enero de 2020, de Tree of Live Web Project website: http://tolweb.org/notes/?note_id=4796

Horiguchi, T. 1995. *Heterocapsa circularisquama* sp. nov. (Peridiniales, Dinophyceae): A new marine dinoflagellate causing mass mortality of bivalves in Japan. Phycological Research, 43(3), 129–136. doi:10.1111/j.1440-1835.1995.tb00016.x

Horner, R.A., Garrison, D.L., Plumley, F.G. 1997. Harmful algal blooms and red tide problems on the U.S west coast. Limnol. Oceanogr. 42, 1076–1088.

Hu, T., Burton, I. W., Cembella, A. D., Curtis, J. M., Quilliam, M. A., Walter, J. A., Wright, J. L. C. 2001. Characterization of spirolides A, C, and 13-desmethyl C, new marine toxins isolated from toxic plankton and contaminated shellfish. Journal of Natural Products, 64(3), 308–312. doi:10.1021/np000416q

Hu, T., Curtis, J.M., Walter, J.A., Wright, J.L. 1996. Characterization of biologically inactive spirolides E and F: identification of the spirolide pharmacophore. Tetrahedron Lett, 37, 7671–7674. doi: 10.1016/0040-4039(96)01721-2

Hu, T., Curtis, J.M., Oshima, Y., Quilliam, M.A., Walter, J.A., Watson-Wright, W.M., Wright, J.L.C. 1995. Spirolides B and D, two novel macrocycles isolated from the digestive glands of shellfish. J. Chem. Soc. Chem. Commun. 2159–2161. doi: 10.1039/C39950002159

Ito, E., Satake, M., Ofuji, K., Kurita, N., McMahon, T., James, K., Yasumoto, T. 2000. Multiple organ damage caused by a new toxin azaspiracid, isolated from mussels produced in Ireland. Toxicon, 38(7), 917–930. doi:10.1016/S0041-0101(99)00203-2

Iwataki, M. 2002. Taxonomic study on the genus *Heterocapsa* Dinophyceae). University pf Tokyo.

Iwataki, M. 2008. Taxonomy and identification of the armored dinoflagellate genus *Heterocapsa* (Peridiniales, Dinophyceae). Plankton and Benthos Research, 3(3), 135–142. doi:10.3800/pbr.3.135

Iwataki, M., Hansen, G., Sawaguchi, T., Hiroishi, S., Fukuyo, Y. 2004. Investigations of body scales in twelve *Heterocapsa* species (Peridiniales, Dinophyceae), including a new species *H. pseudotriquetra* sp. nov. Phycologia, 43(4), 394–403. doi:10.2216/i0031-8884-43-4-394.1

Iwataki, M., Takayama, H., Matsuoka, K., Fukuyo, Y. 2002. *Heterocapsa lanceolata* sp. nov. and *Heterocapsa horiguchii* sp. nov. (Peridiniales, Dinophyceae), two new marine dinoflagellates from coastal Japan. Phycologia, 41(5), 470–479. doi:10.2216/i0031-8884-41-5-470.1

Jacox, M. G., Alexander, M.A., N. Mantua, N.J., Scott, J.D., Hervieux, G., Webb, R.S., Werner, F.E. 2017. Forcing of multiyear extreme ocean temperatures that impacted California Current living marine resources in 2016. Bulletin of the American Meteorological Society. Vol.99 (1). doi: 10.1175/BAMS-D-17-0119.

James, K. J., Lehane, M., Moroney, C., Fernandez-Puente, P., Satake, M., Yasumoto, T., Furey, A. 2002. Azaspiracid shellfish poisoning: unusual toxin dynamics in shellfish and the increased risk of acute human intoxications. Food Additives and Contaminants, 19(6), 555–561. doi:10.1080/02652030210126398

Jauffrais, T., Marcaillou, C., Herrenknecht, C., Truquet, P., Nicolau, E., Tillmann, U., Hess, P. 2012. Azaspiracid accumulation, detoxification and biotransformation in the blue mussels (*Mytilus edulis*) experimentally fed *Azadinium spinosum*. Toxicon, 60(4), 582–595.

Jauffrais, T., Séchet, V., Herrenknecht, C., Truquet, P., Véronique, S., Tillmann, U., Hess, P. 2013. Effect of environmental and nutritional factors on growth and azaspiracid production of the dinoflagellate *Azadinium spinosum*. Harmful Algae, 27(July), 138–148. doi:10.1016/j.hal.2013.05.009

Jensen, M, E., Moestrup, Ø. 1997. Autoecology of the toxic dinoflagellate *Alexandrium ostenfeldii*: life history and growth at different temperatures and salinities. Eur. J. Phycol. 32, 9–312. doi: 10.1080/09541449710001719325

Johnsen, G., Nelson, N. B., Jovine, R. V. M., Prezelin, B. B. 1994. Chromoprotein- and pigment dependent modeling of spectral light absorption in two dinoflagellates, *Prorocentrum minimum* and *Heterocapsa pygmaea*. Marine Ecology Progress Series, 114(3), 245–258. doi:10.3354/meps114245

Ki, J.-S., Han, M.-S. 2007. Rapid molecular identification of the harmful freshwater dinoflagellate Peridinium in various life stages using genus-specific single-cell PCR. Journal of Applied Phycology, 19(5), 467–470. doi:10.1007/s10811-007-9157-8

Ki, J.-S., Jang, G. Y., Han, M.-S. 2004. Integrated method for Single-Cell DNA extraction, PCR amplification, and sequencing of ribosomal DNA from harmful dinoflagellates *Cochlodinium polykrikoides* and *Alexandrium catenella*. Marine Biotechnology, 6(6), 587–593. doi:10.1007/s10126-004-1700-x

Kilcoyne, J., McCoy, A., Burrell, S., Krock, B., Tillmann, U. 2019. Effects of temperature, growth media, and photoperiod on growth and toxin production of *Azadinium spinosum*. Marine Drugs, 17(9), 1–16. doi:10.3390/md17090489

Kim, D., Miyazaki, Y., Nakashima, T., Izvashita, T., Fujita, T., Yamaguchi, K., Choi, K. S., Oda, T. 2008. Cytotoxic action mode of a novel porphyrin derivative isolated from harmful red tide dinoflagellate *Heterocapsa circularisquama*. Journal of Biochemical and Molecular Toxicology, 22(3), 158–165. doi:10.1002/jbt.20216

Kim, J. H., Tillmann, U., Adams, N. G., Krock, B., Stutts, W. L., Deeds, J. R., Han, M. S., Trainer, V. L. 2017. Identification of *Azadinium* species and a new azaspiracid from *Azadinium poporum* in Puget Sound, Washington State, USA. Harmful Algae, 68(September), 152–167. doi:10.1016/j.hal.2017.08.004

Klontz, K. ., Abraham, A., Plakas, S. ., Dickey, R. 2009. Mussel-Associated Azaspiracid Intoxication in the United States. Annals of Internal Medicine, 150(5), 361.

Kremp, A., Tahvanainen, P., Litaker, W., Krock, B., Suikkanen, S., Leaw, C.P., Tomas, C. 2014. Phylogenetic relationships, morphological variation and toxin patterns in the *Alexandrium ostenfeldii* (Dinophyceae) complex: implications for species boundaries and identities. J. Phycol. 50, 81–100. doi:10.1111/jpy.12134

Kremp, A., Lundholm, T., Drebler, N., Erler, K., Gerdts, G., Eirtovaara, S., Leskinen, E. 2009. Bloom forming *Alexandrium ostenfeldii* (Dinophyceae) in shallow waters of the Aland Archipelago Northern Baltic Sea. Harmful Algae. 8, 318–328. doi: 10.1016/j.hal.2008.07.004

Krock, B., Tillmann, U., John, U., Cembella, A. 2008. LC-MS-MS aboard ship: Tandem mass spectrometry in the search for phycotoxins and novel toxigenic plankton from the North Sea. Analytical and Bioanalytical Chemistry, 392(5), 797–803. doi:10.1007/s00216-008-2221-7

Krock, B., Tillmann, U., John, U., Cembella, A. D. 2009. Characterization of azaspiracids in plankton size-fractions and isolation of an azaspiracid producing dinoflagellate from the North Sea. Harmful Algae, 8(2), 254–263. doi:10.1016/j.hal.2008.06.003

Krock, B., Tillmann, U., Voß, D., Koch, B. P., Salas, R., Witt, M., Potvin, É., Jeong, H. J. 2012. New azaspiracids in Amphidomataceae (Dinophyceae). Toxicon, 60(5), 830–839. doi:10.1016/j.toxicon.2012.05.007

Kudela, R. M., Berdalet, E., Bernard, S., Burford, M., Fernand, L., Lu, S., Roy, S., Tester, P., Usup, G., Magnien, R., Anderson, D. M., Cembella, A., Chinain, M., Hallegraeff, G., Reguera, B., Zingone, A., Enevoldsen, H. 2015. Harmful Algal Blooms: A scientific summary for policy makers. En IOC/Unesco. de http://unesdoc.unesco.org/images/0023/002334/233419e.pdf

Kumar, S., Stecher, G., Tamura, K. 2016. MEGA7: Molecular Evolutionary Genetics Analysis Version 7.0 for Bigger Datasets. Molecular Biology and Evolution, 33(7), 1870–1874. doi:10.1093/molbev/msw054

Kyewalyanga, M. 2016. Phytoplankton primary production: Western Indian Ocean. En J. Paula (Ed.), Regional State of the Coast Report (First edit). doi:10.18356/7e303d60-en

Larrañaga, M. . 2013. Variability of surface circulation in the Bay of Todos Santos, Baja California, Mexico. Universidad Autónoma de Baja California, Mexico. 81 pp.

LeGresley, M., McDermott, G. 2010. Counting chamber methods for quantitative phytoplankton analysis -haemocytometer, Palmer-Maloney cell and Sedgewick-Rafter cell. En B. Karlson, C. Cusack, & E. Bresnan (Eds.), Microscopic and molecular methods for quantitative phytoplankton analysis ((IOC 290 M). UNESCO: Paris. p. 109.

Lenaers, G., Scholin, C., Bhaud, Y., Saint-Hilaire, D., Herzog, M. 1991. A molecular phylogeny of dinoflagellate protists (Pyrrhophyta) inferred from the sequence of 24S rRNA divergent domains D1 and D8. Journal of Molecular Evolution, 32(1), 53–63. doi:10.1007/BF02099929

Lewitus, A. J., Horner, R. A., Caron, D. A., Garcia-Mendoza, E., Hickey, B. M., Hunter, M., Huppert, D. D., Kudela, R. M., Langlois, G. W., Largier, J. L., Lessard, E. J., RaLonde, R., Jack Rensel, J. E., Strutton, P. G., Trainer, V. L., Tweddle, J. F. 2012. Harmful algal blooms along the North American west coast region: History, trends, causes, and impacts. Harmful Algae, 19, 133–159. doi:10.1016/j.hal.2012.06.009

Lin, S. 2011. Genomic understanding of dinoflagellates. Research in Microbiology, 162, 151–169. doi:10.1016/j.resmic.2011.04.006

Lin, S., Zhang, H., Hou, Y., Zhuang, Y., Miranda, L. 2009. High-level diversity of dinoflagellates in the natural environment, revealed by assessment of mitochondrial cox1 and cob genes for dinoflagellate DNA barcoding. Applied and Environmental Microbiology, 75(5), 1279–1290. doi:10.1128/AEM.01578-08

Lindholm, T., Nummelin, C. 1999. Red tide of the dinoflagellate *Heterocapsa triquetra* (Dinophyta) in a ferry-mixed coastal inlet. Hydrobiologia, 393, 245–251. doi:10.1023/A:1003563022422

Litaker, R. W., Tester, P. A., Duke, C. S., Kenney, B. E., Pinckney, J. L., Ramus, J. 2002. Seasonal niche strategy of the bloom-forming dinoflagellate *Heterocapsa triquetra*. Marine Ecology Progress Series, 232(June 2014), 45–62. doi:10.3354/meps232045

Litaker, R. W., Vandersea, M. W., Kibler, S. R., Reece, K. S., Stokes, N. A., Lutzoni, F. M., Yonish, B. A., West, M. A., Black, M. N. D., Tester, P. A. 2007. Recognizing dinoflagellate species using ITS rDNA sequences. Journal of Phycology, 43(2), 344–355. doi:10.1111/j.1529-8817.2007.00320.x

Loeblich, A.R., J. ., Loebich, A.R., I. 1966. Index to the genera, subgenera, and sections of the Pyrrophyta. Stud. Trop. Oceanogr., 3, 1–94.

Lomas, M. W., Glibert, P. M. 1999. Interactions between NH+4 and NO−3 uptake and assimilation: comparison of diatoms and dinoflagellates at several growth temperatures. Marine Biology, 133(3), 541–551. doi:10.1007/s002270050494

Lund, J.W.G., Kipling, C., Le Cren, E.D. 1958. The inverted microscope method of estimating algal numbers and the statistical basis of estimations by counting. Hydrobiol. 11, 143–170. doi: 10.1007/BF00007865

Mackenzie, L., White, D., Oshima, Y., Kapa, J. 1996. The resting cyst and toxicity of *Alexandrium ostenfeldii* (Dinophyceae) in New Zealand. Phycologia, 35(2), 148–155. doi:10.2216/i0031-8884-35-2-148.1

MacKinnon, S., Cembella, A., Quilliam, M., LeBlanc, P., Lewis, N., Hardstaff, W., Burton, I., Walter, J. 2004. The characterization of two new spirolides isolated from Danish strains of the toxigenic dinoflagellate *Alexandrium ostenfeldii*. In: Steidinger, K,A., Landsberg, J.H., Tomas, C.R., Vargo, G.A, eds. Proceedings of the 10th International Conference on Harmful Algae, Florida Fish and Wildlife Conservation Commission, Florida Institute of Oceanography and Intergovernmental Oceanographic Commission of UNESCO, Paris, 186–188 p.

McClatchie, S., Goericke, R., Leising, A., Auth, T. D., Bjorkstedt, E., Robertson, R., Brodeur, D., Du, X., Daly, E.A., Morgan, C.A., Chavez, E.F., Debich, A.J., Hildebrand, J., Field, J., Sakuma, K., Jacox, M.G., Kahru, M., Kudela, R., Anderson, C., Lavaniegos, B.E., Gomez-Valdes, J., Jiménez-Rosenberg, S.P.A., McCabe, R., Melin, S.R., Ohman, M.D., Sala, L.M., Peterson, B., Fisher, J., Schroeder, I.D., Bograd, S.J., Hazen, E.L., Schneider, S.R., Golightly, R.T., Suryan, M.R., Gladics, A.J., Loredo, S., Porquez, J.M., Thompson, A.R., Weber, E.D.,Watson, W., Trainer, V., Warzybok, P., Bradley, R., Jahncke, J. 2016. State of the California Current 2015–16: Comparisons with the 1997–98 El Niño. California Cooperative Ocean and Fisheries Investigations Reports (CalCOFI). Vol. 57,5–61.

Maeda-Martínez, A. . 2008. Estado actual del cultivo de moluscos en México. En A. Lovatelli, A. Farías, & I. Uriarte (Eds.), Taller Técnico Regional de la FAO 20-24 de agosto de 2007 (Vol. 12). Roma, Italy. pp. 91–100.

Martín-Morales, E., Mariño, C., Arévalo, F., Correa, J., Moroño, A., Blanco, J. 2013. Marine and Freshwater Toxins Analysis. Fourth Joint Symposium and AOAC Task Force Meeting. Baiona (Spain), MAY 5-9, 2013. doi:10.13140/RG.2.1.2912.6647

Matsuyama, Y. 1999. Harmful effect of dinoflagellate *Heterocapsa circularisquama* on shellfish aquaculture in Japan. JARQ, 33(4), 283–293.

Matsuyama, Y., Uchida, T., Honjo, T. 1997. Toxic effects of the dinoflagellate *Heterocapsa circularisquama* on clearance rate of the blue mussel *Mytilus galloprovincialis*. Marine Ecology Progress Series, 146, 73–80.

Matsuyama, Y., Uchida, T., Honjo, T., Shumway, S. . 2001. Impacts of the harmful dinoflagellate *Heterocapsa circularisquama* bloom on shellfish aquaculture in Japan and some experimental studies on invertebrates. Journal of Shellfish Research, 20(3), 1269–1272.

McMahon, T., Silke, J. 1996. West coast of Ireland; winter toxicity of unknown aetiology in mussels. Harmful Algae News, 14(2), 12.

Medlin, L. K., Orozco, J. 2017. Molecular techniques for the detection of organisms in aquatic environments, with emphasis on harmful algal bloom species. Sensors (Switzerland), 17(5). doi:10.3390/s17051184

Méndez, M. 2008. Desarrollo de métodos para el aislamiento y la detección de toxinas marinas en productos de la pesca y la acuicultura. Universidad de Santiago de Compostela. 111 pp.

Mendoza, R., Ramírez-Martínez, C., Aguilera, C., Meave del Castillo, M. . 2014. Principales vías de introducción de las especies exóticas. En R. Mendoza & P. Koleff (Eds.), Especies acuáticas invasoras en México. Comisión Nacional para el Conocimiento y Uso de la Biodiversidad: México. pp. 43–73.

Millette, N. C., Pierson, J. J., Aceves, A., Stoecker, D. K. 2017. Mixotrophy in *Heterocapsa rotundata*: A mechanism for dominating the winter phytoplankton. Limnology and Oceanography, 62(2), 836–845. doi:10.1002/lno.10470

Miranda Bojórquez, L. 2012. Caracterización de las corrientes en las entradas y alrededores de la Bahía de Todos Santos. Centro de investigación Científica y de Educación Superior de Ensenada Baja California, México. 56 pp.

Miyazaki, Y., Nakashima, T., Iwashita, T., Fujita, T., Yamaguchi, K., Oda, T. 2005. Purification and characterization of photosensitizing hemolytic toxin from harmful red tide phytoplankton, *Heterocapsa circularisquama*. Aquatic Toxicology, 73(4), 382–393. doi:10.1016/j.aquatox.2005.04.005

Mizuno, M. 1991. Influence of cell volume on the growth and size reduction of marine and estuarine diatoms. Journal of Phycology, 27(4), 473–478. doi:10.1111/j.0022-3646.1991.00473.x

Moestrup, Ø., Hansen, P.J. 1988. On the occurrence of the potentially toxic dinoflagellates *Alexandrium tamarense* (=*Gonyaulax excavata*) and *A. ostenfeldii* in Danish and Faroese waters. Ophelia. 28, 195–213. doi: 10.1080/00785326.1988.10430813

Moreno-Moreno, L. ., López-Torres, G. ., Marín, E. 2016. El sector de pesca y acuacultura en Baja California. En Tópicos de Pesca y Acuacultura en el Noroeste de México. Universidad Autónoma de Baja California: Mexicali. pp. 53–86.

Morrill, L. C., Loeblich, A. R. 1981. A survey for body scales in dinoflagellates and a revision of Cachonina and *Heterocapsa* (Pyrrhophyta). Journal of Plankton Research, 3(1), 53–65. doi:10.1093/plankt/3.1.53

Munday, R., Quilliam, M. A., LeBlanc, P., Lewis, N., Gallant, P., Sperker, S. A., Stephen Ewart, H., MacKinnon, S. L. 2012. Investigations into the toxicology of spirolides, a group of marine phycotoxins. Toxins, 4(1), 1–14. doi:10.3390/toxins4010001

Niklas, K. . 1994. Plant Allometry. The Scaling of Form and Process. The University of Chicago Press: Chicago.

Ofuji, K., Satake, M., Oshima, Y., McMahon, T., James, K. J., Yasumoto, T. 1999. A sensitive and specific determination method for azaspiracids by liquid chromatography mass spectrometry. Natural Toxins, 7(6), 247–250. doi:10.1002/1522-7189(199911/12)7:6<247::AID-NT68>3.0.CO;2-T

Orellana-Cepeda, E., Canino-Herrera, R., Santamaría del Angel, E., Granados-Machuca, C., Valdez, M., Morales-Zamoran, L. . 2007. Florecimiento de *Ceratium divaricatum* frente a la costa Noroeste de 623 Ensenada, Baja California, durante la primavera de 2007. En II Taller de Florecimientos Algales Nocivos, Ensenada, Baja California, 2007, CICESE, pp. 12. CICESE: Ensenada, Baja California. p. 12.

Otero, A., Chapela, M.J., Atanassoya, M., Vieites, J.M., Cabado, A.G. 2011. Cyclic imines: chemistry and mechanism of action: A review. Chemical Research in Toxicology. 11, 1817–1829. doi: 10.1021/tx200182m.

Penna, A., Bertozzini, E., Battocchi, C., Galluzzi, L., Giacobbe, M., Vila, M., Garces, E., Luglie, A., Magnani, M. 2007. Monitoring of HAB species in the Mediterranean sea through molecular methods. Journal of Plankton Research, 29, 19–38. doi: 10.1093/plankt/fbl053

Peña-Manjarrez, J.L., Helenes, J., Gaxiola-Castro, G., Orellana-Cepeda, E. 2005. Dinoflagellate cysts and bloom events at Todos Santos Bay, Baja California, México, 1999–2000. Continental Shelf Research. 25:1375–1393. doi:10.1016/j.csr.2005.02.002

Peña Manjarrez, J., Gaxiola-Castro, G., Helenes-Escamilla, J. 2009. Environmental factors influencing the variability of *Lingulodinium polyedrum* and *Scrippsiella trochoidea* (Dinophyceae) cyst production. Ciencias Marinas, 35(1), 1–14. doi:10.7773/cm.v35i1.1406

Percy, L., Morris, S., Higman, W., Stone, D., Hardstaff, W. R., Quilliam, M. A., Lewis, J. 2004. Identification of *Alexandrium ostenfeldii* from the Fal Estuary, UK; morphology, molecular taxonomy and toxin composition. Abstract, XI International Conference on Harmful Algal Blooms, Cape Town, South Africa, 15–19 November, 2004, 209 pp.

Percopo, I., Siano, R., Rossi, R., Soprano, V., Sarno, D., Zingone, A. 2013. A new potentially toxic *Azadinium* species (Dinophyceae) from the Mediterranean Sea, *A. dexteroporum* sp. nov. Journal of Phycology, n/a-n/a. doi:10.1111/jpy.12104

Pérez-Brunius, P., López, M., Pineda, J. 2006. Hydrographic conditions near the coast of northwestern Baja California: 1997–2004. Continental Shelf Research, 26(8), 885–901. doi:10.1016/j.csr.2006.01.017

Potvin, É., Jeong, H. J., Kang, N. S., Tillmann, U., Krock, B. 2012. First report of the photosynthetic dinoflagellate genus *Azadinium* in the Pacific Ocean: Morphology and molecular characterization of *Azadinium cf. poporum*. Journal of Eukaryotic Microbiology, 59(2), 145–156. doi:10.1111/j.1550-7408.2011.00600.x

Raven, J. A., Richardson, K. 1984. Dinoflagellate flagella: a cost-benefit analysis. The New Phytologist, 98(2), 259–276.

Regueiro, J., Rossignoli, A.E., Alvarez, G., Blanco, J. 2011. Automated online solid-phase extraction coupled to liquid chromatography tandem mass spectrometry for determination of lipophilic marine toxins in shellfish. Food Chem. 129 (2), 533–540. doi: 10.1016/j.foodchem.2011.04.054

Richard, D., Arsenault, E., Quilliam, M.A., Cembella, A.D. 2001. Investigations into the toxicology and pharmacology of spirolides, a novel group of shellfish toxins. In: Harmful Algal Blooms 2000. Hallegraeff, G,M., Blackburn, S.I., Bolch, C.J., Lewis, R.J. eds. International Oceanographic Commission (UNESCO), Paris, 383–386 p.

Román, Y., Alfonso, A., Louzao, M. C., de la Rosa, L. A., Leira, F., Vieites, J. M., Vieytes, M. R., Ofuji, K., Satake, M., Yasumoto, T., Botana, L. M. 2002. Azaspiracid-1, a potent, nonapoptotic new phycotoxin with several cell targets. Cellular Signalling, 14(8), 703–716. doi:10.1016/S0898-6568(02)00015-3

Ronquist, F., Huelsenbeck, J. P. 2003. MrBayes 3: Bayesian phylogenetic inference under mixed models. Bioinformatics, 19(12), 1572–1574. doi:10.1093/bioinformatics/btg180

Rossi, R., Dell'Aversano, C., Krock, B., Ciminiello, P., Percopo, I., Tillmann, U., Soprano, V., Zingone, A. 2017. Mediterranean *Azadinium dexteroporum* (Dinophyceae) produces six novel azaspiracids and azaspiracid-35: a structural study by a multi-platform mass spectrometry approach. Analytical and Bioanalytical Chemistry, 409(4), 1121–1134. doi:10.1007/s00216-016-0037-4

Rossini, G. P., Hess, P. 2010. Phycotoxins : chemistry , mechanisms of action and shellfish poisoning. Clinical Toxicology, 2, 65–122.

Ruiz de la Torre, M. C. 2013. Coastal algal blooms, the near-surface diurnal thermocline and wind transport toward the coast; ecological implications. Centro de Investigación Científica y de Educación Superior de Ensenada Baja California. 18–56 pp.

Rundberger, T., Aasen, J.A., Selwood, A.L., Miles C.O. 2011. Pinnatoxins and spirolides in Norwegian blue mussels and seawater. Toxicon. 58 (8), 700–711. doi: 10.1016/j.toxicon.2011.08.008

Salas, R., Tillmann, U., John, U., Kilcoyne, J., Burson, A., Cantwell, C., Hess, P., Jauffrais, T., Silke, J. 2011. The role of *Azadinium spinosum* (Dinophyceae) in the production of azaspiracid shellfish poisoning in mussels. Harmful Algae, 10(6), 774–783. doi:10.1016/j.hal.2011.06.010

Salas, R., Tillmann, U., Kavanagh, S. 2014. Morphological and molecular characterization of the small armoured dinoflagellate *Heterocapsa minima* (Peridiniales, Dinophyceae). European Journal of Phycology, 49(4), 413–428. doi:10.1080/09670262.2014.956800

Salcedo-Garduño, M. G., Castañeda-Chávez, M. del R., Lango-Reynoso, F., Galaviz-Villa, I. 2018. Harmful Algal Blooms (HABS) along Mexican coasts. Preprints, (December), 1–17. doi:10.20944/preprints201812.0352.v1

Sánchez-Bravo, Y. 2013. Concentración de toxinas lipofílicas en el mejillón mediterraneo (*Mytilus galloprovincialis*) asociados a la presencia de dinoflagelados del género *Dinophysis* durante enero a diciembre del 2012, en la Bahía de Todos Santos, B.C., México. Universidad Autónoma de Baja California. 109 pp.

Sánchez, S., Villanueva, P., Carbajo, L. 2004. Distribution and concentration of *Alexandrium peruvianum* (Balech and de Mendiola) in the Peruvian coast (03°24'–18°20' LS) between 1982–2004. In Proceedings of the XI International Conference on Harmful Algal Blooms, Cape Town, South Africa, 15–19 November 2004.

Satake, M., Ofuji, K., Naoki, H., James, K. J., Furey, A., McMahon, T., Silke, J., Yasumoto, T. 1998. Azaspiracid, a New Marine Toxin having unique spiro ring assemblies, isolated from Irish mussels, *Mytilus edulis*. Journal of the American Chemical Society, 120(38), 9967–9968. doi:10.1021/ja981413r

Schwarz, E. 2011. Molecular and Morphological Characterization of *Alexandrium* species (Dinophyceae) from the East Coast, USA. Department of Biology and Marine Biology: University of North Carolina Wilmington, USA.

Seong, K., Jeong, H., Kim, S., Kim, G., Kang, J. 2006. Bacterivory by co-occurring red-tide algae, heterotrophic nanoflagellates, and ciliates. Marine Ecology Progress Series, 322, 85–97. doi:10.3354/meps322085

SEPESCABC. 2018. Boletín Estadístico Reporte de Producción Pesquera y Acuícola de Baja California Perido Información 2017 Cierre Anual preliminar. de http://www.sepescabc.gob.mx/x/estadisticas/docs/PRODUCCION_PESQUERA_Y_ACUICOLA_DE_BC_2017-(PRELIMINAR_05MAR2018).pdf

Sleno, L., Chalmers, M.L., Volmer, D.A. 2004. Structural study of spirolide marine toxins by mass spectrometry. Part II. Mass spectrometric characterization of unknown spirolides and related compounds in a cultured phytoplankton extract. Anal. Bioanal. Chem. 378, 977–986. doi: 10.1007/s00216-003-2296-0

Smayda, T. J., Reynolds, C. S. 2003. Strategies of marine dinoflagellate survival and some rules of assembly. Journal of Sea Research, 49(2), 95–106. doi:10.1016/S1385-1101(02)00219-8

Solórzano, L. 1969. Determinarion of ammonia in natural waters by the phenol hypochlorite method. Limnology and Oceanography, 14(5), 799–801. doi:10.4319/lo.1969.14.5.0799

Steidinger, K. ., Tangen, K. 1996. Dinoflagellates. En C. R. Tomas (Ed.), Identifying Marine Diatoms and Dinoflagellates. Academic Press Inc.: San Diego. pp. 387–598.

Stein, F. 1883. Der organismus der Infusionsthiere nach eigenen forschungen in systematischer reihenfolge bearbeitet. III. Abt. II. Hälfte. Die naturgeschichte der arthrodelen flagellaten. W. Engelmann: Leipzig.

Stern, R. F., Andersen, R. A., Jameson, I., Küpper, F. C., Coffroth, M. A., Vaulot, D., Le Gall, F., Véron, B., Brand, J. J., Skelton, H., Kasai, F., Lilly, E. L., Keeling, P. J. 2012. Evaluating the ribosomal Internal Transcribed Spacer (ITS) as a candidate dinoflagellate barcode marker. PLoS ONE, 7(8). doi:10.1371/journal.pone.0042780

Stern, R. F., Horak, A., Andrew, R. L., Coffroth, M.-A., Andersen, R. A., Küpper, F. C., Jameson, I., Hoppenrath, M., Véron, B., Kasai, F., Brand, J., James, E. R., Keeling, P. J. 2010. Environmental barcoding reveals massive dinoflagellate diversity in marine environments. PLoS ONE, 5(11), e13991. doi:10.1371/journal.pone.0013991

Stobo, L. ., Lacaze, J. ., Scott, A. ., Gallacher, S., Smith, E. ., Quilliam, M. A. 2005. Liquid chromatography with mass spectrometry-detection of lipophilic shellfish toxins. Journal of AOAC International, 88(5), 1371–1382.

Strickland, J. ., Parsons, T. . 1972. A practical handbook of sea water analysis (Second edi; J. . Stevenson, Ed.). Ottawa, KIA 169: Canada.

Strub, P. T., James, C. 2000. Altimeter-derived variability of surface velocities in the California Current System: 2. Seasonal circulation and eddy statistics. Deep Sea Research Part II: Topical Studies in Oceanography, 47(5–6), 831–870. doi:10.1016/S0967-0645(99)00129-0

Suikkanen, S., Kremp, A., Hautala, H., Krock, B. 2013. Paralytic shellfish toxins or spirolides? The role of environmental and genetic factors in toxin production of the *Alexandrium ostenfeldii* complex. Harmful Algae. 26, 52–59. doi: 10.1016/j.hal.2013.04.001

Stocker, T.F., Qin, D., Plattner, G.K., Tignor, M., Allen, S.K., Boschung, J., Nauels, A., Xia, Y., Bex, V., Midgle, P.M. 2013. Climate change 2013: the physical science basis. Contribution of Working Group I to the Fifth Assessment Report of the Intergovernmental Panel on Climate Change Cambridge University Press; Cambridge, United Kingdom and New York, NY USA. 2013. 1535p.

Tarutani, K., Nagasaki, K., Itakura, S., Yamaguchi, M. 2001. Isolation of a virus infecting the novel shellfish-killing dinoflagellate *Heterocapsa circularisquama*. Aquatic Microbial Ecology, 23(2), 103–111. doi:10.3354/ame023103

Taylor, F. J. . 1987. The Biology of dinoflagellates (Second edi; F. J. . Taylor, Ed.). Oxford : Blackwell Scientific.

Thompson, J. D., Gibson, T. J., Plewniak, F., Jeanmougin, F., Higgins, D. G. 1997. The CLUSTAL X windows interface: Flexible strategies for multiple sequence alignment aided by quality analysis tools. Nucleic Acids Research, 25(24), 4876–4882. doi:10.1093/nar/25.24.4876

Throndsen, J., Hasle, G. ., Tangen, K. 2007. Phytoplankton of Norwegian coastal waters. Almater Forlag AS: Oslo, Norway.

Tillmann, Urban, Trefault, N., Krock, B., Parada-Pozo, G., De La Iglesia, R., Vásquez, M. 2017a. Identification of *Azadinium poporum* (Dinophyceae) in the Southeast Pacific: Morphology, molecular phylogeny, and azaspiracid profile characterization. Journal of Plankton Research, 39(2), 350–367. doi:10.1093/plankt/fbw099

Tillmann, U, Jaén, D., Fernández, L., Gottschling, M., Witt, M., Blanco, J., Krock, B. 2017b. *Amphidoma languida* (Amphidomatacea, Dinophyceae) with a novel azaspiracid toxin profile identified as the cause of molluscan contamination at the Atlantic coast of southern Spain. Harmful Algae, 62, 113–126. doi:10.1016/j.hal.2016.12.001

Tillmann, Urban, Hoppenrath, M., Gottschling, M., Kusber, W. H., Elbrächter, M. 2017c. Plate pattern clarification of the marine dinophyte *Heterocapsa triquetra* sensu Stein (Dinophyceae) collected at the Kiel Fjord (Germany). Journal of Phycology, 53(6), 1305–1324. doi:10.1111/jpy.12584

Tillmann, Urban, Sánchez-Ramírez, S., Krock, B., Bernales-Jiménez, A. 2017d. A bloom of *Azadinium prolongum* in coastal waters off Peru. Revista de biología marina y oceanografía, 52(3), 591–610. doi:10.4067/S0718-19572017000300015

Tillmann, U, Gottschling, M., Nézan, E., Krock, B. 2015. First record of *Azadinium dexteroporum* and *Amphidoma languida* (Amphidomataceae, Dinophyceae) from the Irminger Sea off Iceland. Marine Biodiversity Records, 8(148), 11. doi:10.1017/S1755262715001128

Tillmann, Urban, Salas, R., Jauffrais, T., Hess, P., Silke, J. 2014a. AZA: The Producing Organisms—Biology and Trophic Transfer. Seafood and Freshwater Toxins, 773–798. doi:10.1201/b16662-26

Tillmann, Urban, Krock, B., Taylor, B. B. 2014b. *Azadinium caudatum* var. *margalefii*, a poorly known member of the toxigenic genus *Azadinium* (Dinophyceae). Marine Biology Research, 10(10), 941–956. doi:10.1080/17451000.2013.866252

Tillmann, U, Salas, R., Gottschling, M., Krock, B., O'Driscoll, D., Elbrächter, M. 2012a. *Amphidoma languida* sp. nov. (Dinophyceae) Reveals a Close Relationship between *Amphidoma* and *Azadinium*. Protist, 163(5), 701–719. doi:10.1016/j.protis.2011.10.005

Tillmann, Urban, Soehner, S., Nézan, E., Krock, B. 2012b. First record of the genus *Azadinium* (Dinophyceae) from the Shetland Islands, including the description of *Azadinium polongum* sp. nov. Harmful Algae, 20(December), 142–155. doi:10.1016/j.hal.2012.10.001

Tillmann, Urban, Elbrächter, M., John, U., Krock, B. 2011. A new non-toxic species in the dinoflagellate genus *Azadinium* : *A. poporum* sp. nov. European Journal of Phycology, 46(1), 74–87. doi:10.1080/09670262.2011.556753

Tillmann, U, Elbrächter, M., Krock, B., John, U., Cembella, A. 2009a. *Azadinium spinosum* gen. et sp. nov. (Dinophyceae) identified as a primary producer of azaspiracid toxins. European Journal of Phycology, 44(1), 63–79. doi:10.1080/09670260802578534

Tillmann, U, Hansen, P. . 2009b. Allelopathic effects of *Alexandrium tamarense* on other algae: evidence from mixed growth experiments. Aquatic Microbial Ecology, 57, 101–112. doi:10.3354/ame01329

Tillmann, Urban, John, U. 2002. Toxic effects of Alexandrium spp. on heterotrophic dinoflagellates: An allelochemical defence mechanism independent of PSP-toxin content. Marine Ecology Progress Series, 230(1999), 47–58. doi:10.3354/meps230047

Thompson, J.D., Gibson, T.J., Plewniak, F., Jeanmougin, F., Higgins, D.G. 1997. The ClustalX windows interfase: flexible strategies for multiple sequence alignment aided by quality analysis tools. Nucl. Acid Res. 25, 4876–4882.

Toebe, K., Joshi, A. R., Messtorff, P., Tillmann, U., Cembella, A., John, U. 2013a. Molecular discrimination of taxa within the dinoflagellate genus Azadinium, the source of azaspiracid toxins. Journal of Plankton Research, 35(1), 225–230. doi:10.1093/plankt/fbs077

Toebe, K., Alpermann, T. J., Tillmann, U., Krock, B., Cembella, A., John, U. 2013b. Molecular discrimination of toxic and non-toxic Alexandrium species (Dinophyta) in natural phytoplankton assemblages from the Scottish coast of the North Sea. European Journal of Phycology, 48(1), 12–26. doi:10.1080/09670262.2012.752870

Torres, C. ., Mejía, A., Argote, M. ., Ramírez, I., Mancillas, M. 2006. Three-dimensional circulation in Todos Santos Bay, Ensenada, B. C. Mexico. En B. Gámez, D. Ojeda, G. Larrazabal, & M. Cerrolaza (Eds.), Simulación y Modelado en Ingeniería y Ciencias (First edit). SVMNI. pp. 115–122.

Tosteson, T. ., Ballantine, D. ., Winter, A. 1998. Sea surface temperature, benthic dinoflagellate toxicity and toxin transmission in the ciguatera food web. En B. Reguera, J. Blanco, M. Fernandez, & T. Wyatt (Eds.), Proceedings of the VIII International Conference on Harmful Algae. Xunta de Galicia and IOC of UNESCO: Vigo, Spain. pp. 44–48.

Touzet, N., Keady, E., Raine, R., Maher, M. 2009. Evaluation of taxa-species real time PCR, whole-cell FISH and morphotaxonomy analyses for the detection and quantification of the toxic microalgae *Alexandrium minutum* (Dinophyceae), global clade ribotype. FEMS Microbiol. Ecol, 67 2, 329–341. doi: 10.1111/j.1574-6941.2008.00627.x

Touzet, N., Franco, J. M., Raine, R. 2008. Morphogenetic diversity and biotoxin composition of *Alexandrium* (Dinophyceae) in Irish coastal waters. Harmful Algae. 7, 782–97. doi: 10.1016/j.hal.2008.04.001

Trainer, V. L., Moore, L., Bill, B. D., Adams, N. G., Harrington, N., Borchert, J., Da Silva, D. A. M., Eberhart, B. T. L. 2013. Diarrhetic shellfish toxins and other lipophilic toxins of human health concern in Washington State. Marine Drugs, 11(6), 1815–1835. doi:10.3390/md11061815

Twiner, M. J., Rehmann, N., Hess, P., Doucette, G. J. 2008. Azaspiracid shellfish poisoning: A review on the chemistry, ecology, and toxicology with an emphasis on human health impacts. Marine Drugs, 6(2), 39–72. doi:10.3390/md6020039

Vale, P., Bire, R., Hess, P. 2008. Confirmation by LC-MS/MS of azaspiracids in shellfish from the Portuguese north-western coast. Toxicon, 51(8), 1449–1456. doi:10.1016/j.toxicon.2008.03.022

Van de Waal, D. B., Tillmann, U., Martens, H., Krock, B., van Scheppingen, Y., John, U. 2015. Characterization of multiple isolates from an *Alexandrium ostenfeldii* bloom in The Netherlands. Harmful Algae, 49, 94–104. doi:10.1016/j.hal.2015.08.002

Van Dolah, F. M., Fire, S. E., Leighfield, T. A., Mikulski, C. M., Doucette, G. J. 2012. Determination of paralytic shellfish toxins in shellfish by receptor binding assay: collaborative study. Journal of AOAC International, 95(3), 795–812. doi:10.5740/jaoacint.CS2011_27

Van Heukelem, L., Thomas, C. S. 2001. Computer-assisted high-performance liquid chromatography method development with applications to the isolation and analysis of phytoplankton pigments. Journal of Chromatography A, 910(1), 31–49. doi:10.1016/S0378-4347(00)00603-4

Vandersea, M. W., Kibler, S. R., Holland, W. C., Tester, P. A., Schultz, T. F., Faust, M. A., Holmes, M. J., Chinain, M., Wayne Litaker, R. 2012. Development of semi-quantitative PCR assays for the detection and enumeration of *Gambierdiscus* species (Gonyaulacales, Dinophyceae). Journal of Phycology, 48(4), 902–915. doi:10.1111/j.1529-8817.2012.01146.x

Van Wagoner, R.M., Misner, I., Tomas, C.R. Wright, J.L.. 2011. Occurrence of 12- methyl gymnodimine in a spirolide producing dinoflagellate *Alexandrium peruvianum* and the biogenic implications. Tetrahedron Lett. 52, 4243–6. doi: 10.1016/j.tetlet.2011.05.137

Wells, B., Schroeder, J., Santora, E., Hazen, S., Bograd, E., Bjorkstedt, V., Loeb, S., McClatchie, E., Weber, W., Watson, A., Thompson, W., Peterson, R., Brodeur, J., Harding, J., Field, K., Sakuma, S., Hayes, N., Mantua, W., … Kim, F. 2017. State of the California Current 2016 – 17 : Still Anything But " Normal " in the North (Vol. 58).

Wells, M. L., Karlson, B., Wulff, A., Kudela, R., Trick, C., Asnaghi, V., Berdalet, E., Cochlan, W., Davidson, K., De Rijcke, M., Dutkiewicz, S., Hallegraeff, G., Flynn, K. J., Legrand, C., Paerl, H., Silke, J., Suikkanen, S., Thompson, P., Trainer, V. L. 2020. Future HAB science: Directions and challenges in a changing climate. Harmful Algae, 91(June 2019). doi:10.1016/j.hal.2019.101632

Wietkamp, S., Tillmann, U., Clarke, D., Toebe, K. 2019. Molecular detection and quantification of the azaspiracid-producing dinoflagellate *Amphidoma languida* (Amphidomataceae, Dinophyceae). Journal of Plankton Research, 41(2), 101–113. doi:10.1093/plankt/fby052

Wohlrab, S., Iversen, M.H., John, U. 2010. A molecular and co-evolutionary context for grazer induced toxin production in *Alexandrium tamarense*. PLoS ONE. 5(11):e15039. doi: 10.1371/journal.pone.0015039

Wu, H., Yao, J., Guo, M., Tan, M., Zhou, D., Zhai, Y. 2015. Distribution of marine lipophilic toxins in shellfish products collected from the Chinese market. Mar. Drugs. 13(7), 4281–4295. doi: 10.3390/md13074281

Wyatt, T. 2014. Margalef's mandala and phytoplankton bloom strategies. Deep Sea Research Part II: Topical Studies in Oceanography, 101, 32–49. doi:10.1016/j.dsr2.2012.12.006

Xiao, J., Sun, N., Zhang, Y., Sun, P., Li, Y., Pang, M., Li, R. 2018. *Heterocapsa bohaiensis* sp. nov. (Peridiniales: Dinophyceae): a novel marine dinoflagellate from the Liaodong Bay of Bohai Sea, China. Acta Oceanologica Sinica, 37(10), 18–27. doi:10.1007/s13131-018-1296-z

Yang, X., Sun, N., Li, Y., LI, X. 2015. Effects of two harmful species algae on reproduction of rotifer *Brachionus plicatilis* and metamorphosis of zoea of Chinese mitten handed crab *Eriocheir sinensis*. Journal of Dalian Ocean University, 30(4), 351–356.

Yoshida, T., Nakai, R., Seto, H., Wang, M., Iwataki, M., Hiroishi, S. 2003. Sequence analysis of 5.8S rDNA and the Internal Transcribed Spacer Region in dinoflagellate *Heterocapsa* species (Dinophyceae) and development of selective PCR primers for the bivalve killer *Heterocapsa circularisquama*. Microbes and Environments, 18(4), 216–222.

Zapata, M., Fraga, S., Rodríguez, F., Garrido, J. 2012. Pigment-based chloroplast types in dinoflagellates. Marine Ecology Progress Series, 465, 33–52. doi:10.3354/meps09879

Zapata, M., Rodríguez, F., Garrido, J. L. 2000. Separation of chlorophylls and carotenoids from marine phytoplankton: a new HPLC method using a reversed phase C8 column and pyridine-containing mobile phases. Marine Ecology Progress Series, 195, 29–45.

Zaytsev, O., Cervantes Duarte, R., Montante, O., Gallegos García, A. 2003. Coastal upwelling activity on the Pacific shelf of the Baja California Peninsula. Journal of Oceanography, 59, 489–502. doi:10.1023/A:1025544700632

Zehr, J. P., Ward, B. B. 2002. Nitrogen cycling in the ocean: New perspectives on processes and paradigms. Applied and Environmental Microbiology, 68(3), 1015–1024. doi:10.1128/AEM.68.3.1015-1024.2002

Zhang, Y., Feng, T., Qu, J., Sun, N., Liu, L. 2019. Toxicity and haemolytic activity of a newly described dinoflagellate, *Heterocapsa bohainensis* to the rotifer *Brachionus plicatilis*. Harmful Algae, 84, 112–118. doi:10.1016/j.hal.2019.03.007

Zhou, J., Fritz, L. 1994. Okadaic acid antibody localizes to chloroplasts in the DSP-toxin-producing dinoflagellates *Prorocentrum lima* and *Prorocentrum maculosum*. Phycologia, 33(6), 455–461. doi:10.2216/i0031-8884-33-6-455.1

Supplementary material

The effect of the environmental variables in the toxin production of *A. ostenfeldii* strain AON-13 (isolated from Netherlads) was studied at the Alfred-Wegener Institute. This strain is capable of producing gymnodimines, spirolides and saxitoxins. Three different temperatures: 10, 15, and 20 °C and three different irradiances 30, 100 and 200 µmol.m-^{2}.s-^{1} were tested. The control condition was 15 °C and 100 µmol.m-^{2}.s-^{1}. Along of the growth curve (lag phase, early exponential, late exponential and stationary phase) samples to quantify each toxin were obtained by triplicate.

In figure 34, the growth curve at 15 °C with the three irradiances are shown. At the low irradiance, the growth of the cells was lower that in the higher irradiances. Non-stationary phase was recorded after 60 days. The maximum growth rate and maximum density at this irradiance were 0.13 d^{-1} and 4.7 x 10^{2} cell mL^{-1}, respectively (Fig. 34). The growth rate was similar in 100 and 200 µmol.m-^{2}.s-^{1} with 0.21 and 0.23 d^{-1} respectively and the exponential phase occurred around day 10.

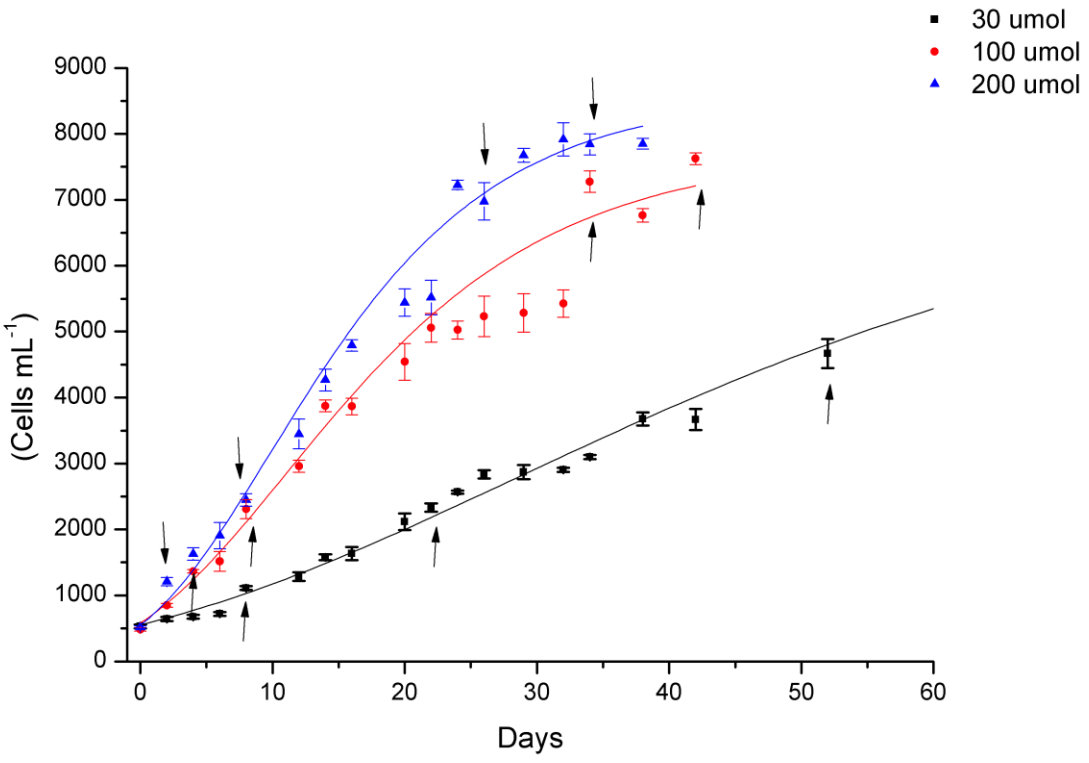

Figure 34. Growth curve of *A. ostenfeldii*, strain AON-13 at the control temperature of 15 °C and the three experimental irradiances: 30, 100, and 200 µmol.m^{-2}.s^{-1}.

As expected, the growth of *A. ostenfeldii* at 20 °C and 30 µmol.m-^{2}.s-^{1} was 50% of the obtained with the highest irradiance (200 µmol m-^{2} s-^{1}) (Fig.35). Even though the early exponential phases occurred at day 16 for the irradiance 30, the highest cell density was recorded at the end of the culture (8 x 10^{3} cell mL^{-1}). (Fig. 35). The maximum growth rate was similar at the three irradiances with 0.21 d^{-1} at 30 µmol.m^{2}.s-^{1}, 0.22 d^{-1} at 100 µmol.m^{2}.s-^{1}, and 0.23 d^{-1} at 200 µmol.m^{2}.s-^{1}. After 45 days of the experiment non stationary phase could be recorded in the low irradiance.

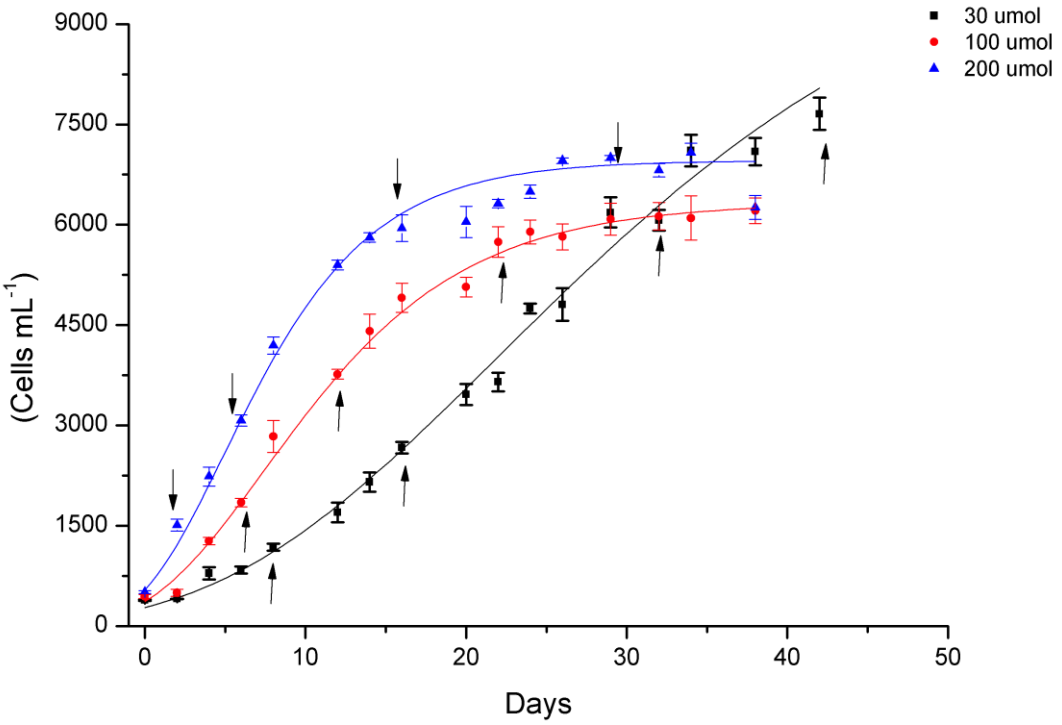

Figure 35. Growth curve of *A. ostenfeldii*, strain AON-13 at the control temperature of 20 °C and the three experimental irradiances: 30, 100, and 200 µmol.m^{2}.s^{-1}.

At 10 °C, no growth of the AON-13 strain was observed. At the beginning of the experiment with the higher irradiance, it seemed that the cells were growing; however, after six days, the cell density decreased like in the other two irradiances (Fig. 36). At this temperature, the cells excreted a mucilage to adhere to the bottom, and between the cells, there was also the formation of cysts. These results were unlike what had been reported before for *A. ostenfeldii*, and could be related to the low cell abundance (5 x 10^{2} cell mL^{-1}) with which the experiment began.

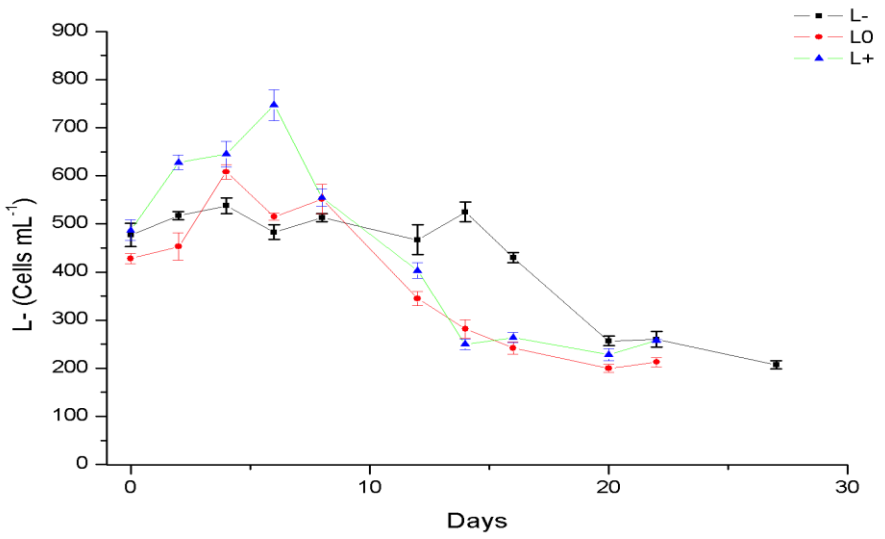

Figure 36. Growth curve of *A. ostenfeldii*, strain AON-13 at the control temperature of 10 °C and the three experimental irradiance: 30, 100 and 200 µmol.m^2.s^{-1}.

At the beginning of the experiment, the toxins were measured at control conditions (15 °C and 100 µmol.m^2.s-^{1}). In Figure 37, the content of 13 desm- SPXC per cell is shown in the experiment at 15°C. At control conditions, the cell produced 2.78 pg cell^{-1} of 13 desm- SPXC. In the T1 (lag phase) the production of the toxin was reduced but was similar at the three irradiances (mean of 1.60 pg cell^{-1}), but in the early and late exponential phases, there was a higher production of the toxin at the highest irradiance (200 µmol.m^2.s-^{1} and 100 µmol.m^2.s-^{1}) with 4.05 and 3.59 pg cell^{-1} of 13 desm- SPXC, respectively (Fig. 37).

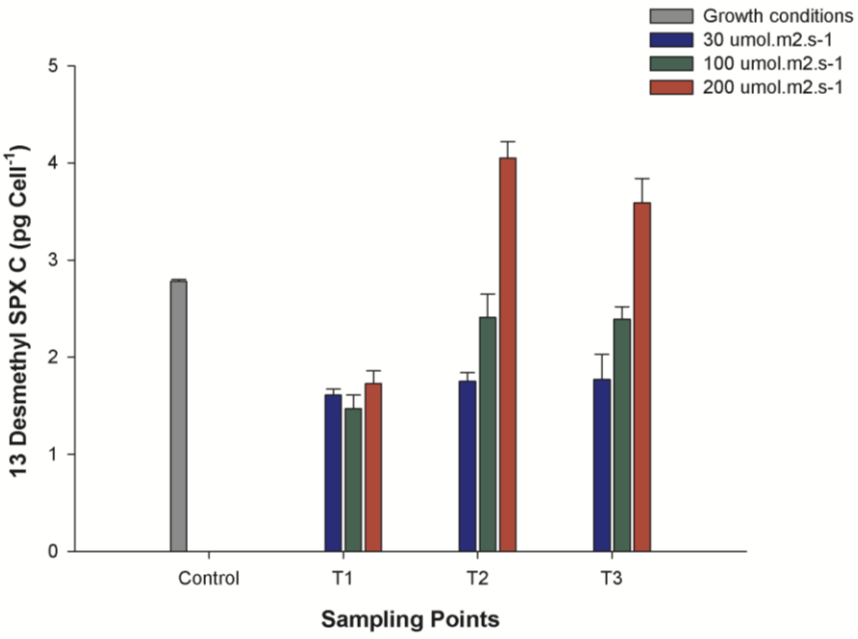

Figure 37. Production of 13 Desm-SPXC in *A. ostenfeldii*, strain AON-13 at the control temperature of 15 °C and the three experimental irradiances: 30 (blue bar), 100 (green bar) and 200 (red bar) µmol.m^2.s^{-1}. Toxin production is shown along with the growth curve T1 (lag phase) T2 (early exponential phase) T3 (late exponential phase).

The production of the spirolides at 20 °C had the same tendency as at 15 °C: a higher toxin production as irradiance increased. The effect between toxin and irradiance became more evident upon reaching the stationary phase. The maximum concentration of the 13 Desm-SPXC at 20 °C was 3.74 pg $cell^{-1}$ at T4 (Fig. 38). The stationary phase were only achieved in in the two higher irradiances (100 and 200 µmol.m^2.s^{-1}) (Fig. 38). The temperature affected the toxin production linked with the growth rate. For example in T3 at 15 ° C the toxin production was more evident than at 20 ° C, the highest cellular density was recorded at 30 µmol.m^2.s^{-1} due to cell division, which reduced the quota per cell, reflecting the lowest toxin production of 0.94 pg $cell^{-1}$ in the late exponential phase.

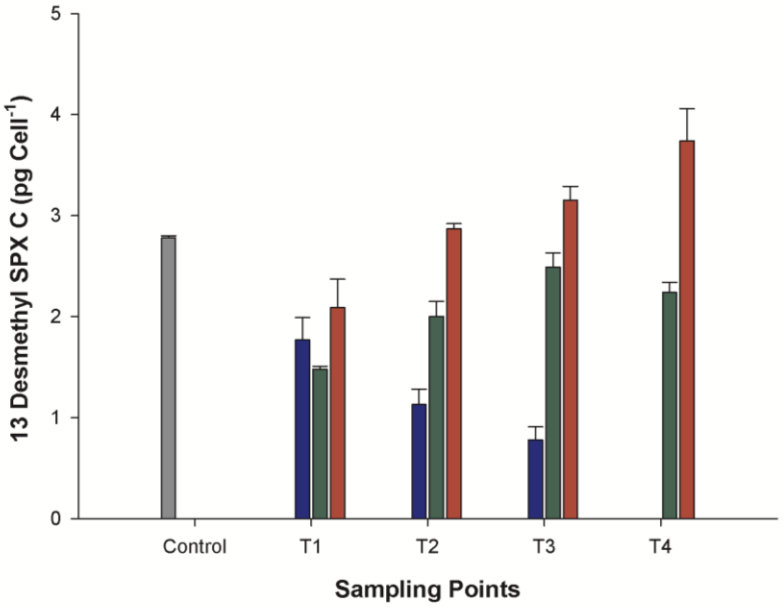

Figure 38. Production of 13 Desm-SPXC in *A. ostenfeldii*, strain AON-13 at the experimental temperature of 20 °C and the three experimental irradiance: 30 (blue bar), 100 (green bar) and 200 (red bar) µmol.m^{2}.s^{-1}. Toxin production is shown along the growth curve T1 (lag phase) T2 (early exponential phase) T3 (late exponential phase) and T4 (stationary phase).

The AON-13 strain has a lower production of gymnodimines (Gym) compared to spirolides. At the control condition, the strain produced 1.73 pg cell^{-1} of Gym A. As in the case of the spirolides at higher irradiance, higher production of toxin. During the lag phase the production of the toxin decreases with a mean of 1.08 pg cell^{-1} in the three irradiances. In the late stacionary phase the maximum production of 2.58 pg cell^{-1} was recorded at 200 µmol.m^{2}.s-^{1} (Fig. 39).

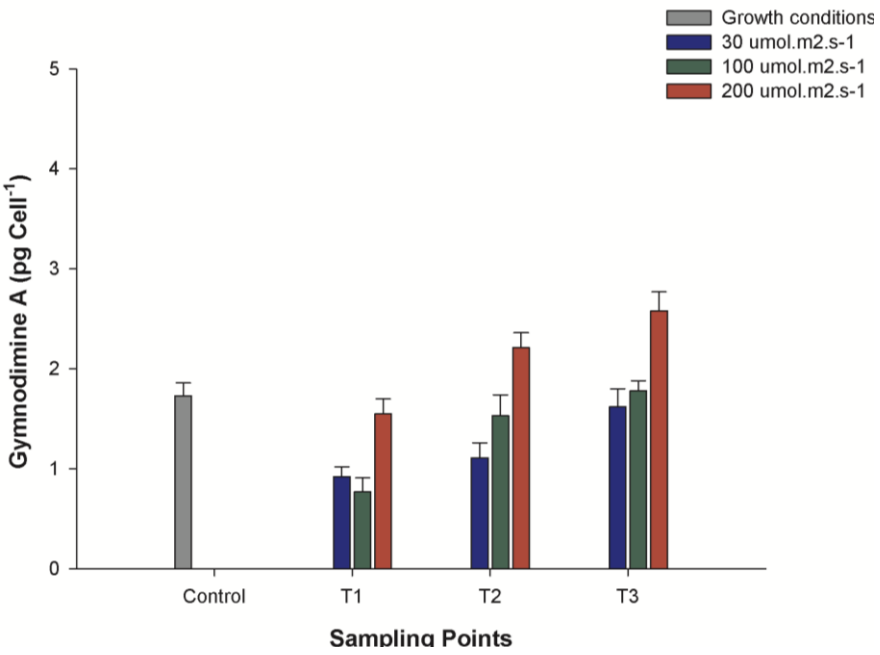

Figure 39. Production of Gymnodimine A in *A. ostenfeldii*, strain AON-13 at the control temperature of 15 °C and the three experimental irradiance: 30 (blue bar), 100 (green bar) and 200 (red bar) µmol.m^2.s^{-1}. Toxin production is shown along the growth curve T1 (lag phase) T2 (early exponential phase) T3 (late exponential phase).

As can be observed in Figure 40, as in the case of the spirolides, the production of gymnodimine A at 20 °C was reduced in low irradiances (30 µmol.m^2.s^{-1}). Following the growth curve, the higher production of the toxin (2.60 pg $cell^{-1}$ of Gym A) in the stationary phase was recorded at 200 µmol.m^2.s^{-1}. Apparently the photosyntethic machinary is closely related with the production of polyether toxins having a direct effect.

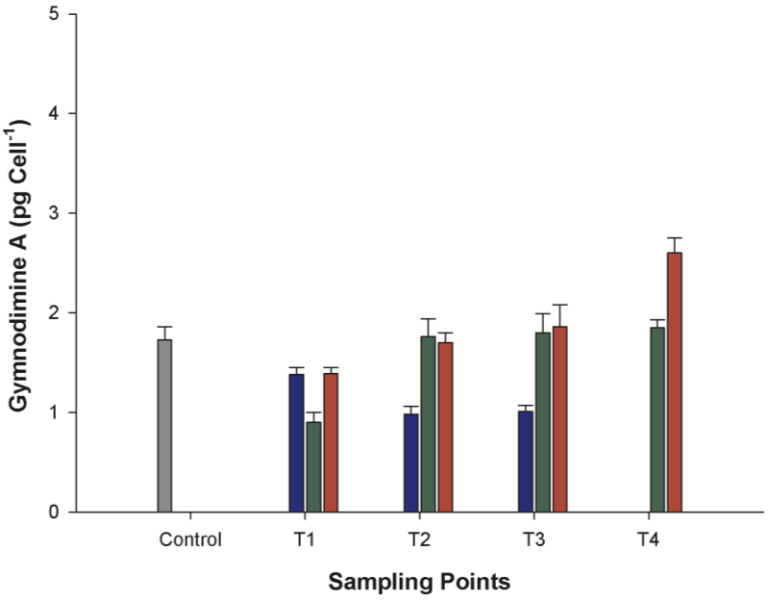

Figure 40. Production of 13 Gymnodimine A in *A. ostenfeldii*, strain AON-13 at the experimental temperature of 20 °C and the three experimental irradiance: 30 (blue bar), 100 (green bar) and 200 (red bar) µmol.m^2.s^{-1}. Toxin production is shown along the growth curve T1 (lag phase) T2 (early exponential phase) T3 (late exponential phase) and T4 (stationary phase).

The strain AON13 produced PSP toxins, their toxin profile was: C1/C2, GTX 2 and 3, dc GTX3 and STX, the quantification of all analogs is given in STX eq. cell $^{-1}$. In control conditions, the strain produced 7.79 pg STX eq. cell $^{-1}$. Unlike to the polyether toxins, during the lag phase the highest toxin production of 16.19 pg STX eq. cell $^{-1}$ was recorded at 200 µmol.m^2.s-^{1} (Fig. 41) In the early exponential phase the highest irradiance had similar toxin production with 14.38 pg at 200 µmol.m^2.s-^{1} and 14.02 pg at 100 µmol.m^2.s-^{1}. And in the late exponential phase the PSP production was higher (15.29 pg STX eq. cell $^{-1}$) at the high irradiance (Fig. 41).

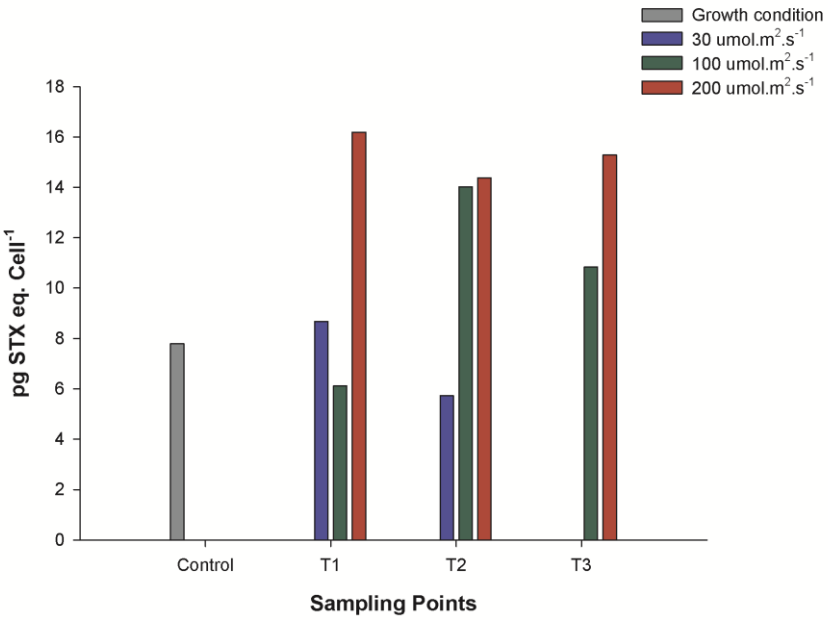

Figure 41. Production of PSP toxins in *A. ostenfeldii*, strain AON-13 at the control temperature of 15 °C and the three experimental irradiances: 30 (blue bar), 100 (green bar) and 200 (red bar) µmol.m^2.s^{-1}. Toxin production is shown along the growth curve T1 (lag phase) T2 (early exponential phase) T3 (late exponential phase).

At 20 ° C the effect that temperature had on toxin production was observed. Unlike the consistently high production of toxin at highest irradiance (200 µmol.m^2.s-^{1}). At 20 the highest production was in the late exponential phase at 30 µmol.m^2.s-^{1} with 11.54 pg STX eq. cell $^{-1}$ (Fig. 42). Would have been interesting to end the growth curve in low irradiance to confirm the highest toxin production, but was not possible then at the stationary phase the highest PSP production was at 200 µmol.m^2.s-^{1} with 19.12 pg STX eq. cell $^{-1}$.

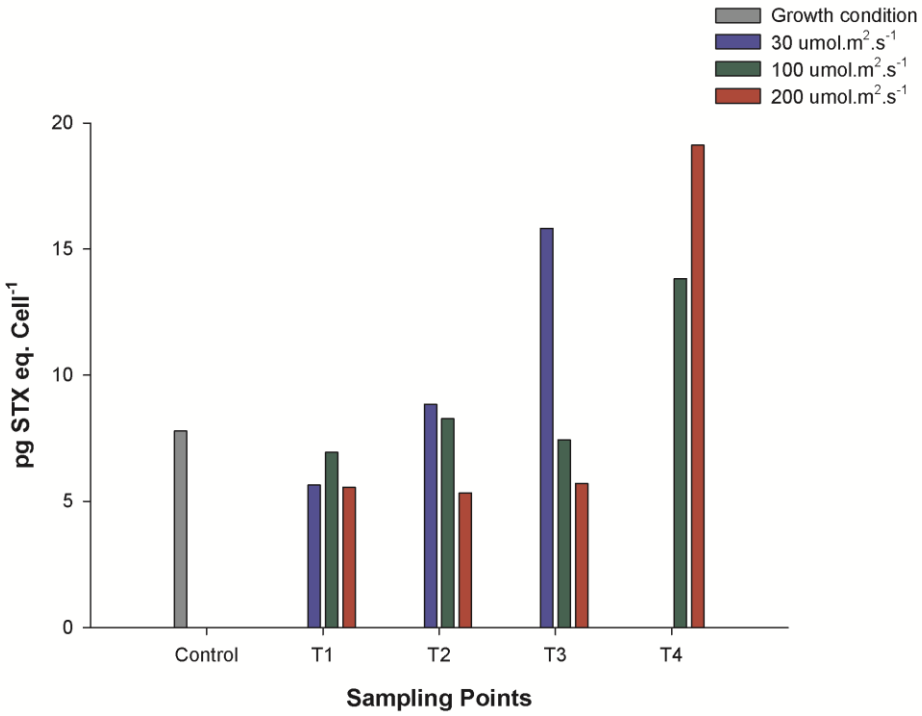

Figure 42. Production of PSP toxins in *A. ostenfeldii*, strain AON-13 at the experimental temperature of 20 °C and the three experimental irradiances: 30 (blue bar), 100 (green bar) and 200 (red bar) µmol.m^2.s^{-1}. Toxin production is shown along the growth curve T1 (lag phase) T2 (early exponential phase) T3 (late exponential phase) and T4 (stationary phase).